Homologous Recombinational DNA Repair: From Prokaryotes to Eukaryotes

A Dissertation Presented

By

Anthony L. Forget

Submitted to the Faculty of the
University of Massachusetts Graduate School of Biomedical Sciences, Worcester
In partial fulfillment of the requirements for the degree of

DOCTOR OF PHILOSOPHY

August 17, 2004

Biochemistry & Molecular Pharmacology

Homologous Recombinational DNA Repair:

From Prokaryotes to Eukaryotes

A Dissertation Presented

By

Anthony L. Forget

Approved as to style and content by:

Anthony Carruthers, Ph.D., Chair of Committee

Sharon Cantor, Ph.D., Member of Committee

William R. Robertz, Ph.D., Member of Committee

Susan T. Lovett, Ph.D., Member of Committee

Craig L. Peterson, Ph.D, Member of Committee

Kendall L. Knight, Ph.D., Dissertation Mentor

Anthony Carruthers, Ph.D., Dean of the Graduate School of Biomedical Sciences

Biochemistry & Molecular Pharmacology
August 17, 2004

ACKNOWLEDGMENTS

The successful completion of the work presented here as well as my entire graduate career at UMASS would not have been possible with out the support of many individuals with a list too long to mention everyone who contributed. For those whom I do not mention specifically, let me begin by saying thanks to you. To my family, Mom, Dad and Jenn thanks for standing behind my on my decision to return to school and leave a perfectly good job for greater intellectual challenge. Thanks for also listening to my practice talks and trying to read articles I brought home to you even though they probably seemed as if they were in a foreign language, you have to admit the pictures were nice though. Janell thank you for your support and patience in the last few years of my stay at UMASS, you couldn't have come along at a better time. The little things like understanding (or putting up with) my enthusiasm of a black picture with some colored dots on it mean more than you could ever imagine.

Thanks to members of my committee for providing helpful scientific guidance throughout my career at UMASS. Many members of the department including the Carruthers Lab, Gilmore Lab, Zamore Lab for sharing ideas, protocols and reagents. Thanks to past and current members of the Knight lab: Karen, Julie and Jan thanks for my first real exposure to biomedical research and more importantly how to work in the lab as the only guy with all women. Thanks to the departmental support staff Annette, Karen and Denise things wouldn't happen with out you. Thanks to my fellow graduate students particularly the ones on my softball team (you know who you are) for providing moral support which helped me maintain a decent level of sanity when needed.

Last but certainly not least I want to thank Ken for being an amazing mentor and friend throughout my stay in his lab. We have developed a relationship that I only hope will continue through the years. His open door and stocked fridge provided a great atmosphere to bounce my next experiment off you or discuss our plans for the upcoming weekend. That atmosphere was invaluable in helping me to achieve what I have thus far for that I am truly thankful. I only hope that I can be as successful in this next stage of my scientific career so that I may return that same mentor student experience someday in the near future, only next time as the role of the mentor in my own lab.

ABSTRACT

The error free repair of DNA double strand breaks through the homologous recombinational repair pathway is essential for organisms of all types to sustain life. A detailed structural and mechanistic understanding of this pathway has been the target of intense study since the identification of bacterial *recA*, the gene whose product is responsible for the catalysis of DNA strand exchange, in 1965. The work presented here began with defining residues that are important for the assembly and stability of the RecA filament, and progressed to the identification of residues critical for the transfer of ATP-mediated allosteric information between subunits in the protein's helical filament structure. My work then evolved to investigate similar mechanistic details concerning the role of ATP in the human RecA homolog, Rad51.

Results from non-conservative mutagenesis studies of the N-terminal region of one subunit and the corresponding interacting surface on the neighboring subunit within the RecA protein, led to the identification of residues critical for the formation of the inactive RecA filament but not the active nucleoprotein filament. Through the use of specifically engineered cysteine substitutions we observed an ATP-induced change in the efficiency of cross subunit disulfide bond formation and concluded that the position of residues in this region as defined by the current crystal structure may not accurately reflect the active form of the protein.

These ATP induced changes in positioning led to the further investigation of the allosteric mechanism resulting in the identification of residue Phe217 as the key mediator for ATP-induced information transfer from one subunit to the next.

In transitioning to investigate homologous mechanisms in the human pathway I designed a system whereby we can now analyze mutant human proteins in human cells. This was accomplished through the use of RNA interference, fluorescent transgenes, confocal microscopy and measurements of DNA repair. In the process of establishing the system, I made the first reported observation of the cellular localization of one of the Rad51 paralogs, Xrcc3, before and after DNA damage. In addition we found that a damage induced reorganization of the protein does not require the presence of Rad51 and the localization to DNA breaks occurs within 10 minutes.

In efforts to characterize the role of ATP in human Rad51 mediated homologous repair of double strand breaks we analyzed two mutations in Rad51 specifically affecting ATP hydrolysis, K133A and K133R. Data presented here suggests that, in the case of human cells, ATP hydrolysis and therefore binding, by Rad51 is essential for successful repair of induced damage.

TABLE OF CONTENTS

Signature page ii
Aknowledgments ..... **Error! Bookmark not defined.**
Abstract iv
Table of Contents vi
List of Figures viii
List of Tables xi
Abbreviations xii

CHAPTER I Introduction and Background 1

Preface for CHAPTER II 9

CHAPTER II Mutations in the N-terminal Region of RecA Which Disrupt the Stability of Free Protein Oligomers but not RecA-DNA Complexes 10
- Abstract 10
- Introduction 11
- Results 14
- Discussion 23
- Materials and Methods 29

Preface for CHAPTER III 34

CHAPTER III ATP-mediated Changes in Cross-subunit Interactions in the RecA Protein 35
- Abstract 35
- Introduction 35
- Results 37
- Discussion 48
- Materials and Methods 53

Preface for CHAPTER IV 57

CHAPTER IV Phe217 Regulates the Transfer of Allosteric Information Across the Subunit Interface of the RecA Protein Filament 58
- Introduction 58
- Results 60
- Discussion 67
- Materials and methods 76

Preface for CHAPTER V 79

CHAPTER V Xrcc3 is Recruited to DNA Double Strand Breaks Early and Independent of Rad51 79
Abstract 80
Introduction 81
Results 83
Discussion 88
Materials and Methods 91

Preface for CHAPTER VI 95

CHAPTER VI ATP Binding and Hydrolysis is Essential for the Ability of Human Rad51 to Repair Ionizing Radiation Induced DNA Damage 96
Introduction 96
Results 100
Discussion 103
Materials and Methods 104

CHAPTER VII Future Directions 108

References 110

LIST OF FIGURES

CHAPTER I

Figure 1.1 Homologous Recombination Strand Exchange Model

Figure 1.2 Key Proteins involved in Homologous Recombination

Figure 1.3 Extended and Compressed States of RecA

CHAPTER II

Figure 2.1 Details of the oligomeric interactions of RecA

Figure 2.2 Superose 6 gel filtration profiles of wild type RecA and Lys6→Ala, Asp139→Ala, Lys6→Asp/Asp139→Lys mutant RecA proteins

Figure 2.3 Superose 6 gel filtration profiles of wild type RecA and Arg28→Ala, Asn113→Ala, Arg28→Asn/Asn113→Arg mutant RecA proteins

Figure 2.4 Electron micrographs of wild type, Lys6→Ala and Arg28→Ala RecA proteins

Figure 2.5 Single-stranded DNA binding by wild type, Lys6→Ala and Arg28→Ala RecA proteins

Figure 2.6 DNA strand exchange catalyzed by wild type, Lys6→Ala and Arg28→Ala RecA proteins

CHAPTER III

Figure 3.1 Details of the oligomeric interactions in RecA

Figure 3.2 Gel shift DNA binding assays

Figure 3.3 Negative stained electron micrographs of protein and protein-ssDNA complexes

Figure 3.4 Gel filtration profiles of wild type RecA and the three double Cys mutant proteins

Figure 3.5 Disulfide cross-linking performed using the engineered double Cys mutant proteins

Figure 3.6 Disulfide cross-linking performed using wild type RecA and the T150C/F217C mutant protein

Figure 3.7 Disulfide cross-linking followed by incubation with βME

CHAPTER IV

Figure 4.1 Negative stained electron micrographs of protein and protein-ssDNA complexes

Figure 4.2 Biosensor DNA binding time courses

Figure 4.3 DNA binding as a function of protein concentration

Figure 4.4 ATPase activity of both wild type RecA and the Phe217Tyr mutant protein as a function of ATP concentration

Figure 4.5 Structure of the RecA protein and specific interactions at the subunit interface

Figure 4.6 Molecular surface of the neighboring subunit with which residue 217 interacts

CHAPTER V

Figure 5.1 Localization of Xrcc3 to DNA double strand breaks does not require Rad51

Figure 5.2 RNAi-mediated knock-down of Rad51 and rescue using a Rad51-GFP fusion protein

Figure 5.3 Rad51 and Xrcc3 localize to DNA double strand breaks within 10 min following exposure to ionizing radiation

Figure 5.4 Model for an early function of Xrcc3 in the homologous recombination pathway

CHAPTER VI

Figure 6.1 Model for ATP regulation of events at a DSB

Figure 6.2 Comet Assay

Figure 6.3 Co-immunoprecipitation assay

LIST OF TABLES

CHAPTER I

Table 1.1 - Proteins associated with Double strand break repair through homologous recombination

CHAPTER II

Table 2.1 - In vivo recombinational DNA repair activity of mutant RecA proteins

CHAPTER III

Table 3.1 - $C\beta_1$-$C\beta_2$ cross-subunit distances between indicated residues

Table 3.2 - In vivo DNA repair and Coprotease Activities

Table 3.3 - DNA binding and ATPase Activities

CHAPTER IV

Table 4.1 - DNA binding parameters

ABBREVIATIONS

γH2AX	phosphorylated histone2A variant X
ATCC	American Type Culture Collection
ATP	adenosine triphosphate
ATPγS	adenosine 5´-O-(3-thio) triphosphate
BRCA	Breast Cancer Associated
BSA	bovine serum albumin
DAPI	4´, 6´-diamidino-2-phenylindole
DMEM	Dulbecco's modified eagle media
DNA	deoxyribonucleic acid.
DSB	DNA double strand break.
dsDNA	double-strand DNA
EDTA	ethylene diamine tetra-acetic acid
EM	electron microscopy
FBS	fetal bovine serum
GFP	green fluorescent protein
HEK293 -	human embryonic kidney 293
HR	homologous recombination.
IPTG	isopropyl-1-β-D-galactopyranoside
IR	ionizing radiation
NEM	N-ethylmaleamide
NTP	nucleoside triphosphate
PCR	polymerase chain reaction
PEI	poly-ethylenimine
PVDF	polyvinylidene fluoride
RAD	genes in which mutations result in radiation sensitivity.
RIPA	radioimmuno precipitation assay
RNA	ribonucleic acid
RNAi	RNA interference.
SDS	sodium dodecyl sulfate
SSB	single strand DNA binding protein.
ssDNA	single-strand DNA
TAE	tris acetate EDTA
U.V.	ultra violet
XRCC	X-ray cross complementing

CHAPTER I

INTRODUCTION AND BACKGROUND

Insult to deoxyribonucleic acid (DNA) can arise from many different environmental factors and *in vivo* processes such as radiation, chemical exposure, free radicals from normal metabolic processes, and errors in DNA synthesis. Different classifications of DNA damage can by separated into the following general categories: DNA modifications (i.e., cross-links), single strand breaks, or double strand breaks (DSBs). To overcome DNA damage cells of all type have inherent repair mechanisms specific to the form of damage including single strand annealing, non-homologous end joining, base excision repair, and homologous recombination (HR). Given the critical importance of maintaining genome integrity, it is not surprising that defects in these DNA repair pathways are associated with cancer, conditions that occur by either a predisposition to genetic disorders through chromosome instability or the occurrence of somatic mutations in genes essential to the repair pathway that contribute to carcinogenesis (Thompson and Schild, 2002).

The work presented here focuses on understanding the high fidelity repair of DSBs carried out by HR. Methods of repair other than HR have a much greater propensity to be error prone rather than error free. Figure 1.1 represents a basic model for HR that can be broken down into four critical steps: **I.** Initiation, **II**. Homologous pairing and strand exchange, **III**. Branch migration and **IV**. Resolution. The Initiation step involves the processing of double strand ends by nucleases and/or helicases to produce free 3´ tails of

single strand DNA. This step also involves binding of single stranded binding proteins to remove any secondary structure introduced in the newly created single strand tails facilitating the loading of the major catalytic protein in the next step. Homologous pairing and strand exchange begins with the key catalytic component, RecA or Rad51, forming a cooperative nucleoprotein filament on the newly processed 3′ tail in a 5′ to 3′ manner. A fast and efficient scan for homology results in joint molecule formation. Once homologous sequences are aligned crossover structures known as Holliday junctions are formed. The next step, branch migration, involves a specialized class of helicases to catalyze translocation of the heteroduplex joints. The fourth and final step, resolution, is the nucleolytic cleavage of the crossover structures resulting in either spliced or patched products (Figure 1.1).

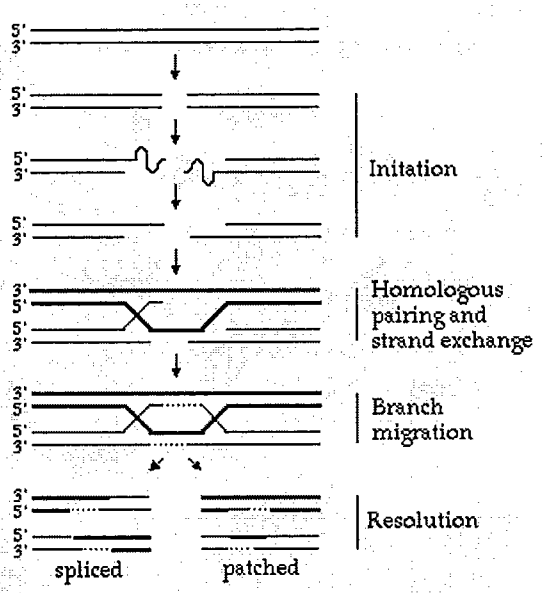


Figure 1.1 - Homologous Recombination Strand Exchange Model

An abbreviated model of HR strand exchange shown in Figure 1.2 illustrates selected key components of the pathway. Although the pathway illustrated here is representative of human proteins the mechanism is similar for the prokaryotic homologs. Upon the appearance of a DSB (steps I-II) the ends of DNA at the break are processed in 5′ to 3′

directional manner by exonucleases (steps II-III). The resected ends of a break are initially bound by RPA (*E. coli* SSB) (steps III-IV) which, among other functions, serves to remove any secondary structure in the single strand tails facilitating accessibility to other DNA proteins. By virtue of its affinity for ssDNA, and perhaps RPA, Rad52 binds to the RPA-coated resected break (steps IV-V). BRCA2 promotes recruitment of Rad51 (*E. coli* RecA) (steps V-VI). Rad52 may stabilize interactions between Rad51 and the Rad51-paralog proteins e.g. Xrcc3, as well as interactions between various Rad51-paralog proteins.

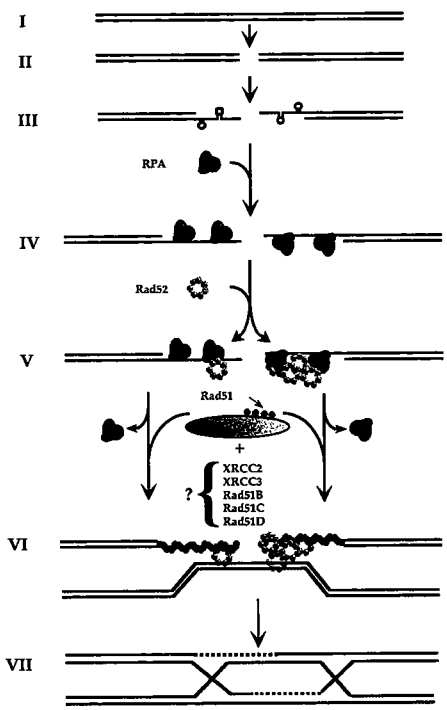


Figure 1.2 - Key proteins involved in Homologous Recombination

Table 1.1 lists the known gene products involved in homologous recombination for bacteria, yeast and humans grouped into categories where they are known and or hypothesized to function in the pathway (Figure 1.1). The purpose of this table is to illustrate the high degree of conservation of proteins across species. The *recA* gene was discovered by Clark and Margulies in 1965 and is responsible for catalyzing HR in *E. coli* as discussed here but also plays an essential role in the induction of the SOS response (Clark and Margulies, 1965). This activity is carried out through cleavage of the LexA

	E. coli	*S. cerevisiae*	*H. sapians*
INITIATION	RecBCD	-	-
	SbcCD	Mre11; Rad50; Xrs2	Mre11/Rda50/Nbs1
	RecQ	Sgs1	RecQ1,4,5; BLM;WRN
	RecJ	Exo1	Exo1
	UvrD	Srs2	-
HOMOLOGOUS PAIRING AND STRAND EXCHANGE	RecA	Rad51	Rad51
	SSB	RPA	RPA
	RecF, RecR	Rad55,57	Rad51B,C,D; Xrcc2,3
	RecO	Rad52	Rda52
	-	Rad59	-
	-	Rad54; Rdh54	Rad54, 54B
	-	-	Brca2
BRANCH MIGRATION	RuvAB	Rad54	Rad54
	RecG	-	-
	RecQ	Sgs1	RecQ1,4,5; BLM; WRN
RESOLUTION	RuvC	-	-
	-	Mus81; Mms4	Mus81; Mms4
	RecQ; TopoIII	Sgs1; TopoIII	BLM; TopoIIIa
	-	-	Xrcc3

Table1.1 Proteins associated with Double strand break repair through homologous recombination

repressor in response to DNA damage resulting in activation of more than 20 genes involved in DNA repair. Given the essential role of RecA in recombinational repair widespread efforts to identify DNA damage repair associated proteins in eukaryotes resulted in the identification of the *S. cerevisiae RAD52* epistasis group, a gene family in which mutations resulted in increased sensitivity to ionizing radiation. This group includes *RAD50, RAD51, RAD52, RAD54, RAD55, RAD57, RAD59, MRE11* and *XRS2* (Game and Mortimer, 1974). It wasn't until 1992 that the *S. cerevisiae* Rad51 protein was characterized as a RecA homolog followed by discovery of homologs in chicken (Bezzubova et al., 1993), mouse (Morita et al., 1993; Shinohara et al., 1993), fission yeast (Shinohara et al., 1993), human (Shinohara et al., 1993) and *Xenopus laevis* (Maeshima et al., 1995). Additionally, five *RAD51* paralog genes were identified based on their sequence homology of the corresponding protein to Rad51 (20-30%): *RAD51B* (Albala et al., 1997; Rice et al., 1997; Cartwright et al., 1998), *RAD51C* (Dosanjh et al., 1998), *RAD51D* (Cartwright et al., 1998; Pittman et al., 1998), *XRCC2* (Cartwright et al., 1998;

Liu et al., 1998), and *XRCC3* (Tebbs et al., 1995; Cartwright et al., 1998; Liu et al., 1998). Deletion of any of the paralog genes in chicken or hamster cells leads to defects in HR, increased chromosomal aberrations and increased sensitivity to DNA damaging agents (Takata et al., 2001; Tebbs et al., 1995; Cui et al., 1999). Studies of the specific function of these proteins is currently the focus of many researchers in the field.

Both RecA and Rad51 can bind and hydrolyze ATP in a ssDNA dependent manner, bind to ssDNA or dsDNA and promote strand annealing, homologous pairing and strand exchange (Baumann et al., 1996; Gupta et al., 1997; Benson et al., 1994). While showing a high degree of homology in the 207 amino acid core domain and a 51% overall homology, studies of RecA and Rad51 have revealed significant differences in the way they function. Bacteria carrying a *recA* deletion are compromised for homologous recombination events but remain viable yet *RAD51* knock-out mice show embryonic lethality, and a *RAD51* deletion in various cell lines results in extreme sensitivity to DNA damaging agents, defective repair of DSBs and ultimately cell death (Tsuzuki et al., 1996; Sonoda et al., 1998). Biochemical analyses have also revealed important mechanistic differences between RecA and human Rad51. RecA requires ATP to efficiently bind DNA while human Rad51 does not (Knight & DeZutter unpublished). The rate of ATP hydrolysis also differs. RecA is much more efficient than Rad51 with $k_{cat} \approx 30\ min^{-1}$ and $0.16\ min^{-1}$, respectively (Kowalczykowski, 1991; Baumann et al., 1996). RecA can catalyze *in vitro* strand exchange efficiently in the absence of other cofactors while Rad51 requires the assistance of accessory proteins such as RPA, Rad52

or Rad54 to efficiently catalyze the reaction (Roman and Kowalczykowski, 1986; Benson et al., 1998; Baumann and West, 1997).

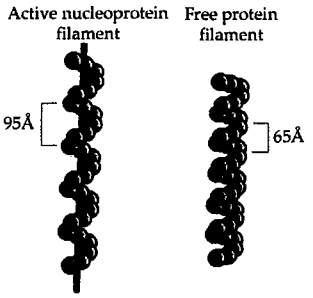


Figure – 1.3 Extended and compressed states of RecA

Although RecA has been the focus of intense studies since its discovery and we now have a good understanding of most of the basic mechanistic features of RecA, important questions remain as to how the protein coordinates its various domains to carry out its regulatory and catalytic activities. Electron microscopic analyses of RecA revealed that the protein filament formed in the absence of ATP (the inactive filament) assumes a more compressed state (≈ 65 – 70Å pitch) relative to the active filament formed in the presence of ATP in which bound DNA is extended and the filament pitch is ≈ 95Å (Figure 1.3)(Egelman and Stasiak, 1986). Given this dramatic change in pitch there must be significant conformational changes that occur upon ATP and/or DNA binding to allow for this. Specifically addressed in the following chapters, we have identified critical residues involved in free protein filament formation *vs.* those essential for active filament formation, and have shown that ATP binding induces a significant conformational change at the subunit interface (Chapters II & III). We have also characterized important molecular determinants of the allosteric pathway involved in the transmission of ATP-mediated conformational changes between subunits of the RecA filament (Chapter IV).

The focus of my research shifted from the prokaryotic RecA to the human homolog Rad51 to determine if similar mechanisms were involved in its catalytic activity. Biochemical assays were in place to evaluate mutant proteins *in vitro* yet there was a need to establish a system to evaluate mutants in the context of living cells. The data obtained from a combination of more traditional biochemical assays in combination with genetic and *ex vivo* (cell culture) assays allows us to see how specific mechanistic defects in Rad51 affect its functions in the cell. Therefore, I established a system using RNA interference (RNAi), transient expression of mutant proteins, confocal microscopy and DNA damage assays to address the functionality of mutant human proteins in human cells (Chapters V & VI). In the process of establishing this system we showed for the first time that Xrcc3 forms distinct cellular foci, both cytoplasmic and nuclear, and upon DNA damage the protein is redistributed to the nucleus and associates with DSBs independent of Rad51 (Forget et al., 2004).

One of the initial questions to be addressed with this system is the role of ATP binding/hydrolysis for Rad51 function. Given that Rad51 and each of the five Rad51 paralog proteins has an ATP binding site, regulation of protein-protein interactions required for the establishment of active repair complexes in the HR pathway may be mediated by specific ATP binding and turnover events. In fact, recent studies suggest that Xrcc2 acts as an NTP exchange factor by stimulating ATP processing by Rad51 in a Rad51D-dependent manner (Shim et al., 2004). Recent data also shows that the stability of the Rad51C/Xrcc3 dimer is regulated by ATP binding and hydrolysis by Xrcc3 (Yamada et al., 2004). Studies in mouse and chicken cells have led to conflicting results regarding the requirement for ATP

binding/hydrolysis by human Rad51 to carry out its DNA repair function (Morrison et al., 1999; Stark et al., 2002). Our recent analyses of human Rad51 ATP site mutants using DNA repair assays in HEK293 cells as well as two-hydrid, co-ip and biochemical analyses provide novel mechanistic insights into the use of ATP by Rad51. This work is described in Chapter VI.

Development of the cellular system and RNAi methods now allows us to analyze many of the components of the HR pathway in human cells, and will provide a better understanding of both their overall importance and specific function, as well as the links between HR other cellular pathways involved in DNA damaging signaling, DNA replication and cell cycle progression.

PREFACE FOR CHAPTER II

In Chapter II we provide evidence that cross-subunit contacts in one region of the RecA protein interface are different for free RecA protein filaments *vs.* RecA-DNA nucleoprotein filaments. We have identified Lys6 and Arg28 as important determinants of RecA oligomer formation and stability in the absence of DNA. In contrast, these side chains are not essential to the function or stability of the RecA nucleoprotein filament but do play a role in optimizing its catalytic efficiency. Our results suggest that in the active RecA/ATP/ssDNA nucleoprotein filament each of these side chains makes cross-subunit contacts other than those observed in the RecA crystal structure.

This work was accomplished through the combined efforts of Sherif Eldin, Ph.D., who contributed to the formulation of the fundamental questions and data represented in Table 2.1, Karen Logan who contributed to mutant protein purification and performed strand exchange represented in Figure 2.6, and Danielle Lindenmuth who contributed to data in Table 2.1. I contributed to the overall experimental design, constructed mutants, purified proteins and collected all the data in the remaining Figures (2.2 – 2.5). I also contributed to data interpretation and editing/revising the final manuscript.

The data presented in this chapter was published in the **Journal of Molecular Biology**, Volume 299, Issue 1 (May 2000).

CHAPTER II

MUTATIONS IN THE N-TERMINAL REGION OF RECA WHICH DISRUPT THE STABILITY OF FREE PROTEIN OLIGOMERS BUT NOT RECA-DNA COMPLEXES

Abstract

We have introduced targeted mutations in two areas that make up part of the RecA subunit interface. In the RecA crystal structure cross-subunit interactions are observed between the Lys6 and Asp139 side chains, and between the Arg28 and Asn113 side chains. Unexpectedly, we find that mutations at Lys6 and Arg28 impose severe defects on the oligomeric stability of free RecA protein, whereas mutations at Asn113 or Asp139 do not. However, Lys6 and Arg28 mutant proteins showed an apparent normal formation of RecA-DNA complexes. These results suggest that cross-subunit contacts in this region of the protein are different for free RecA protein filaments *vs.* RecA-DNA nucleoprotein filaments. Mutant proteins with substitutions at either Lys6 or Arg28 show partial inhibition of DNA strand exchange activity, yet the mechanistic reasons for this inhibition appear to be distinct. Although Lys6 and Arg28 appear to be more important to the stability of free RecA protein as opposed to the stability of the catalytically active nucleoprotein filament, our results support the idea that the cross-subunit interactions made by each residue play an important role in optimizing the catalytic organization of the active RecA oligomer.

Introduction

Catalysis of genetic recombination and recombinational DNA repair by the RecA protein requires formation of a nucleoprotein filament consisting of RecA, single-stranded DNA and ATP (Radding, 1989; West, 1992; Kowalczykowski et al., 1994; Roca and Cox, 1997). Structural studies show that in both the absence and presence of DNA, the RecA protein forms long helical polymers with approximately 6 monomers per turn (Di Capua et al., 1982; Egelman and Stasiak, 1988; Heuser and Griffith, 1989; Brenner et al., 1988; Story et al., 1992). Two different forms of the RecA filament, the inactive and active, have been defined by electron microscopic studies (Egelman and Stasiak, 1993). The inactive structure is seen in the absence of nucleotide cofactor and DNA, and is characterized by a helical pitch of approximately 65 Å. In the presence of both DNA and ATP, RecA forms the active structure which has a helical pitch of approximately 95 Å. The X-ray structure of the RecA protein filament displays a helical pitch (82.7 Å) that is intermediate between the inactive and the active form, and therefore, may not reveal the position of certain amino acid side chains at the subunit interface as they would exist in the catalytically active form of the enzyme (Egelman 1993; Egelman and Stasiak, 1993).

To identify specific determinants of RecA oligomer stability and function we have mutagenized regions of the protein involved in subunit-subunit contacts. Previously, we introduced a variety of mutations at 5 residues (Skiba and Knight, 1994) which are shown in the crystal structure to make specific contacts with positions in the neighboring monomer (Story et al., 1992). Analysis of recombination and recombinational DNA

repair activities showed that only 3 of these 5 (Lys216, Phe217 and Arg222) are important for RecA function (Skiba and Knight, 1994). Only the most conservative amino acid substitution at each of these 3 positions retained wild type-like recombination activity, but despite this, each of these mutations (Lys216→Arg, Phe217→Tyr and Arg222→Lys) imposed defects in oligomer formation by free protein, i.e. RecA protein in the absence of DNA and ATP (Logan et al., 1997).

In the present study we have targeted 2 different areas of the RecA structure that make up

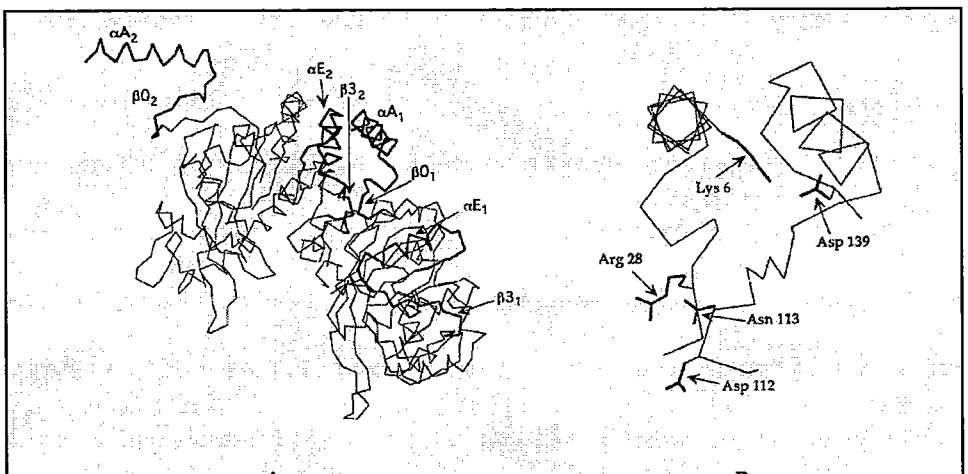


Figure 2.1 - Details of the oligomeric interactions of RecA. **(A)** RecA dimer as shown in the crystal structure (Story et al., 1992). Highlighted areas correspond to α-helix A and β-strand 0, and β-strand 3 and α-helix E. Subunit 1 is on the right and subunit 2 on the left. Complementary oligomeric surfaces which interact are shown in bold in the center of the image, αA_1-$\beta 0_1$ with $\beta 3_2$-αE_2. **(B)** Cross-subunit proximity between Lys6 (subunit 1) and Asp139 (subunit 2), and Arg28 (subunit 1) and Asp112/Asn113 (subunit 2; see text for description of distances). This image has been rotated approximately 180° around the Y-axis relative to that in panel A such that the N-terminal α-helix of subunit 1 (αA_1) is on the left. Side chains of residues 6, 28, 112, 113 and 139 are in bold

part of the oligomeric interface. These are shown in Figure 2.1, and consist of α-helix A and β-strand 0 (residues 6 - 30) in one monomer (designated subunit 1; Figure 2.1A) and β-strand 3 and α-helix E (residues 111 - 140) in the neighboring monomer (designated

subunit 2; Figure 2.1A). Within these two complementary surfaces, cross-subunit interactions are largely hydrophobic in nature as 7 hydrophobic side chains are within van der Waals distance (≤ 4 Å) of 8 hydrophobic side chains in the neighboring monomer. In addition, the structure reveals ionic and polar interactions between several residues that flank this hydrophobic area. The ε-NH_3 group of Lys6 is 2.9 Å from one of the carboxylate oxygens of the Asp139 side chain in the neighboring subunit (Figure 2.1B). In addition, one of the nitrogens in the guanidinium group of Arg28 (Nε) is 3.5 Å from the carbonyl oxygen (Oδ1) of the Asn113 side chain (Figure 2.1B), and two of the nitrogens (Nε and Nη1) are within 3.0 Å of the main chain carbonyl oxygen of Asp112.

To determine the importance of these ionic and polar interactions to both the RecA oligomeric structure and enzyme function we have introduced several amino acid substitutions at positions 6, 28, 112, 113 and 139. The results show that mutations at positions 6 and 28 have a much more dramatic effect on the oligomer stability of free RecA protein than do mutations at 112, 113 and 139. However, formation of active nucleoprotein filaments is not effected by these mutations and RecA function is not significantly disrupted. Our results support the idea that the N-terminal region of RecA interacts with the neighboring monomer differently in the inactive *vs.* active form of the protein.

Results

Gel Filtration Analysis of Mutant RecA Proteins - We have developed a gel filtration assay in which the oligomeric distribution of the RecA protein can be analyzed in treated cell extracts (Logan et al., 1997). Previously, we demonstrated that the observed population of oligomers is a true measure of the oligomeric distribution of free RecA protein, i.e. RecA (wild type or any of the mutants studied) does not form complexes with residual RNA in the extract, nor does RecA show non-specific interactions with other proteins remaining in the extract (Logan et al., 1997). A Superose 6 gel filtration profile for wild type RecA is shown in Figure 2.2A.

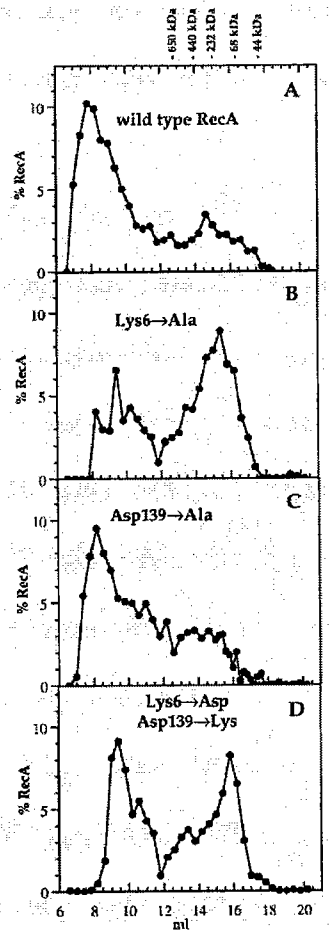


Figure 2.2 - Superose 6 gel filtration profiles of wild type RecA and Lys6→Ala, Asp139→Ala, Lys6→Asp/Asp139→Lys mutant RecA proteins. Protein from treated cell extracts was loaded onto the column such that the concentration of RecA was ≥ 26 μM. Cell extracts were prepared and column profiles analyzed as described in **Materials and Methods**. Molecular weight standards were thyroglobulin (650 kDa), ferritin (440 kDa), catalase (232 kDa), BSA (68 kDa) and ovalbumin (44 kDa).

Protein eluting at the column void volume (≤ 8.0 ml) has a relative molecular weight ≥ 5 x 10^6 Da and corresponds approximately to RecA filaments ≥ 130 monomers and bundles

of filaments. Protein eluting between 8.0 - 13.5 ml corresponds approximately to RecA filaments ranging in size from 100 - 10 monomers, and the peak centered at 14.6 ml corresponds to hexamer-sized RecA oligomers. Electron microscopic analysis of a mutant RecA protein which is trapped in this latter oligomeric state confirms that this peak corresponds to ring-shaped oligomers containing approximately 6 subunits (C.S. Lange and K.L.K., unpublished results).

Replacement of the Lys6 side chain with Ala imposes a significant destabilization of the RecA filament (Figure 2.2B). A significant amount of the Lys6→Ala protein elutes between 13 and 17.4 ml, showing a broad distribution of oligomers ranging in size from approximately 500,000 to 40,000 Da. These molecular weights correspond roughly to RecA filaments containing 13 subunits and monomeric RecA, respectively. Surprisingly, although the RecA crystal structure shows a well defined cross-subunit ionic interaction between Lys6 and Asp139, replacement of Asp139 with Ala has only a minimal effect on the oligomeric stability of the RecA filament (Figure 2.2C). We also created a mutant in which the positions of these 2 residues were switched (Lys6→Asp/Asp139→Lys). The gel filtration profile of this protein (Figure 2.2D) shows no larger oligomers eluting in the column void. The majority of protein elutes in two regions of the profile centered at approximately 9.5 ml and 15.5 ml. This switch mutant does cause a slight suppression of the oligomeric defect seen for the Lys6→Ala mutant, as more RecA appears as larger molecular weight oligomers eluting from 8.0 – 11.5 ml. However, it is clear that overall oligomeric stability relative to wild type RecA has been significantly compromised. Gel filtration profiles of the corresponding single mutants show that the Lys6→Asp mutation

inhibits oligomer stability to a far greater extent than the Asp139→Lys mutation (data not shown). Therefore, despite the fact the RecA crystal structure shows a well-defined cross-subunit interaction between Lys6 and Asp139, only substitutions at Lys6 have a significant effect on RecA oligomer stability.

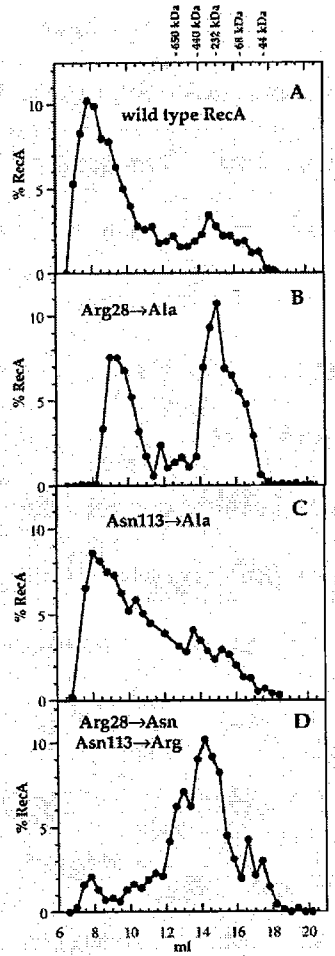


Figure 2.3 - Superose 6 gel filtration profiles of wild type RecA and Arg28→Ala, Asn113→Ala, Arg28→Asn/Asn113→Arg mutant RecA proteins. Protein from treated cell extracts was loaded onto the column such that the concentration of RecA was ≥ 26 μM. Cell extracts were prepared and column profiles analyzed as described in **Experimental Procedures**.

Mutation of another pair of residues involved in a cross-subunit interaction in this area of the oligomeric interface, Arg28 and Asn113, results in a pattern of oligomeric disruption very similar to that seen for substitution of Lys6 and Asp139, i.e. mutation of the residue in subunit 1 (Arg28) is far more deleterious to RecA oligomer stability than mutation of the residue in subunit 2, Asn113. The Arg28→Ala mutant protein no longer forms large molecular weight oligomers that elute in the column void (compare Figure 2.3A and 2.3B). Although some larger oligomers elute between 8 – 11 ml, the majority of the mutant protein elutes in a broad peak centered at 15 ml which

approximates the molecular weight of hexameric RecA. In contrast, the Asn113→Ala mutant protein shows a distribution of oligomers very much like wild type RecA (Figure 2.3C). A mutant protein carrying two substitutions that switch the position of the wild type side chains (Arg28→Asn/Asn113→Arg) shows severe oligomeric defects (Figure 2.3D). Gel filtration profiles of the corresponding single mutants show that the Arg28→Asn protein is far more defective in oligomer formation than is the Asn113→Arg protein (data not shown). These results lend strong support to the idea that the Arg28 side chain is an important determinant of RecA oligomeric stability.

Given that mutations at positions 113 and 139 did not significantly effect the oligomeric stability of RecA, we re-examined the crystal structure for other side chains that may serve as cross-subunit partners for either Lys6 or Arg28. Other than Asp139, the only other side chain in subunit 2 which is close to the ε-NH_3 group of Lys6 is Thr89, whose -OH group is 4.1 Å away (the Thr89 -OH is also 9.8 Å from Nε of the Arg28 side chain in subunit 1). However, we created mutant proteins carrying either a Thr89→Ala or Val substitution and showed that each has an oligomeric profile virtually identical to wild type RecA (data not shown).

Mutations introduced at Asp112 (Ala or Arg) also showed far less of a defect in oligomer stability than would be expected if this side chain was involved in making a cross-subunit contact (data not shown; see **DISCUSSION**).

Effects of Mutations on in vivo DNA Repair Function – The effect of all mutations on RecA recombinational DNA repair activity, a function that requires formation of an active nucleoprotein filament, was examined by U.V. survival assays. Most mutations in either subunit 1 or 2 had little, if any effect, on this RecA activity (Table 2.1). For example, despite imposing significant defects in the oligomeric stability of free protein, substitutions at Lys6 and Arg28 result in virtually no decrease in repair activity. Previous genetic studies of the Lys6→Ala mutant are consistent with our results (Morimatsu and Horii, 1995). Note that the U.V. survival assays are performed in the absence of isopropyl-1-thio-β-D-galactopyranoside (IPTG) whereas

amino acid substitution	fractional UV survival
I. *mutations in subunit 1*	
K6A	0.95
K6D	0.95
R28A	1.00
R28D	1.00
R28N	0.90
II. *mutations in subunit 2*	
T89A	0.70
T89V	0.70
D112R	0.90
N113A	1.00
N113R	0.90
D139A	1.00
D139K	0.80
III. *mutations in subunits 1 and 2*	
K6D/D139K	0.90
R28N/N113R	0.75
R28D/D112R	0.90

Table 2.1 - in vivo recombinational DNA repair activity of mutant RecA proteins. Recombinational DNA repair activity was determined by measuring cell survival following exposure to varying doses of U.V. irradiation (0 - 1.52 J/m^2/sec) and is reported as fractional survival relative to wild type RecA protein (pTRecA420 in strain DE1663′). Strain DE1663′ carrying plasmid pZ150 (Nastri and Knight, 1994) served as the negative control and had a fractional survival = 0.

for analysis of RecA oligomeric defects *recA* gene expression is induced with IPTG. Therefore, potential functional defects of these mutants are not being masked by artificially high levels of RecA protein. Additionally, the double switch mutants, Lys6→Asp/Asp139→Lys and Arg28→Asn/Asn113→Arg, as well as their corresponding single mutants show no significant defect in recombinational DNA repair (Table 2.1). These results demonstrate that although the oligomeric stability of the free protein is compromised, these mutant proteins must still be capable of forming an active nucleoprotein filament upon binding to a single-stranded DNA substrate. Biochemical analysis of two mutant proteins described below shows that this is, indeed, the case.

Electron microscopic analysis of the Lys6→Ala and Arg28→Ala mutant proteins supports the idea that while the oligomeric stability of free protein is disrupted, both proteins maintain the ability to form wild type-like nucleoprotein filaments on single-

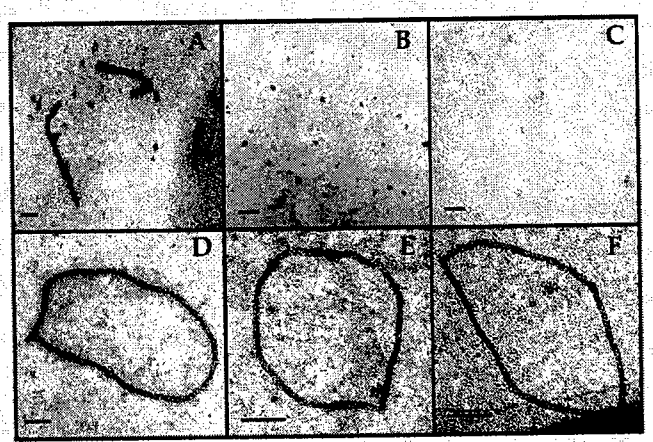


Figure 2.4 - Electron micrographs of wild type, Lys6→Ala and Arg28→Ala RecA proteins. Nega stained electron micrographs of wild type RecA protein (**A, D**), the Lys6→Ala mutant protein (**B, I** and the Arg28→Ala mutant protein (**C, F**). In the absence of DNA (**A, B, C**) the protein concentra is 2.0 μM. In the presence of 3 μM ϕX174 ssDNA (**D, E, F**) the protein concentration is 0.8 μM a samples also included 0.03 μM SSB. Black bar in each panel equals 0.1 μm.

stranded DNA. In the absence of DNA wild type RecA forms various length filaments and smaller oligomers (Figure 2.4A) while both the Lys6→Ala and Arg28→Ala mutant proteins form no observable oligomeric species (Figures 2.4B and 2.4C, respectively). In the presence of single-stranded DNA, however, both mutant proteins form nucleoprotein filaments identical to those formed by wild type RecA (Figures 2.4D, 2.4E and 2.4F).

Effect of Mutations on in vitro RecA Activities - Despite the fact that both the Lys6→Ala and Arg28→Ala mutant proteins form wild type-like nucleoprotein filaments and show

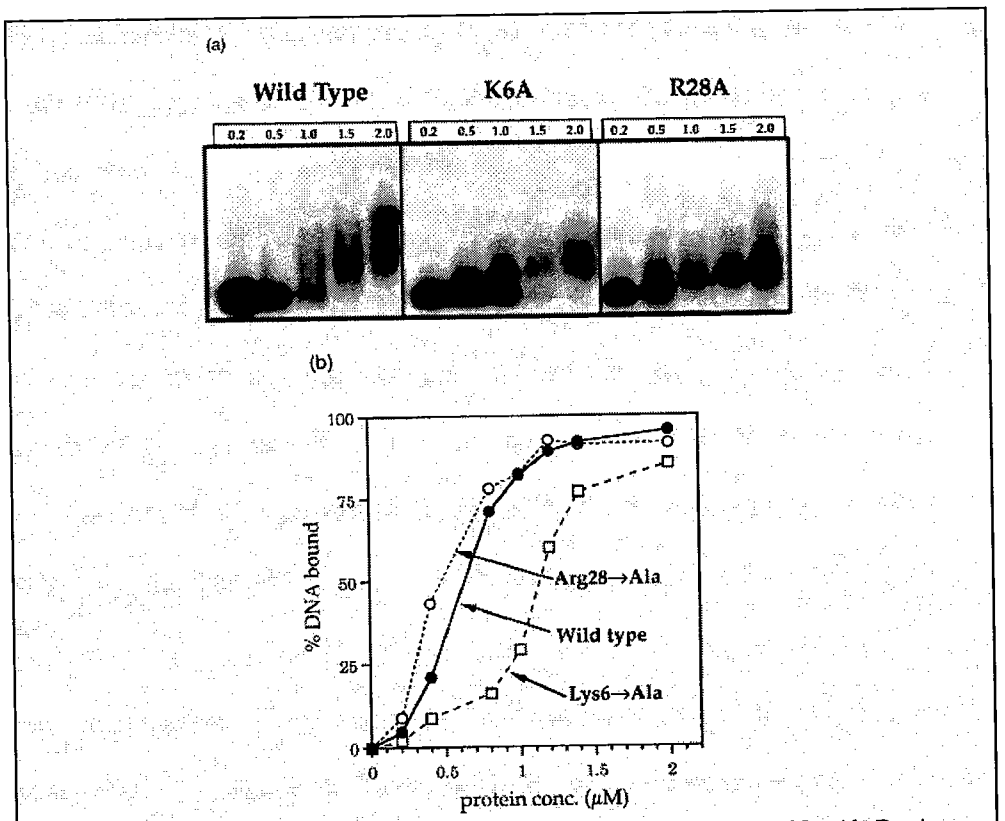


Figure 2.5 - Single-stranded DNA binding by wild type, Lys6→Ala and Arg28→Ala RecA proteins. (**A**) Gel shift assays included the indicated concentration of each protein, 10 μM ^{32}P-labeled 97 base oligonucleotide and 0.5 mM ATPγS. Reactions were incubated for 1 hr at 37 °C prior to electrophoresis as described (see **Materials and Methods**). (**B**) Plot of gel shift data expressed as % labeled oligonucleotide bound as a function of protein concentration. Procedure is identical to that in (**A**) but represents a different experiment.

little defect in carrying out repair of U.V. damage *in vivo*, each mutant protein displays observable changes of several functional properties including, (***i***) binding to ssDNA, (***ii***) catalysis of DNA-dependent ATP turnover and (***iii***) DNA strand exchange.

Gel shift DNA binding assays were performed using a 97 base oligonucleotide substrate. Titration of protein using a constant amount of labeled DNA shows that the Arg28→Ala mutant protein forms a protein-DNA complex with slightly better efficiency than wild type RecA and with significantly better efficiency than the Lys6→Ala protein (compare the 1.0 μM lane in each panel of Figure 2.5A). Because gel shift assays with RecA give rise to a diffuse protein-DNA shifted complex we used the disappearance of free oligonucleotide as a quantitative measure of relative binding. From Figure 2.5B, which plots gel shift data from an experiment independent of that in Figure 2.5A, we estimate that half-maximal binding of DNA for the wild type, Lys6→Ala and Arg28→Ala proteins occurs at concentrations of approximately 0.60 μM, 1.10 μM and 0.45 μM, respectively. Similar gel shift assays were repeated several times and consistently showed the Arg28→Ala protein binding to ssDNA with slightly higher affinity than wild type RecA while the Lys6→Ala protein showed significantly reduced affinity.

Each mutant protein showed a slight inhibition of ssDNA-dependent ATPase activity relative to wild type RecA. Rates of ATP hydrolysis were determined to be 18.6, 9.0 and 15.8 mol ADP•min^{-1}•mol^{-1} enzyme for wild type RecA and the Lys6→Ala and Arg28→Ala proteins, respectively.

DNA strand exchange assays were performed using single-stranded circular and homologous linearized duplex ϕX174 DNAs. Comparison of the reaction catalyzed by wild type RecA and the two mutant proteins shows several interesting differences. For wild type RecA, small amounts of initial joint molecules are observed as early as 30 sec into the time course. This is followed by the accumulation of slower mobility joint molecules that can be observed from 2 min through the end of the time course (60 min). Nicked circular products begin to appear at 6 min and reach a maximum between 30 and 60 min. For the Lys6→Ala mutant the appearance of initial and slower mobility joint molecules is similar to that seen for wild type RecA. However, there is a marked delay in the appearance of nicked circular product molecules as well as their accumulation during the 60 min time course. In contrast to wild type RecA and the Lys6→Ala mutant, strand exchange catalyzed by the Arg28→Ala mutant results in initial joint molecules appearing more quickly and accumulating to a significantly greater degree during the first 4 minutes of the reaction. However, this mutant also shows a significant delay in the appearance of nicked circular product molecules as well as a decrease in their overall accumulation. Additionally, the Arg28→Ala mutant displays a time dependent increase in the amount of DNA remaining in the gel well which does not occur with either wild type RecA or the Lys6→Ala mutant. Formation of these larger protein-DNA complexes may result from multiple initiation events in which more than one RecA-coated single-stranded circular DNA has formed a joint molecule with a single molecule of duplex DNA. Together, the results suggest that while both mutant proteins are partially inhibited for DNA strand exchange activity, the mechanism of their inhibition may be different (see **DISCUSSION**).

Discussion

The crystal structure of the RecA protein (Story et al., 1992) provided an explanation to earlier genetic results which demonstrated that a peptide consisting of the N-terminal 77 residues (Yarranton and Sedgwick, 1982) or the N-terminal 50 residues (Kiselev et al., 1988) could form mixed oligomers with wild type protein and inhibit its recombination function. Subsequent biochemical studies have demonstrated the importance of the N-terminal 33 residues to RecA self-assembly and function (Mikawa et al., 1995), and also suggest that folding of α-helix A is coupled to RecA monomer-monomer interactions and regulation of RecA filament formation (Masui et al., 1997). Recent studies of *recA* deletion mutants support the idea that residue 6 defines the minimum length for the N-terminus of RecA required to form active nucleoprotein filaments (Zaitsev and Kowalczykowski, 1998). In the present study we have identified Lys6 and Arg28 as important determinants of RecA oligomer formation and stability in the absence of DNA. In contrast, these side chains are not essential to the function or stability of the RecA nucleoprotein filament but do play a role in optimizing its catalytic efficiency. Our results suggest that each of these side chains makes cross-subunit contacts other than those observed in the RecA crystal structure.

In the RecA crystal structure, the ε-NH_3 group of Lys6 is within 2.9 Å of one of the carboxylate oxygens of Asp139 in the neighboring subunit (Story et al., 1992). However, while substitution of Lys6 with Ala blocks formation of larger RecA filaments, an

Asp139→Ala mutation has no significant effect on the oligomeric properties of RecA. Likewise, the Arg28 side chain in subunit 1 is within interacting distance of the Asn113 side chain in subunit 2. Again, however, while substitution of Arg28 with Ala imposes a significant defect in RecA oligomer formation, the Asn113→Ala mutation shows an oligomeric profile much like wild type RecA. This suggests that the specific cross-subunit contacts made by the Lys6 and Arg28 side chains that are important for oligomer stability of free protein are not apparent in the crystal structure. Another interpretation is that the Lys6↔Asp139 and Arg28↔Asn113 interactions seen in the structure are important for oligomer stability, but in the absence of their normal interacting partners the length of the Lys6 and Arg28 side chains permits them to find alternative cross-subunit positions with which to interact. The crystallographic B-factors are somewhat high for the Lys6 and Arg28 side chains (Lys6 NZ = 52.4; the mean for atoms in the Arg28 guanidinium group = 50.0) suggesting that they are quite mobile and capable of interacting with alternative positions in the neighboring monomer. Our data also show that, despite its proximity, Thr89 is unlikely to act as a cross-subunit partner for either Lys6 or Arg28.

In contrast to the stability of free RecA filaments, mutation of Lys6 or Arg 28 has little effect on the formation and function of RecA-DNA complexes. Using electron microscopy we have confirmed that mutant proteins carrying either a Lys6→Ala or Arg28→Ala substitution fail to form stable oligomers in the absence of DNA, yet form wild type-like nucleoprotein filaments in the presence of ssDNA.

Our results are not necessarily predicted by the degree of conservation of each of these residues across 63 different bacterial RecA sequences (Karlin and Brocchieri, 1996; Roca and Cox, 1997). Despite the fact that mutation of Asp139 has no significant effect on either RecA structure or function, it is very highly conserved, with 61 of 63 sequences having Asp at position 139. The chemical and steric nature of residue 6 is also very highly conserved (48 Lys, 15 Arg). Residues 28 and 113 are somewhat less well conserved with 56 of 63 sequences having Arg or Lys at position 28, and 54 of 63 sequences having either Asn, Asp or Glu at position 113.

Our data for Asp112 are consistent with the interaction between its main chain carbonyl oxygen and the Arg28 guanidinium group as seen in the crystal structure. The structure shows the Asp112 side chain pointing inward and within 3.5 Å of Arg105 in the same monomer. Therefore, the slight oligomeric defects observed for the Asp112→Arg mutation likely derive not from loss of a specific cross-subunit interaction, rather from a general disruption of the interacting surfaces between subunits.

The severity of the effect of individual subunit interface mutations on RecA function is clearly context dependent. Previous studies have shown that certain single mutations within another region of the subunit interface completely inhibit oligomer formation and enzyme function (Nguyen et al., 1993; Skiba and Knight, 1994; Logan et al., 1997). For example, a Lys216→Ala or Arg222→Ala substitution blocks formation of long filaments and inhibits RecA recombination activity (Skiba and Knight, 1994; Logan et al., 1997). In the present study however, mutants carrying either a Lys6→Ala or Arg28→Ala

substitution cannot form larger filaments in the absence of DNA, yet form wild type-like nucleoprotein filaments on ssDNA and show little or no effect on the *in vivo* recombination functions of RecA (Table 2.1). When bound to DNA the interacting surfaces must be able to accommodate either of these defects. In the absence of either a Lys or Arg at positions 6 and 28, respectively, other cross-subunit interactions in this area must provide sufficient oligomeric stability to promote formation of an active nucleoprotein filament. There is, in fact, a much more extensive set of cross-subunit hydrophobic interactions between the surfaces defined by residues 6 - 30 and 111 - 140 than between that defined by residues 213 - 222 and its cross-subunit complementary surface (Story et al., 1992; Skiba and Knight, 1994). Recent studies support the idea that cross-subunit hydrophobic interactions may account for most of the oligomeric stability within this region of the RecA subunit interface (Zaitsev and Kowalczykowski, 1999). At present it is not known what contribution these hydrophobic interactions make to the overall stability of RecA nucleoprotein filaments, but our data show that hydrophobic interactions alone are not sufficient for stabilization of the free protein filament.

Given that the recombinational DNA repair activity of RecA is not significantly affected by mutations at Lys6 or Arg28, are they important to the catalytically active form of the protein? Our data argue that while neither is a critical determinant of the structure or function of the RecA nucleoprotein filament, each does contribute to the overall catalytic efficiency of the protein. The Lys6→Ala mutant protein shows a clear defect in binding to ssDNA and hydrolyzes ATP at approximately 50% the rate of wild type RecA. Nayak & Bryant (1999) have recently demonstrated that the rate of strand exchange catalyzed by

RecA is directly proportional to its rate of NTP hydrolysis. Therefore, the partial inhibition of both ssDNA binding and ATPase activity likely account for the observed

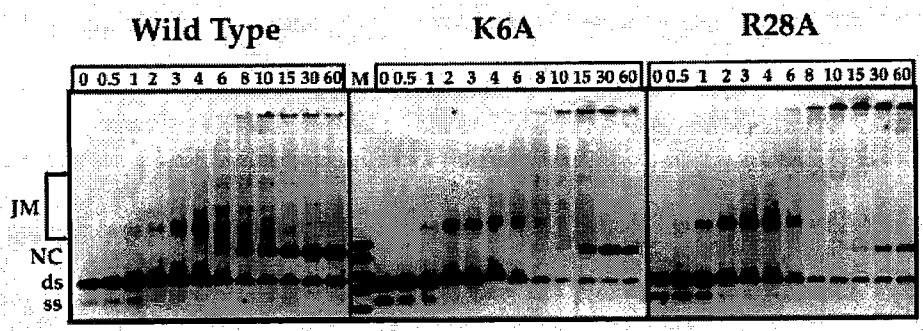


Figure 2.6 - DNA strand exchange catalyzed by wild type, Lys6→Ala and Arg28→Ala RecA proteins. Strand exchange reactions contained 6.7 μM protein, single- and double-stranded ϕX174 DNAs (ss and ds, respectively; 20 μM each), dATP (3 mM) and SSB (2 μM). At the times indicated (min, above each lane) samples were removed and added to stop buffer (see **Materials and Methods**). Samples were electrophoresed on a 0.8% agarose gel in TAE buffer and DNAs were visualized by staining with ethidium bromide. Products of the reaction include joint molecules (JM) and nicked circular heteroduplex DNA (NC).

defect in strand exchange. In contrast, the Arg28→Ala mutant protein shows a slight but significant increase in ssDNA binding affinity over wild type RecA and only a slight decrease in the rate of ATP hydrolysis. However, this mutant also shows a decrease in the rate of DNA strand exchange. Results of the strand exchange assay for this mutant protein are consistent with the idea that a single nucleoprotein filament (RecA + ϕX174 circular ssDNA) mediates multiple initiation events that give rise to larger protein-DNA complexes which move very slowly on agarose gels (see Figure 2.6). This would be expected to inhibit efficient progression of RecA-mediated branch migration of the joint molecule and slow the appearance of nicked circular products. Therefore, while the Lys6 and Arg28 side chains have little effect on the stability of the RecA nucleoprotein filament, they clearly contribute to optimizing the catalytic efficiency of the protein.

Although the X-ray structure differs from the inactive and active filament structures as defined by electron microscopy, several studies have shown that the crystal structure accurately reflects the positions of many residues within the subunit interface as they are likely to exist in the active form of the enzyme (Nguyen et al., 1993; Skiba and Knight, 1994; Yu et al., 1998; Skiba et al., 1999). Particularly relevant to our study of the N-terminal region of RecA is recent work by Zaitsev & Kowalczykowski (1999) in which the authors were able to explain the identity of a specific suppressor mutation within this region of the subunit interface based on its position in the RecA crystal structure. In the present study we have demonstrated that Lys6 and Arg28 are particularly important determinants of the oligomeric stability of free RecA protein. However, our data suggest that the cross-subunit interactions observed in the crystal structure may not show the positions with which they interact in the neighboring subunit. While formation of stable nucleoprotein filaments appears not to be effected by mutation of these residues, functional defects are apparent, demonstrating that the wild type Lys6 and Arg28 serve to optimize the catalytic proficiency of the protein. Given the flexibility of α-helix A, we suggest that this is one of the regions that undergoes significant changes with regard to its interaction with the neighboring subunit when the protein shifts from the inactive (- ATP, - ssDNA) to the active form (+ ATP, + DNA). Further studies have been designed to address how various mutations within the subunit interface regions effect assembly and disassembly of both free RecA protein oligomers as well as RecA nucleoprotein filaments, and how changes in these processes effect RecA function.

Materials and Methods

Materials - Media (LB, Superbroth) was from Bio 101, Inc. and antibiotics were added when appropriate (100 μg/ml ampicillin, 50 μg/ml kanamycin). IPTG was from BioWorld. Mutagenic oligonucleotides, sequencing primers and the 97mer used for gel shift DNA binding assays were made using an ABI 392 DNA/RNA synthesizer. Restriction enzymes, T4 DNA ligase and ΦX174 DNAs were from New England Biolabs. Sequenase version 2.0 was from Amersham. Single-stranded circular RV-1 DNA (a derivative of M13) was prepared as described (Logan and Knight, 1993). ATPγS, ATP, ATP-agarose and a protease inhibitor cocktail (40x contains 8 mM 4-(2-aminoethyl)-benzensulfonyl fluoride, 4 mM EDTA, 0,5 mM bestatin, 5.6 μM E64, 4 μM leupeptin, 0.3 μM aprotonin) were from Sigma. RNase-free DNase was from Promega. R-buffer contains 20 mM Tris-HCl (pH 7.5), 5% glycerol (w/v), 5 mM β-mercapto-ethanol (β-ME) and 0.1 mM EDTA. R-filtration buffer is R-buffer plus 30 mM NH_4Cl and 15 mM $MgCl_2$. P-buffer contains 20 mM KH_2PO_4/K_2HPO_4 (pH 6.8), 5% glycerol, 5 mM β-ME and 0.1 mM EDTA. A-buffer contains 20 mM Tris-HCl (pH 7.5), 20 mM KCl, 10 mM $MgCl_2$ and 0.5 mM EDTA.

Strains and plasmids - Mutant *recA* genes are carried on plasmids derived from pTRecA230, pTRecA420 or pTRecA430 in which *recA* expression is regulated by the *tac* promoter (Logan and Knight, 1993). These plasmids are identical except for the position of unique restriction sites within the *recA* gene. For cassette mutagenesis procedures we used the following restriction sites in the indicated plasmids. Except for the AccI site

(codons V138, D139) which occurs naturally in the *recA* gene, sites were introduced using standard site-directed mutagenesis procedures: *pTRecA230* - NotI (codons A81 - A83); BssHII (codons A104, R105); *pTRecA420* - NcoI (codons -1, fMet and A1); EagI (codons A11 - A13); BglII (codons R33, S34); SalI/AccI (codons V109, D110); AccI (codons V138, D139): *pTRecA430* - AccI (codons V138, D139); SalI/AccI (codons V143, D144). Plasmids were propagated in either of two Δ*recA E. coli* strains, MV1190 (Logan & Knight, 1993) or DE1663′ (Nastri and Knight, 1994).

Mutagenesis - Amino acid substitutions were introduced using modifications of a previously described cassette mutagenesis procedure (Skiba and Knight, 1994) or a PCR-based procedure (QuikChange; Stratagene). For example, three mutations (Ala, Glu or Asp) were introduced at Lys6 using a synthetic oligonucleotide cassette containing a G(A/C)(G/C) sequence at codon 6, the wild type *recA* sequence at all other codons, and NcoI and EagI overhangs at the 5′ and 3′ ends, respectively. Top and bottom strands were each 36 bases long and the duplex cassette was cloned into NcoI/EagI-digested pTRecA420. Amino acid substitutions were identified by DNA sequencing.

Recombinational DNA Repair Activity in Vivo - Recombinational DNA repair activity was characterized by measuring cell survival following exposure to different doses of UV irradiation as previously described (Nastri and Knight, 1994).

Determining the Size of Mutant RecA Protein Oligomers - We have designed a gel filtration assay which displays the oligomeric size of RecA protein in treated cell extracts,

thereby allowing analyses of a fairly large number of mutant proteins without the need to purify each one (Logan et al., 1997). The RecA protein concentration in the extract was determined by comparison with a series of RecA standards on SDS gels which were analyzed using a Fluor-S MultiImager (Bio-Rad). Before loading onto gel filtration columns, the sample volume was adjusted to give a final concentration of 26 μM RecA and DNase was added (30 u for 5 min at room temperature with 10 mM $CaCl_2$). Using a BioLogic Chromatography system (Bio-Rad), samples were loaded onto a Superose 6 HR gel filtration column (Pharmacia/LKB) equilibrated in R-filtration buffer. Columns were maintained at 4°C. Fractions were collected and aliquots electrophoresed on 10% SDS polyacrylamide gels. To determine the percent RecA in each fraction gels were analyzed using a Fluor-S MuiltiImager and Multi-Analyst 1.0.2 software (Bio-Rad). The size of RecA oligomers was estimated by comparison to protein standards: thyroglobulin (650 kDa), ferritin (440 kDa), catalase (232 kDa), BSA (68 kDa) and ovalbumin (44 kDa). The elution volumes of standards are an average of at least 3 runs.

Protein Purification - Wild type RecA protein was purified as described previously (Konola et al., 1995). The Lys6→Ala and Arg28→Ala mutant proteins were purified as follows starting with 10 l of cell culture. All steps through cell lysis and extraction with poly-ethylenimine (PEI) were as for wild type RecA (Konola et al., 1995), and a protease inhibitor cocktail was added according to the manufacturer's recommendations (Sigma). Protein was buffer exchanged into R-buffer containing 50 mM NH_4Cl, loaded onto a DE-52 column (25 ml) and eluted in a 50 - 450 mM NH_4Cl gradient. Fractions containing the mutant RecA protein were pooled, dialyzed in A-buffer, mixed with ATP-agarose resin

(5 ml), washed with 100 ml A-buffer and the mutant RecA protein was eluted specifically in 3 ml of A-buffer plus 1 mM ATP.

Gel shift DNA binding assay – Reactions (30 μl) were performed in A-buffer containing 0.5 mM adenosine 5′-O-(thiotriphosphate) (ATPγS) and were initiated with addition of a 5′-end labeled 97 base oligonucleotide to a final concentration of 10 μM (bases). Incubation was continued at 37 °C for 1 hr followed by addition of glycerol to a final concentration of 12.5%. Samples were loaded onto a 1.2% agarose gel and electrophoresed in TAE buffer. Gels were analyzed using a Molecular Imager FX and QuantityOne software (Bio-Rad).

ATPase Activity - Single-strand DNA dependent hydrolysis of ATP was measured as described (Weinstock et al., 1981; Konola et al., 1995). PEI chromatography plates were analyzed using a Molecular Imager FX and QuantityOne software (Bio-Rad).

DNA strand exchange assay – DNA strand exchange activity was measured as follows. Reactions (120 μl) were performed in buffer containing 25 mM TrisOAc (pH 7.5), 10 mM MgOAc, 1 mM dithiothreitol and 5% (w/v) glycerol. RecA protein (6.7 μM) was incubated with both single- and double-stranded ΦX174 DNAs (20 μM each) in reaction buffer for 10 min at 37 °C. Reactions were started by simultaneous addition of dATP (3 mM) and SSB (2 μM). Aliquots (9 μl) were removed at the indicated times and added to stop solution such that the final concentrations of SDS, glycerol and EDTA were 1% (w/v), 5% (w/v) and 10 mM. Samples were electrophoresed on a 0.8% agarose gel in

TAE buffer and DNAs were visualized by staining with ethidium bromide. Gels were displayed using a FluorS MultiImager (Bio-Rad).

Electron microscopy – Samples were prepared for electron microscopy by incubating wild type or mutant RecA proteins at 2.0 μM in the absence of DNA, or 0.8 μM in the presence of 3.0 μM RV-1 single-stranded circular DNA. All reactions containing DNA included *E. coli* single-stranded DNA binding protein (0.03 μM) and were pre-incubated at 37 °C for 5 min. Reaction buffer included 25 mM triethanolamine-HCl (pH 7.5), 50 mM KCl, 5 mM $MgCl_2$ and 1 mM ATPγS. Upon addition of RecA reactions were incubated for 15 min at 37 °C. Reactions were spread onto thin carbon films on holey carbon grids (400 mesh) and stained with 1% uranyl acetate. Samples were visualized using either a Philips CM10 or a Philips EM400 electron microscope.

PREFACE FOR CHAPTER III

The work in Chapter III provides evidence for an ATP induced conformational change at the subunit interface within the RecA protein filament, specifically in the an area defined by the N-terminal region of one subunit (residues 6 – 30) and the complementary interacting surface on the neighboring, residues 111 – 140 (the same region investigated using alanine mutations in Chapter II).

Through the use of pair-wise designed cysteine mutations we show here that the efficiency of cross-subunit disulfide bond formation at certain positions in the interface changes in the presence of ATP or ATP/DNA. These results further support the previous findings that specific cross-subunit interactions at the subunit interface are different in RecA/ATP/DNA nucleoprotein filaments *vs.* free RecA protein filaments.

This work was the result of combined efforts of Karen Logan and John Paul Verderese. I contributed specifically to the overall design of the experiments, data analysis, the construction and purification of some of the mutant proteins, all of the electron microscopy and final compilation and editing of the manuscript.

The data presented in this chapter was published in the journal **Biochemistry**, Volume 40, (September 2001).

CHAPTER III

ATP-MEDIATED CHANGES IN CROSS-SUBUNIT INTERACTIONS IN THE RECA PROTEIN

Abstract

RecA protein undergoes ATP- and DNA-induced conformational changes that result in different helical parameters for RecA/ATP/DNA nucleoprotein filaments *vs.* free protein filaments. Previous mutational studies of a particular region of the RecA oligomeric interface suggested that cross-subunit contacts made by residues K6 and R28 were more important for stabilization of free protein oligomers than nucleoprotein filaments (Eldin et al., 2000). Using mutant proteins with specifically engineered Cys substitutions we show here that the efficiency of cross-subunit disulfide bond formation at certain positions in this region changes in the presence of ATP or ATP/DNA. Our results support the idea that specific cross-subunit interactions that occur within this region of the subunit interface are different in RecA/ATP/DNA nucleoprotein filaments *vs.* free RecA protein filaments.

Introduction

The bacterial RecA protein mediates genetic recombination by catalyzing strand exchange between DNAs of related sequence. In the presence of ATP, RecA binds to ssDNA with high affinity and it is this RecA/ATP/ssDNA nucleoprotein filament that is the catalytically active form of the protein (Radding, 1989; Eggleston and West, 1996; Roca and Cox, 1997; Bianco et al., 1998). Recent studies have shown that ATP promotes

high affinity ssDNA binding by increasing the cooperative association of subunits rather than by increasing the inherent affinity of monomeric RecA for ssDNA (De Zutter and Knight, 1999). Therefore, our studies of the oligomeric properties of RecA have involved the identification and characterization of residues within different regions of the interface that play important roles in the transmission of ATP-mediated allosteric information as well as in the stabilization of the oligomeric structure of the protein filament.

The present study focuses on an area of the interface defined by the N-terminal region of RecA in one subunit (residues 6 – 30) and the complementary interacting surface on the neighboring subunit defined by residues 111 – 140 (Figure 3.1) (Story et al., 1992). Early genetic studies using peptides consisting of the N-terminal 77 residues (Yarranton and Sedgwick, 1982) or the N-terminal 50 residues (Kiselev et al., 1988) suggested that these formed mixed oligomers with wild type RecA thereby inhibiting its activity. Subsequent biochemical studies demonstrated the importance of the N-terminal 33 residues for RecA self-assembly (Mikawa et al., 1995) and also supported the idea that folding of the N-terminal α-helix (residues 3 – 21) is coupled to RecA self-assembly (Masui et al., 1997). Although cross-subunit interactions in this region of the interface are largely hydrophobic, the RecA crystal structure shows the following cross-subunit ionic and polar interactions as well: K6↔D139, R28↔D112 and R28↔N113. Unexpectedly, we have found that mutations at K6 and R28 impose severe defects on the oligomeric stability of free RecA protein, whereas mutations at D112, N113 and D139 do not (Eldin et al., 2000). However, K6 and R28 mutant proteins showed an apparent

normal formation of nucleoprotein filaments and had nearly wild type-like catalytic abilities. These results suggested that cross-subunit contacts made by K6 and R28 with positions in the neighboring subunit are different in the active *vs.* inactive form of the protein.

In this study we have created a series of mutant RecA proteins with pair-wise Cys substitutions at positions 6/139, 28/112 and 28/113 to test the efficiency of disulfide bond formation under various conditions. Our data provide a direct demonstration of ATP-induced changes in cross-subunit interactions made between residues in this region of the subunit interface.

Results

Design of Cys Mutations. The RecA crystal structure (Story et al., 1992) shows that the

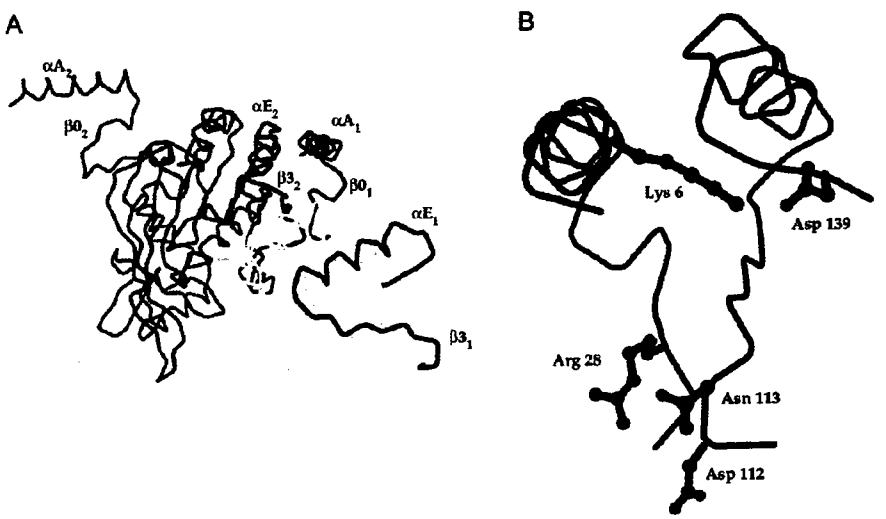


Figure 3.1 - Details of the oligomeric interactions in RecA. (A) An α-carbon trace of a RecA dimer taken from the crystal structure of the helical RecA protein filament (Story et al, 1992). Subunit 1 is on the right (yellow α-carbon backbone) and subunit 2 is on the left (aqua α-carbon backbone). Highlighted areas include αA/β0 (green) and β3/αE (violet). Complementary interacting surfaces ($\alpha A_1/\beta 0_1$ with $\beta 3_2/\alpha E_2$) are in the center of the image. (B) Cross-subunit proximity of K6 (subunit 1)/D139 (subunit 2), and R28 (subunit 1)/D112/N113 (subunit 2). This image has been rotated 180° around the Y-axis relative to the image in (A).

N-terminal region of the protein, defined by α-helix A and β-strand 0 (residues 6 – 30), interacts with a region of the neighboring subunit defined by β-strand 3 and α-helix E (residues 111 – 140; Figure 3.1). The majority of the interactions between these two complementary surfaces are hydrophobic. Seven non-polar side chains in subunit 1 are within van der Waals distance of eight non-polar side chains in subunit 2. However, the structure shows that this large hydrophobic cluster is flanked by polar and ionic cross-subunit contacts. The ε-NH_3 group of Lys6 is 2.9 Å from one of the carboxylate oxygens of Asp139 in the neighboring subunit (Figure 3.1B). Also, one of the nitrogens in the guanidinium group of Arg28 (Nε) is 3.5 Å from the carbonyl oxygen of the Asn113 side chain (Figure 3.1B), and two of the nitrogens (Nε and Nη1) are within 3.0 Å of the main chain carbonyl oxygen of Asp112. Double mutants were made with Cys at positions 6/139, 28/112 and 28/113. Single Cys mutants were also created at positions 6, 28, 112, 113 and 139. All mutant proteins could be overproduced and purified.

Table 3.1: $C\beta_1$-$C\beta_2$ cross-subunit distances between indicated residues.

cross-subunit pair	$C\beta_1$-$C\beta_2$ distance (Å)
Lys6↔Asp139	9.6
Arg28↔Asp112	6.8
Arg28↔Asn113	6.3
Phe217↔Thr150	6.6

In vivo Function of Mutant RecA Proteins. As shown in Table 3.2 all single and double Cys mutants maintain a high level of recombinational DNA repair function as measured by survival in the presence of mitomycin C or following exposure to UV irradiation. All proteins maintain ≥ 75% of wild type recombination activity. All mutants also retained substantial levels of either inducible or constitutively activated coprotease function.

These results demonstrate that each of the engineered Cys substitutions do not significantly impair RecA function.

Table 3.2: In vivo DNA repair and Coprotease Activities

Cys mutant	fractional UV survival/30 s	survival in the presence of MMC (0.3/0.6 $\mu g \cdot ml^{-1}$)	coprotease[a]
wild type	1.00	1.00/1.00	i
6	0.75	1.00/0.75	i
28	1.00	1.00/1.00	c
112	1.00	1.00/1.00	i
113	1.00	1.00/1.00	i
139	1.00	1.00/0.85	i
6/139	0.75	0.75/0.75	i
28/112	1.00	1.00/0.75	c
28/113	1.00	1.00/0.75	c

[a] i indicates "inducible" activity in the presence of DNA damage. c indicates "constitutive" activity in the absence of DNA damage. All assays were repeated a minimum of 4 times and the range of standard errors is 5 – 15%.

Function of Mutant RecA Nucleoprotein Filaments. We tested the ability of each mutant protein to form catalytically active nucleoprotein filaments *in vitro* by assaying for DNA binding and ATPase activity. The gels in Figure 3.2 show that each protein maintains the ability to bind ssDNA although for the K6C/D139C mutant protein there is a substantial decrease in affinity. From plots of ssDNA bound *vs.* RecA concentration

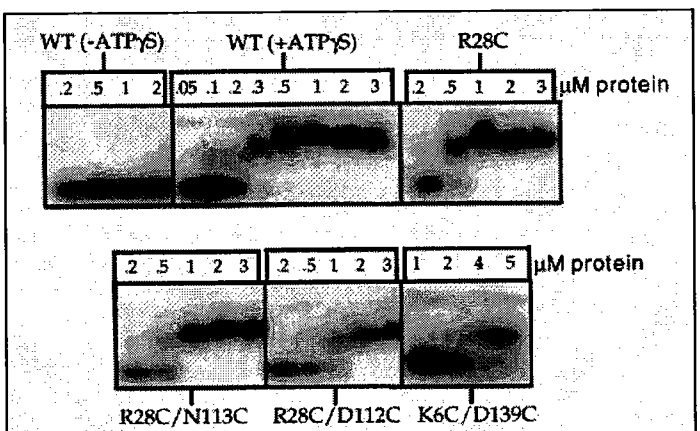


Figure 3.2 - Gel shift DNA binding assays. Indicated concentrations proteins were incubated with a 5′-end-labeled 97 base oligonucleotide and samples were electrophoresed on a 1.2% agarose gel. Reactions with wild type RecA were done in the absence or presence of 0.5 mM ATPγS. Reactions with mutant proteins all contained 0.5 mM ATPγS.

(not shown) we estimate a $K_{D\ app}$ of 0.2 μM for wild type and 0.4 μM for the R28C single mutant (Table 3.3). Values of $K_{D\ app}$ for the double mutants R28C/N113C, R28C/D112C and K6C/D139C were estimated to be 0.5 μM, 1.2 μM and 3.0 μM, respectively (Table 3.3). As for wild type RecA, binding to ssDNA by all mutant proteins is dependent on the presence of ATP (or ATPγS).

Table 3.3: DNA binding and ATPase Activities

Cys mutant	ssDNA binding $K_{D\ app}$ (μM)[a]	V_i/E (mol ADP•min^{-1}•mol RecA^{-1})
wild type	0.2	22.5
28	0.4	23.0
28/113	0.5	12.5
28/112	1.2	3.2
6/139	3.0	1.3

[a] $K_{D\ app}$ was determined from plots of DNA bound *vs.* protein concentration and represents the protein concentration at which 50% of substrate DNA is bound. DNA binding and ATPase assays were repeated 3 times and the standard errors approximated 20%.

Turnover numbers for the ssDNA-dependent ATPase activity were calculated for each protein (Table 3.3). For wild type RecA and the R28C single mutant $V_i/E \approx 23.0$ mol ADP•min^{-1}•mol RecA^{-1}, whereas the double Cys mutant proteins showed varying degrees of inhibition with the K6C/D139C protein showing almost an 18 – fold decrease in ATPase catalytic proficiency (Table 3.3).

Analyses of Oligomeric Properties. The oligomeric structure of the double Cys mutant proteins in both the presence and absence of ATP and ssDNA was analyzed by electron microscopy. In Figure 3.3 (panels A – D) we show negative stained electron micrographs of wild type RecA and the 3 double Cys mutants in the presence of ATPγS. As seen previously (Di Capua et al., 1982; Egelman and Stasiak, 1988; Brenner et al., 1988; Heuser and Griffith, 1989), wild type RecA forms a heterogeneous population of oligomeric structures including helical filaments that range in length from 0.03 - 0.15 μm. For the double Cys mutant proteins no filaments are observed indicating that each

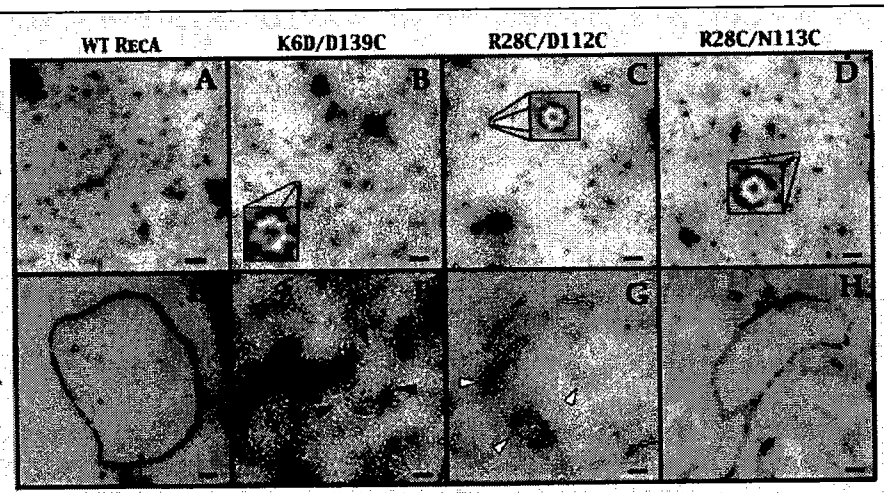


Figure 3.3 - Negative stained electron micrographs of protein and protein-ssDNA complexes. Wild type RecA and the three double Cys mutant proteins were incubated in the presence of 1.0 mM ATPγS and absence of ssDNA (A-D) or in the presence of 1.0 mM ATPγS and 3.0 μM phage circular ssDNA (E-H). Protein concentration in the absence of ssDNA (A-D) was 2.0 μM. Protein concentration in the presence of ssDNA for wild type, R28C/D112C and R28C/N113C was 0.8 μM, while the concentration of K6C/D139C was 4.0 μM. White arrows in panel G indicate regions of ssDNA not bound by protein. Black arrows in panel F indicate the single nucleoprotein filament observed in this field. Black bar in each panel equals 0.1 μm.

pair of Cys substitutions destabilizes subunit interactions that are important for extended polymerization in the absence of ssDNA. Although not shown in Figure 3.3, occasional longer filaments (≈ 1.0 μm in length) were observed for the R28C/N113C protein in the presence of ATPγS, although these represented an extremely small percent of the total

protein. These results are consistent with previous studies in which we showed that either a K6A or R28A substitution inhibited the stability of free protein filaments (Eldin et al., 2000). Interestingly, all 3 double Cys mutant proteins form a significant amount of 7-membered ring shaped oligomers (Figure 3.3, inserts in panels B, C and D).

In the presence of ssDNA and ATPγS each double Cys mutant protein forms a nucleoprotein filament (Figure 3.3F, G and H), but the two that are most compromised in their DNA binding affinity (K6C/D139C, R28C/D112C) show distinct differences compared to wild type RecA. As expected under the conditions used (0.8 μM protein, 3.0 μM bases of ssDNA), very little wild type RecA remains in a free state and all DNA molecules with bound protein are fully covered, indicating cooperative filament formation by RecA on the ssDNA substrate (Figure 3.3E). The R28C/N113C mutant (Figure 3.3H) forms nucleoprotein filaments that look similar to those formed by wild type RecA. The R28C/D112C mutant (Figure 3.3G) shows a defect in cooperative filament assembly on ssDNA as most of the DNA molecules with bound protein are only partially covered. Arrows in Figure 3.3G indicate regions of ssDNA not bound by protein. The K6C/D139C mutant has the lowest affinity for ssDNA (see above and Figure 3.2) and even at elevated protein concentrations (4.0 μM in Figure 3.3F) a significant percentage of the protein is not bound to ssDNA. Similar to the R28C/N112C mutant, the K6C/D139C nucleoprotein filaments that do form show regions of ssDNA not bound by protein. The helical pitch of nucleoprotein filaments formed by the mutant proteins is similar to that formed by wild type RecA (≈ 90–95 Å). Together, the functional and structural analyses show that despite defects in DNA binding affinity and

cooperative filament assembly on ssDNA, cross-subunit disulfide formation between the engineered Cys residues in the mutant proteins should accurately reflect the position of these side chains in the catalytically active form of the RecA filament.

The oligomeric properties of the mutant proteins were also analyzed by gel filtration under conditions that closely matched those used in the disulfide cross-linking experiments, i.e. at protein concentrations ≈ 30 μM. The Superose 6 profile in Figure

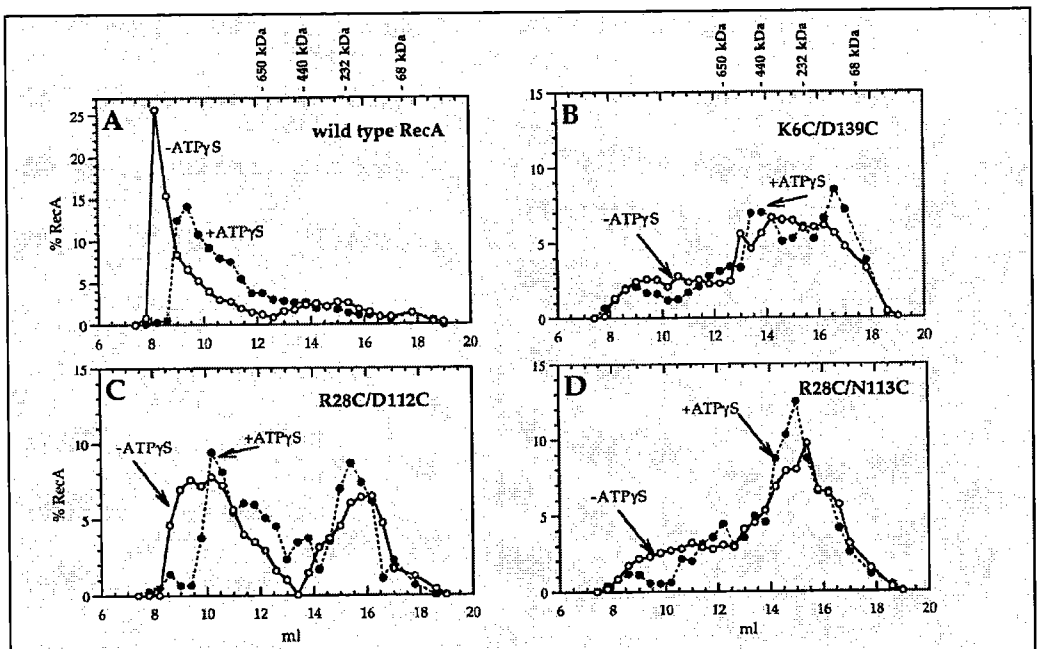


Figure 3.4 - Gel filtration profiles of wild type RecA and the three double Cys mutant proteins. Superose 6 gel filtration profiles reveal that the engineered Cys mutations inhibit formation larger oligomeric species. Larger oligomers observed with wild type RecA (A) and the R28C/D112C protein (C) undergo an ATP-induced shift to smaller sizes, whereas the oligomeric distribution of K6C/D139C (B) and R28C/N113C (D) is largely unaffected by the presence of ATP. Size markers are thyroglobulin (650 kDa), ferritin (440 kDa), catalase (232 kDa) and BSA (68 kDa).

3.4A shows that wild type RecA forms a heterogeneous mix of oligomers ranging from ≥5 x 10^6 Da to 68 kDa. In the presence of ATPγS the oligomeric population undergoes a general shift to smaller sizes, a result that is consistent with previous studies using electron microscopy, light scattering and gel filtration (Brenner et al., 1988; Heuser and

Griffith, 1989; Wilson and Benight, 1990; Ruigrok and DiCapua, 1991). In contrast, each of the mutant proteins shows a profile suggesting that the Cys mutations limit stable filament formation in either the absence or presence of ATPγS. The R28C/D112C protein retains some ability to form larger oligomers, and these shift to a smaller size in the presence of ATPγS. However, in this assay ATPγS does not show a significant effect on the oligomeric distribution of the K6C/D139C and R28C/N113C proteins.

Formation of Cross-subunit Disulfide Bonds. Formation of cross-subunit disulfides was determined for each of the double Cys mutant proteins under 3 different conditions, in the absence of ATPγS and ssDNA, in the presence of ATPγS alone, and in the presence of both ATPγS and ssDNA. We found that the efficiency of disulfide formation was not affected by addition of oxidizing reagents, therefore all disulfides observed in this study result from spontaneous cross-linking due to the proximity of the interacting Cys residues.

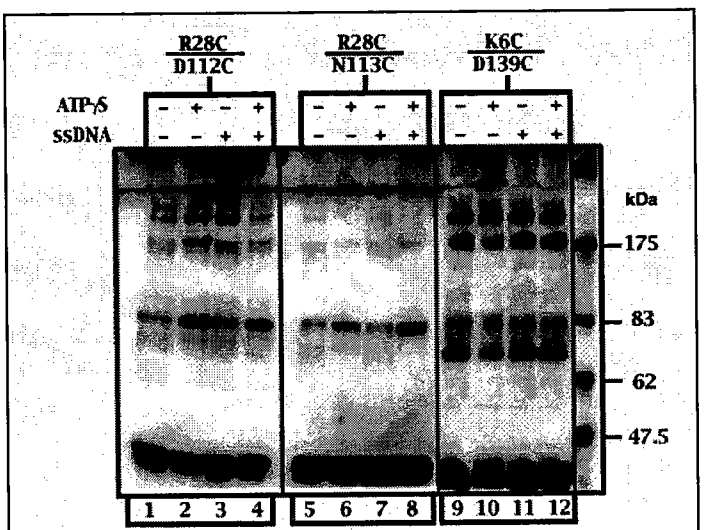


Figure 3.5 - Disulfide cross-linking performed using the engineered double Cys mutant proteins. Proteins (30 μM) were incubated at 37 °C for 60 min in the absence or presence of ATPγS and ssDNA as indicated, and processed as described in **EXPERIMENTAL PROCEDURES**. Monomeric RecA (38 kDa) runs near the bottom of the gel while slower mobility bands represent disulfide cross-linked dimers, trimers, etc. The efficiency of disulfide formation increases in the R28C/D112C and R28C/N113C proteins in the presence of either ATPγS or ATPγS/ssDNA.

Cross-linking reactions were performed using the 3 double Cys mutant proteins (R28C/D112C, R28C/N113C and K6C/D139C) and the resulting SDS-polyacrylamide gel run under non-reducing conditions is displayed in Figure 3.5. Monomeric RecA runs just beneath the 47.5 kDa marker, and disulfide formation between the engineered Cys substitutions results in a series of slower mobility bands. Judging by the staining intensity, the cysteines at positions 6 and 139 form a disulfide bond with greater efficiency than those at positions 28/112 or 28/113. This result was observed consistently during the course of this work. This is an unexpected result given that the $C\beta_1$-$C\beta_2$ distance between residues 6 and 139 is 9.6 Å, whereas those between residues 28/112 and 28/113 are 6.8 Å and 6.3 Å, respectively (Table 3.1; see **DISCUSSION**). Most interestingly, we find that both the R28C/D112C and R28C/N113C mutants show an increase in disulfide formation when cross-linking is done in the presence of ATPγS or ATPγS/ssDNA. ATPγS or ATPγS/ssDNA have no effect on the efficiency of disulfide formation in the K6C/D139C mutant. These data suggest that binding of ATPγS by RecA results in a conformational change that brings residues 28 and 112, as well as 28 and 113, into closer proximity, but does not significantly affect the proximity of residues 6 and 139 (see **DISCUSSION**).

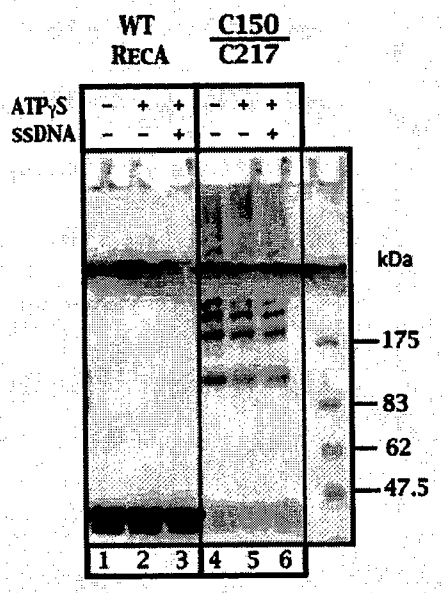


Figure 3.6 - Disulfide cross-linking performed using wild type RecA and the T150C/F217C mutant protein. Proteins (30 μM) were incubated at 37 °C for 60 min in the absence or presence of ATPγS and ssDNA as indicated, and processed as described in **EXPERIMENTAL PROCEDURES**. The three Cys residues in wild type RecA do not show any disulfide formation that results in subunit cross-linking while the T150C/F217C mutant protein shows very efficient formation of cross-subunit disulfides that is not affected by the presence of either ATPγS or ATPγS/ssDNA.

In previous work we performed similar disulfide cross-linking between a F217C substitution and several engineered Cys mutations in the neighboring subunit (Skiba et al., 1999). One double Cys mutant that was particularly efficient at disulfide formation was the F217C/T150C mutant. The gel in Figure 3.6 (lanes 4 – 6) shows that this mutant gives rise to a ladder of bands that extends well up into the gel well. During the time of cross-linking nearly all monomeric RecA is converted to higher molecular weight forms. The fact that the efficiency of disulfide formation does not correlate with the $C\beta_1$-$C\beta_2$ distances between residues 28/112, 28/113 and 217/150 (6.8Å, 6.3Å and 6.6Å, respectively; Table 3.1) suggests that cross-subunit distances seen in the RecA crystal structure may not accurately reflect those in the solution form of the RecA filament (see **DISCUSSION**).

In a control experiment we show that none of the three native Cys residues in wild type RecA formed disulfides that would interfere with our analyses of the cross-linking efficiency of the engineered Cys mutations (Figure 3.6, lanes 1 - 3). The X-ray structure of RecA also shows that none of the three native cysteine side chains are close enough to form a disulfide with cysteines introduced at positions 6, 28, 112, 113 or 139 (not shown). Therefore, although previous work has shown that none of the native Cys residues is critical for RecA function (Weisemann and Weinstock, 1988) we chose not to mutate these in order to avoid any further compromise to the structural and functional integrity of the designed mutant proteins in this study.

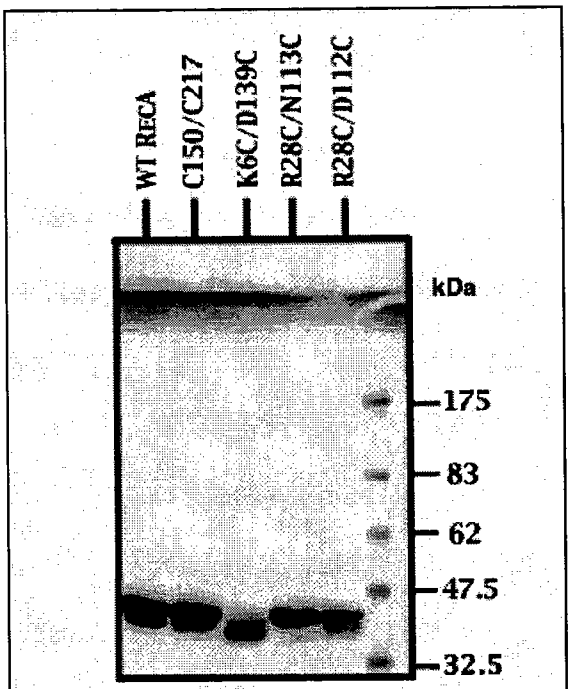


Figure 3.7 - Disulfide cross-linking followed by incubation with βME. Disulfide cross-linking experiments were performed as described (**EXPERIMENTAL PROCEDURES**) followed by incubation with βME (150 mM). All proteins migrate at the position of monomeric RecA and show no slower mobility bands.

Additional controls included cross-linking reactions with each protein followed by incubation with excess βME. Samples were run on an SDS gel under reducing conditions and the results in Figure 3.7 show that all proteins migrate as a single band at the position of monomeric RecA. This demonstrates that the slower mobility bands in

Figures 3.5 and 3.6 result exclusively from formation of cross-subunit disulfides between the engineered Cys residues in the mutant proteins.

Discussion

In this study we provide direct biochemical evidence for an ATP-induced movement of specific side chains within the subunit interface of the RecA protein. In the RecA crystal structure Arg28 is close to both Asp112 and Asn113 in the neighboring subunit (Figure 3.1). Formation of a specific cross-subunit disulfide bond results when pair-wise Cys substitutions are introduced at positions 28 and 112, or positions 28 and 113, and in both cases the efficiency of disulfide formation is increased in the presence of ATPγS or ATPγS/ssDNA. We performed a series of assays to assess the effects of the designed Cys mutations on both the functional and structural properties of RecA, and based on these we conclude that the observed changes in disulfide formation reflect a genuine ATP-induced reorientation of these positions in the wild type protein. First, *in vivo* analyses of recombination proficiency show that all single and double Cys mutants maintain at least 75% of wild type RecA function (Table 3.2). Second, the 3 double Cys mutant proteins maintain both an ATP-dependent ssDNA binding activity as well as a DNA-dependent ATPase activity, although the K6C/D139C mutant shows a significant decrease in both functions (Table 3.3). Third, electron microscopic analyses reveal that each of the 3 double Cys mutant proteins forms a nucleoprotein filament with dimensions, e.g. diameter and pitch, virtually identical to wild type RecA, despite the fact that the R28C/D112C and K6C/D139C proteins show a defect in cooperative filament assembly on ssDNA. The fact that the K6C/D139C protein does show some level of *in*

vivo and *in vitro* function eliminates the possibility that no ATP-induced change in disulfide cross-linking is seen simply because the protein does not bind ATP.

The helical filaments formed by RecA in either the absence or presence of ATP and DNA have distinct structural parameters. This has been most clearly demonstrated by electron microscopy (Egelman and Stasiak, 1993; Egelman and , 1993), and additionally with the use of hydrodynamic and biochemical methods (Wilson and Benight, 1990; Kobayashi et al., 1987). EM reconstructions reveal that filaments formed in the absence of any cofactor (the "inactive" form) have ≈ 6.1 subunits per helical turn and a pitch of 76 Å, while filaments formed in the presence of ATPγS (or ADP-AlF_4) and DNA (the "active" form) have ≈ 6.2 subunits per helical turn and a pitch of 95 Å (Egelman and Stasiak, 1993). In the RecA crystal structure the protein filament has 6.0 subunits per turn and a pitch of 82.7 Å in the absence of cofactors (Story et al., 1992) and 83.1 Å in the presence of ADP (Story and Steitz, 1992). Therefore, there must be some differences in the arrangement of amino acid side chains at the subunit interface when comparing the crystal structure with EM reconstructions of the active filament form. Ideally, for these Cys crosslinking studies we would like to compare the efficiency of disulfide formation in the inactive *vs.* active form of the filament. In fact, in our earlier work mutant proteins carrying a F217C substitution and another Cys substitution on the surface of the neighboring subunit were able to form both catalytically active nucleoprotein filaments as well as inactive filaments in the absence of ATPγS and DNA (Skiba et al., 1999). In the present study, each of the double Cys mutants can form a catalytically active nucleoprotein filament yet formation of filaments in the absence of ATPγS and DNA is

limited, even at protein concentrations used in the cross-linking reactions (≈ 30 mM). At this higher protein concentration the oligomeric distribution of the R28C/D112C protein is shifted to smaller sizes upon incubation with ATPγS, and this may contribute in part to the observed ATP-induced changes in the efficiency of disulfide formation. However, ATPγS does not significantly affect the oligomeric distribution of the R28C/N113C protein and the observed increase in disulfide formation with this protein is most simply explained by an ATP-induced conformational change occurring within each RecA subunit that adjusts the cross-subunit proximity of residues 28 and 113. Given the heterogeneity of the oligomeric population for all three mutant proteins in the absence of ATP and DNA at the concentrations used in the cross-linking experiments (Figure 3.4), we are not strictly comparing the efficiency of disulfide formation between the inactive *vs.* active filament forms of each protein. However, our data does indicate that conformational changes at the subunit interface induced by binding of ATPγS and ATPγS/ssDNA can be monitored by changes in the efficiency of disulfide formation between the engineered Cys residues.

The acceptable limits for $C\beta_1$ - $C\beta_2$ distances in disulfide bonds is 2.9 – 4.6 Å as determined by measurements of disulfides in protein structures and by modeling (Hazes and Dijkstra, 1988; Sowdhamini et al., 1989). Although the $C\beta_1$ - $C\beta_2$ distance for each pair of residues in this study (6.3 – 9.6 Å) is greater than 4.6 Å, clearly the Cys substitutions introduced at positions 6/139, 28/112 and 28/113 are close enough to result in some degree of disulfide formation. Interestingly, the $C\beta_1$ - $C\beta_2$ distances and the orientation of the side chains for these three pairs in the crystal structure would predict

the following order for the efficiency of disulfide cross-linking: 28/113 > 28/112 > 6/139. In fact, exactly the opposite is observed. The K6C/D139C protein shows the greatest amount of disulfide formation despite the fact that the $C\beta_1$ - $C\beta_2$ distance of 9.6 Å is ≈ 3 Å greater than the other pairs. However, given the flexibility of the extreme N-terminal region of RecA (crystallographic B-factors for all atoms at positions 3 – 7 are ≥ 52.4 $Å^2$), Cys substitutions at residues 6 and 139 likely spend more time within bonding distance than is indicated by the $C\beta_1$ - $C\beta_2$ distance in the structure. The $C\beta_1$ - $C\beta_2$ distance for the 28/112 pair is 0.5 Å greater than 28/113 and the crystal structure shows that the N113 side chain is directed toward the subunit interface and R28, while D112 is directed more inward toward its own subunit (Figure 3.1). However, the 28/112 pair consistently cross-links with greater efficiency than the 28/113 pair. Additionally, the F217C/T150C mutant protein forms an intersubunit disulfide very efficiently (Figure 3.6) (Skiba et al., 1999), yet has a $C\beta_1$ - $C\beta_2$ distance intermediate between the 28/112 and 28/113 pairs (Table 3.1). Therefore, the $C\beta_1$ - $C\beta_2$ distances derived from the crystal structure do not necessarily correspond to the observed efficiency of disulfide formation. While we certainly recognize that the oligomeric defects resulting from the paired Cys mutations at positions 6/139, 28/112 and 28/113 may play a role in the unexpected "reverse" order of cross-linking (see Figures 3.3 and 3.4), the results also suggest that the crystal structure may not accurately display the relative distances between these side chains as they occur in the solution structure of the protein.

The "head-to-tail" polymeric arrangement of the RecA protein filament creates a rather complex mixture of surfaces that make up the subunit interface. In our studies of

different regions of the interface we have attempted to identify two general classes of cross-subunit interactions, those that are important for stabilization of the protein oligomeric structure and those that are involved in the transmission of allosteric information across the interface. Of course, these two classes are not necessarily mutually exclusive. Recently, we have demonstrated that Phe217, which lies in another area of the subunit interface, plays a direct role in transmitting ATP-induced allosteric information throughout the RecA filament (Kelley De Zutter et al., 2001). Analysis of the oligomeric properties of various mutant proteins with substitutions at position 217 suggest that this residue is less important for the overall stabilization of the RecA filament, rather its primary role is in allosteric information transfer (Logan et al., 1997; Kelley De Zutter et al., 2001). However, other residues in this same area do play important roles in stabilizing the oligomeric structure of the protein (Logan et al., 1997). The region of the subunit interface that is the focus of the present study appears to be involved exclusively in stabilizing the filament structure of RecA and is unlikely to play any direct role in the transmission of allosteric information. Several pieces of evidence support this idea. Mutant proteins carrying a F217C substitution paired with various other Cys mutations on the surface of the neighboring subunit form disulfide cross-links but show no ATP-induced change in the efficiency of disulfide formation (Skiba et al., 1999). In contrast, ATP does change the efficiency of disulfide formation between pairs of Cys substitutions at positions 28/112 and 28/113. Additionally, a conservative F217Y mutation increases ATP-mediated cooperative filament assembly > 250-fold (Kelley De Zutter et al., 2001). Together these data are consistent with the idea that it is Phe217 that mediates ATP-induced shifts in the positions of residues at the subunit interface and that

residues 28, 112 and 113 are not involved in this signaling process. This idea is also supported by results from Zaitsev and Kowalczykowski (Zaitsev and Kowalczykowski, 1999) in which they showed that the *recA*⁻ phenotype of a *recA*Δ9 mutant (a truncation that removes the first 9 residues) is suppressed by a second site mutation that apparently increases the stability of cross-subunit interactions in this area of the interface. Therefore, in the wild type protein any cross-subunit interactions mediated by residues 1 – 9 and their partners on the neighboring surface, e.g. Lys6↔Asp139, cannot play important roles in a mechanistic process involving allosteric information transfer.

Further studies are aimed at clarifying molecular interactions within various areas of the RecA subunit interface and how they contribute to stable assembly of RecA filaments and optimization of catalytic function.

Materials and Methods

Plasmids and Proteins. Wild type and all mutant *recA* genes are carried on plasmids in which *recA* expression is regulated by the *tac* promoter (Logan and Knight, 1993). Screens for *in vivo* function were carried out in either of two Δ*recA E. coli* strains, MV1190 (Logan and Knight, 1993) or DE1663′ (Nastri and Knight, 1994). ϕX174 circular ssDNA was purchased from New England Biolabs, and RV-1 circular ssDNA was made as previously described (Levinson et al., 1984). RecA proteins were purified using variations of a previously described procedure (Konola et al., 1995). All buffers used in purification of mutant proteins contained 20 mM βME to prevent spontaneous disulfide bond formation. Purification protocols were slightly different for each mutant

protein and involved the use of one or more of the following chromatographic steps: ATP-agarose, heparin agarose, ceramic hydroxyapatite, Superose 6 gel filtration or Sephacryl S-1000 gel filtration.

Mutagenesis. Amino acid substitutions were introduced using modifications of a previously described cassette mutagenesis procedure (Skiba and Knight, 1994) or a PCR-based method (QuikChange; Stratagene).

In vivo activities of recA mutants. Assays for recombinational DNA repair involved measurements of cell survival following exposure to UV light or mitomycin C and were performed as previously described (Nastri and Knight, 1994). Cell growth across a series of time zones of exposure was ranked from zero to 4, and fractional survival at 30 s was calculated from the slope of a line resulting from a plot of relative growth *vs.* time. RecA-mediated cleavage of the LexA protein was measured using MacConkey-lactose plates as previously described (Nastri and Knight, 1994).

Determination of the oligomeric properties of mutant RecA proteins. The effect of mutations on the oligomeric properties of RecA was determined by analyzing the elution profile of each protein on a Superose 6 HR gel filtration column as previously described (Logan et al., 1997). Column buffers contained 20 mM βME. The concentration of RecA protein in the column load was always ≥ 26 μM.

Electron microscopy. Samples were prepared for electron microscopy by incubating wild type or mutant RecA proteins at the indicated concentrations in the absence or presence 3.0 μM single-stranded circular DNA (ϕX174 or RV-1). All reactions containing DNA included *E. coli* single-stranded DNA binding protein (0.03 μM) and were pre-incubated at 37 °C for 5 min. Reaction buffer included 25 mM triethanolamine-HCl (pH 7.5), 50 mM KCl, 5 mM $MgCl_2$, 1 mM ATPγS and 5 mM βME. Upon addition of RecA reactions were incubated for 15 min at 37 °C. Reactions were spread onto thin carbon films on holey carbon grids (400 mesh) and stained with 1% uranyl acetate. Samples were visualized using a Philips CM10 electron microscope.

Gel shift DNA binding assay – Reactions (30 µl) were performed in a buffer containing 20 mM Tris-HCl (pH 7.5), 20 mM KCl, 10 mM $MgCl_2$, 0.5 mM EDTA, 0.5 mM ATPγS and 5 mM βME. Reactions were initiated with addition of a 5′-end labeled 97 base oligonucleotide to a final concentration of 10 µM (bases). Incubation was continued at 37 °C for 1 hr followed by addition of glycerol to a final concentration of 12.5%. Samples were loaded onto a 1.2% agarose gel and electrophoresed in TAE buffer at 4 V/cm. Gels were analyzed using a Personal Molecular Imager FX and QuantityOne software (Bio-Rad).

ATPase Activity - Single-strand DNA dependent hydrolysis of ATP was measured as described (Konola et al., 1995; Weinstock et al., 1981). Reaction buffer contained 2 mM DTT. PEI chromatography plates were analyzed using a Personal Molecular Imager FX and QuantityOne software (Bio-Rad).

Intersubunit Disulfide Crosslinks. Formation and analysis of intersubunit disulfide crosslinks was performed as follows. Protein (50 μg) was pre-reduced in the presence of 20 mM βME (20 min, 22 °C) and desalted into reaction buffer (100 mM Tris-HCl, pH 8.5/0.1 mM EDTA/30 mM NaCl/15 mM $MgCl_2$/5% glycerol) using a Microcon concentrator (Amicon). Disulfide crosslinks formed spontaneously by incubating protein (30 μM final concentration) 60 min at 37 °C in the presence or absence of ATPγS and/or ssDNA. NEM was added to a final concentration of 30 mM, followed immediately by addition of SDS to a final concentration of 1.0%. Previously, we showed that addition of NEM at this step is important for preventing formation of random disulfides when SDS is added (Skiba et al., 1999). The reaction containing NEM was incubated for 10 min at 22 °C, Laemmli loading dye (-βME) was added and samples were electrophoresed on 8% SDS-polyacrylamide gels. Control experiments to ensure that all higher molecular weight bands observed on gels contained reducible disulfides were performed by incubating reactions with βME (150 mM final concentration) following crosslinking. Gels were stained with Coomassie blue (R250), or Western blots were performed using polyclonal rabbit anti-RecA antibodies as previously described (Logan and Knight, 1993). Gels and blots were analyzed using a FluorS MultiImager (Biorad). Reactions done in the presence of nucleotide cofactors contained either 1.0 mM ATP or 0.5 mM ATPγS. When present, single-stranded M13 DNA was added to a final concentration of 70 μM (nucleotides).

PREFACE TO CHAPTER IV

Through the use of electron microscopy and biosensor studies we discovered a subunit interface residue in RecA (Phe217) that plays a critical role in regulating the flow of ATP-mediated allosteric events throughout the protein filament structure. We propose a model describing the allosteric mechanism, or intersubunit communication, leading to ATP-mediated cooperative filament assembly and high affinity binding to ssDNA.

This work was the results of combined efforts of Julie Kelley De Zutter, Ph.D. who performed the IAsys binding studies and Karen Logan who contributed to protein purification and initial biosensor studies. My contributions were protein purification and the electron microscopy leading to the initial observation that F217Y was a cooperativity mutant. I also contributed to data interpretation and final revising of the manuscript.

The data presented in this chapter was published in **Structure**, Volume 9, (January 2001).

CHAPTER IV

PHE217 REGULATES THE TRANSFER OF ALLOSTERIC INFORMATION ACROSS THE SUBUNIT INTERFACE OF THE RECA PROTEIN FILAMENT

Introduction

The bacterial RecA protein is a multifunctional enzyme that plays a central role in recombinational DNA repair, homologous genetic recombination and induction of the cellular SOS response (Eggleston and West, 1996; Roca and Cox, 1997). Each of these activities requires a common initial step, formation of a RecA-ATP-ssDNA nucleoprotein filament (Eggleston and West, 1996; Roca and Cox, 1997; Radding, 1989). Studies of related DNA repair and recombination proteins including UvsX from bacteriophage T4 (Griffith and Formosa, 1985) and both yeast and human Rad51 (Ogawa et al., 1993; Benson et al., 1994) show that such an oligomeric filament is a common structure found in RecA homologs among a wide variety of prokaryotic and eukaryotic organisms. RecA function is regulated in classic allosteric fashion, whereby the binding of ATP greatly enhances the protein's affinity for ssDNA binding and activates it for its catalytic activities (Silver and Fersht, 1982; Menetski and Kowalczykowski, 1985). Recent work suggests that this effect of ATP on DNA affinity is a result of an increase in the cooperative assembly of the protein itself rather than an increase in the intrinsic affinity for DNA (De Zutter and Knight, 1999). Analysis of the RecA crystal structure shows that 55 of the 303 residues in the structure participate in subunit-subunit interactions

(Story et al., 1992). Our studies of different areas of the subunit interface have addressed two fundamental questions: (*i*) which of the intersubunit contacts observed in the structure are actually important for RecA function and oligomer stability and (*ii*) which specific residues are important for the transmission of allosteric information across the protein's oligomeric interface. Initial work focused on a region defined by residues 213-222, which shows 5 side chains that make specific contacts with positions in the neighboring subunit. Through mutational analyses and the use of engineered disulfides (Skiba and Knight, 1994; Logan et al., 1997; Skiba et al., 1999) we have demonstrated the importance of one particular residue within this region, Phe217, for maintenance of both the structural and functional integrity of the protein. While a Phe217Tyr mutation maintains wild type recombination activities *in vivo*, all other substitutions result in a significant decrease or complete inhibition of RecA function (Skiba and Knight, 1994). In the present study we compare various biochemical properties of wild type RecA and the Phe217Tyr mutant protein. These data identify Phe217 as a key residue within the RecA subunit interface required for the transmission of ATP-mediated allosteric information throughout the oligomeric structure of the protein.

Results

Negative stained samples of both wild type RecA and the Phe217Tyr mutant are shown in Figure 4.1. In the absence of both ATPγS and DNA the wild type protein forms short filaments (Figure 4.1A) whereas the mutant forms no detectable oligomeric structures

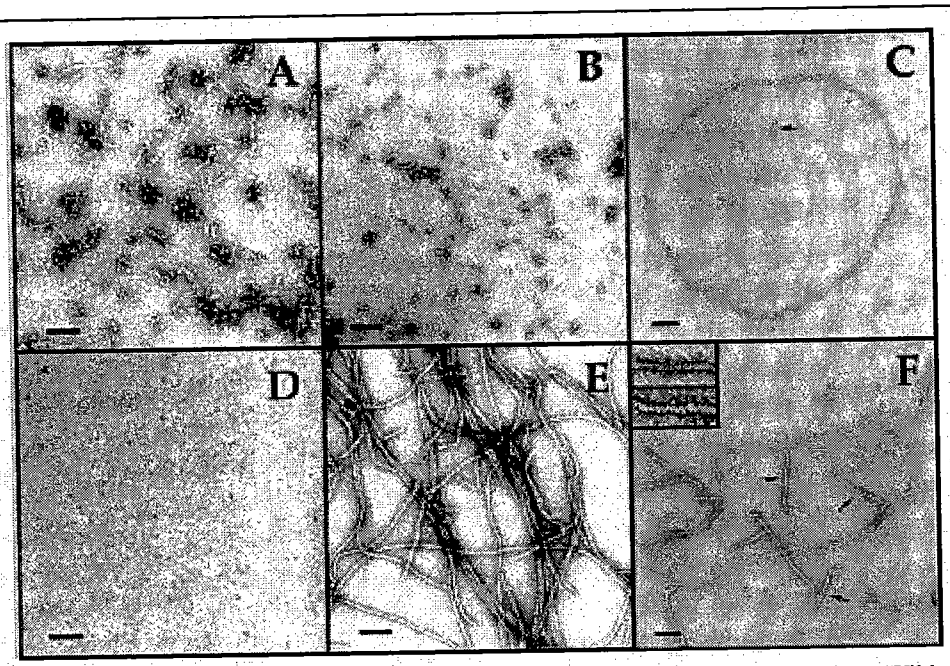


Figure 4.1 – Negative stained electron micrographs of protein and protein-ssDNA complexes. Wild type RecA (A-C) and the Phe217Tyr protein (D-F) were incubated as described in **Materials and methods** in the absence of ATPγS and ssDNA (A, D; protein = 4.0 μM), in the presence of 1.0. mM ATPγS (B, E; protein = 4.0 μM) or in the presence of both ATPγS and 0.5 μM φX174 single-stranded circular DNA (C ,F; protein = 2.0 μM). Inset in panel F shows a 3.6-fold magnification of a free protein filament (top) and a nucleoprotein filament (bottom). Black bar in each panel equals 0.1 μm.

(Figure 4.1D). In the presence of DNA and ATPγS both proteins form well defined nucleoprotein filaments (Figure 4.1C and F). Strikingly, in the absence of DNA the mutant shows a dramatic increase in filament length with addition of ATPγS (Figure 4.1E), whereas the length of wild type filaments clearly decreases (Figure 4.1B). Results for wild type RecA are consistent with previous electron microscopic and hydrodynamic analyses (Brenner et al., 1988; Wilson and Benight, 1990) whereas the ATP-dependent

increase in polymer length for the Phe217Tyr mutant is the first demonstration of such an occurrence for a mutant RecA protein. These data suggest that position 217 plays a key role in regulating polymerization of the RecA protein filament. To provide a quantitative understanding of the effect of the Tyr substitution on RecA polymerization we performed a series of biosensor DNA binding studies.

Binding of both wild type RecA and the Phe217Tyr mutant to ssDNA was measured using an IAsys biosensor. We have previously demonstrated that this technique provides a reliable and quantitative measurement of the DNA binding properties of both RecA and the human Rad51 protein (De Zutter and Knight, 1999). Binding time courses for wild type RecA and the mutant protein in the presence of ATPγS are shown in Figure 4.2. Both proteins showed similar low levels of DNA binding in the absence of ATPγS (not shown). From these curves the extent of binding (binding response at equilibrium) was calculated for each protein concentration. Data were fit to the form of the Hill equation shown below.

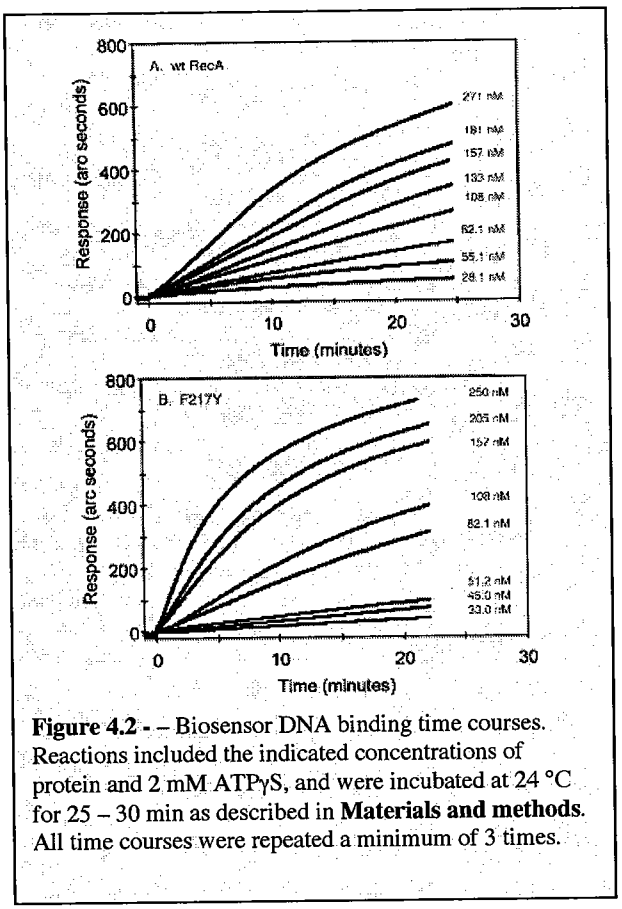


Figure 4.2 - – Biosensor DNA binding time courses. Reactions included the indicated concentrations of protein and 2 mM ATPγS, and were incubated at 24 °C for 25 – 30 min as described in **Materials and methods**. All time courses were repeated a minimum of 3 times.

$$\text{(extent bound) } b = \frac{B_{max} S^{n(app)}}{K' + S^{n(app)}}$$

B_{max} is the maximum amount of protein-DNA complex at equilibrium (reported as the maximum extent of binding in arc seconds), S is protein concentration (free) and K' is a complex constant comprising interaction factors which reflect successive binding and dissociation steps along the cooperative binding pathway (Segel, 1975). Assuming that RecA polymer assembly progresses by addition of individual subunits to the growing chain (Menetski and Kowalczykowski, 1985), we have interpreted the Hill coefficient (n_{app}) as the minimum number of interacting subunits during growth of the nucleoprotein filament which give rise to the observed cooperative binding parameters. $S_{0.5}$, the protein concentration at the mid-point of the titration curve, is calculated as $S_{0.5} = \sqrt[n_{app}]{K'}$ (Segel, 1975). The sigmoidal curves in Figure 4.3 indicate cooperative binding of both proteins to ssDNA, with the mutant showing a dramatic transition from 10 – 90% binding over an extremely narrow range of protein concentration. Calculated values for B_{max}, K', n_{app} and $S_{0.5}$, appear in Table 4.1. Values for wild type RecA are consistent with those determined previously (Menetski and

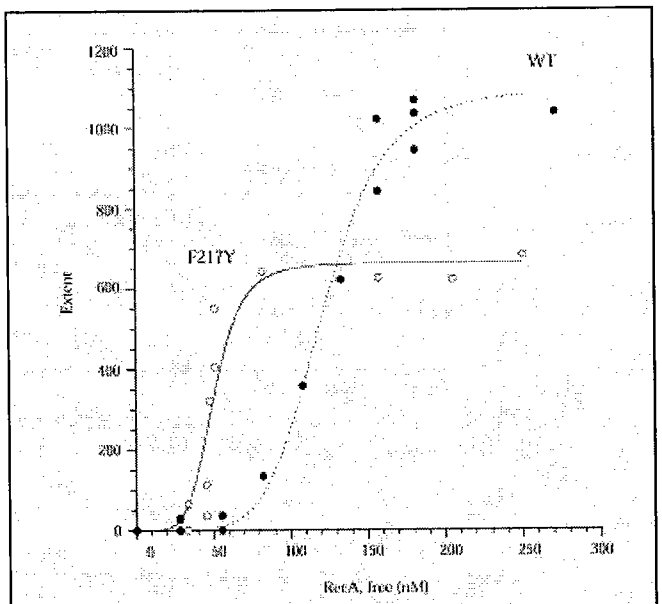


Figure 4.3 - DNA binding as a function of protein concentration. Data from time courses in Figure 4.2 were fit to the Hill equation as described in the text. Extent is the calculated maximum binding at equilibrium in arc seconds for each protein concentration.

Kowalczykowski, 1985; De Zutter and Knight, 1999). The mutant protein shows a slight decrease in B_{max} and a 2.5-fold increase in

	Wild type RecA	Phe217→Tyr
	Hill analysis	
B_{max}	1120.0	765.0
n_{app}	5.8	5.8
K´	7.2×10^{-41}	2.5×10^{-43}
$S_{0.5}$ (nM)	120.0	45.2
	McGhee/von Hippel analysis	
K (M^{-1})	1.1×10^{5}	1.0×10^{3}
ω	75.8	2.0×10^{4}
$(K\omega)^{-1}$ (nM)	120.0	50.0

Table 4.1 - DNA binding parameters were calculated as described in the text. DNA binding time courses were repeated a minimum of 3 times and errors for all parameters shown ranged from 5 – 20%.

affinity ($S_{0.5}$ = 120 and 45.2 nM for wild type and mutant, respectively). Additionally, n_{app} = 5.8 for wild type RecA and the mutant. This suggests that the DNA binding properties of the entire RecA filament are defined by the interaction of the initial 6 subunits for both wild type and mutant proteins. Therefore, when the data is analyzed using this standard form of the Hill equation the Phe217Tyr substitution seems to impose no significant change in the DNA binding properties of the protein. However, analysis of the binding data using a procedure that separates intrinsic DNA binding affinity from cooperative protein-protein interactions (McGhee and von Hippel, 1974) reveals that the Phe217Tyr mutation has a dramatic effect on RecA polymerization.

To investigate potential changes in cooperative filament assembly resulting from the Phe217Tyr mutation we analyzed our data as previously described (De Zutter and Knight, 1999; McGhee and von Hippel, 1974) using the equation below.

$$L = \frac{v}{K(1-nv)\left[\frac{(2\omega-1)(1-nv)+v-\left\{(1-(n+1)v)^2+4\omega v(1-nv)\right\}^{1/2}}{2(\omega-1)(1-nv)}\right]^{n-1}\left[\frac{1-(n+1)v+\left\{(1-(n+1)v)^2+4\omega v(1-nv)\right\}^{1/2}}{2(1-nv)}\right]^{2}}$$

In this expression, L is the concentration of free ligand, n is the number of bases bound by a single RecA subunit (binding site size), v is the binding density of RecA on DNA (fractional maximum extent of binding/n), K is the intrinsic binding constant of a single RecA monomer for DNA and ω is the cooperativity parameter. ω is defined as the relative affinity of an incoming ligand for a singly contiguous site *vs.* an isolated site (McGhee and von Hippel, 1974; Kowalczykowski et al., 1981). A value of $n = 3$ was used as the binding site size (Roca and Cox, 1997; Zlotnick et al., 1993). This expression accommodates two aspects of a widely accepted model for RecA filament assembly onto ssDNA, it proceeds by (***i***) directional binding to an established site (Register and Griffith, 1985) and by (***ii***) addition of protein monomers to the growing filament (Menetski and Kowalczykowski, 1985). Best fits for K and ω were obtained by iterative non-linear regression analysis using the software package KaleidaGraph™ 3.08d (Synergy Software, Reading, PA.). Values for K, ω and $(K\omega)^{-1}$ are shown in Table 4.1. As expected $(K\omega)^{-1}$ approximates the values of $S_{0.5}$ for both the wild type and mutant proteins. However, the analysis reveals a dramatic increase in the cooperative nature of

filament assembly for the mutant protein. The Phe217Tyr substitution increases ω by more than 250-fold (ω = 75.8 and 20,000 for the wild type and Phe217Tyr proteins, respectively).

Although the Phe217Tyr mutant also shows a significant decrease in K, we feel that this does not accurately reflect a true measure of the inherent binding affinity for the following reason. In contrast to wild type RecA, the Phe217Tyr protein polymerizes readily in the presence of ATP (see Figure 4.1E, 4.1F), and it is likely that some portion of the protein in the DNA binding assay exists as free protein filaments. Because free RecA filaments and nucleoprotein filaments are not directly interconvertible (Egelman and , 1993; Yu and Egelman, 1992; Morrical and Cox, 1985), the free filaments must disassemble prior to reassembly on DNA. Therefore, the actual concentration of protein that is immediately available for binding to DNA may be overestimated, resulting in an underestimation of the DNA binding affinity. Experiments are currently in progress in an effort to resolve these competing filamentation events.

RecA filaments have been shown to pack in a side-by-side manner in the absence of DNA to create ordered bundles (Egelman and Stasiak, 1986). Because biosensor measurements simply record the accumulation of mass within the optical window, experiments were designed to ask whether our measurements were also recording fortuitous interactions between free protein filaments and RecA-ATPγS-ssDNA complexes. Electron microscopic analyses were carried out using an excess of protein relative to ssDNA (protein monomers:DNA bases = 4:1). The results showed normal

nucleoprotein filament formation for both wild type RecA (Figure 4.1C) and the mutant protein (Figure 4.1F). For wild type RecA occasional short filaments of free protein were seen (arrow in Figure 4.1C), whereas a much larger percentage of the unbound mutant protein formed elongated filaments (arrows in Figure 4.1F). Differences in the helical pattern of free protein *vs.* nucleoprotein filaments (inset in Figure 4.1F) reflect the fact that when bound to DNA the pitch of the RecA filament is ≈ 95 Å, whereas in the absence of DNA it is ≈ 65 Å (Egelman and , 1993; Egelman and , 1993). There was no appearance of free RecA protein bundling in a side-by-side manner with protein already in complex with DNA. Therefore, our biosensor measurements are recording only the growth of single RecA filaments on the immobilized ssDNA substrate.

We analyzed ssDNA-dependent ATP hydrolysis as a function of ATP concentration for both wild type and the Phe217Tyr mutant protein. As shown in Figure 4.4 the mutant protein has both a higher V_{max} and a higher affinity for ATP. Analysis of the data using the Hill equation (see **Materials and methods**) shows that the mutant protein displays an approximate 1.2-fold increase in V_{max} and a 1.7-fold increase in affinity for ATP ($S_{0.5}$ = 36.6 and 62.2

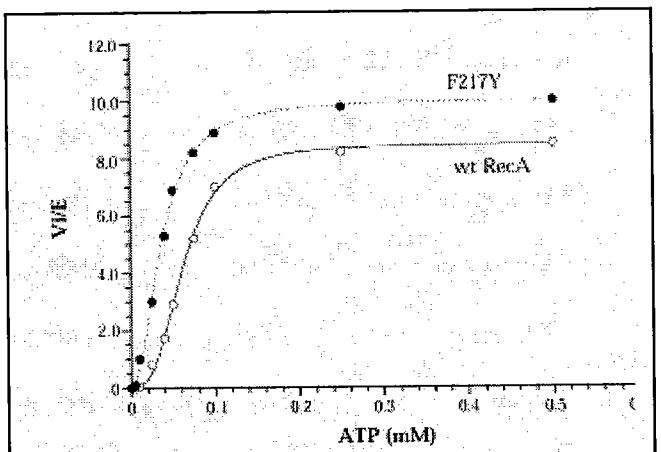


Figure 4.4 – ATPase activity of both wild type RecA and the Phe217Tyr mutant protein as a function of ATP concentration. Reactions included 2 μM protein, 6 μM ϕX174 single-stranded circular DNA, the indicated concentrations of ATP and were incubated as described in **Materials and methods**. Data were fit to the Hill equation as described in **Materials and methods**.

μM for the mutant and wild type proteins, respectively). The Hill coefficient for ATP binding was not changed significantly by the mutation, (n_{app} = 2.1 ± 0.1 and 2.9 ± 0.1 for the mutant and wild type proteins, respectively). Both proteins showed an equivalent basal level of ATP hydrolysis in the absence of ssDNA ($V_i/E \approx 0.1$). Together with the DNA binding data, these results show that the Phe217Tyr mutation increases both cooperative protein-protein interactions and affinity for ATP.

Discussion

Previous genetic analyses of a number of mutant RecA proteins carrying substitutions in one region of the subunit interface revealed that Phe217 was particularly sensitive to mutation (Skiba and Knight, 1994). The RecA crystal structure shows that the Phe217 side chain is within van der Waals contact distance of the Thr150 and I155 side chains in the neighboring subunit (Figure 4.5A and 4.5B). However, a Thr150→Ser substitution imposes no defect in RecA function or structure, and I155 can tolerate a variety of polar and non-polar substitutions (Nastri and Knight, 1994). Therefore, these cross-subunit hydrophobic interactions seen in the structure are not important, and we suggested that Phe217 can form stable interactions with positions further within the neighboring subunit than is apparent in the structure (Skiba and Knight, 1994; Skiba et al., 1999). In the present study we find that a Tyr substitution at position 217 results in a dramatic increase in ATP-dependent cooperative filament assembly, and we propose that ATP-mediated allosteric information is transmitted across the RecA filament via the following mechanism. Gln194 serves as the γ-phosphate sensor within the ATP binding site (Story

and Steitz, 1992; Kelley and Knight, 1997), and its interaction with bound ATP triggers a conformational change in disordered loop 2 (L2, residues 195 – 209; Figure 4.5B). Phe217 is within a small helix (helix G)

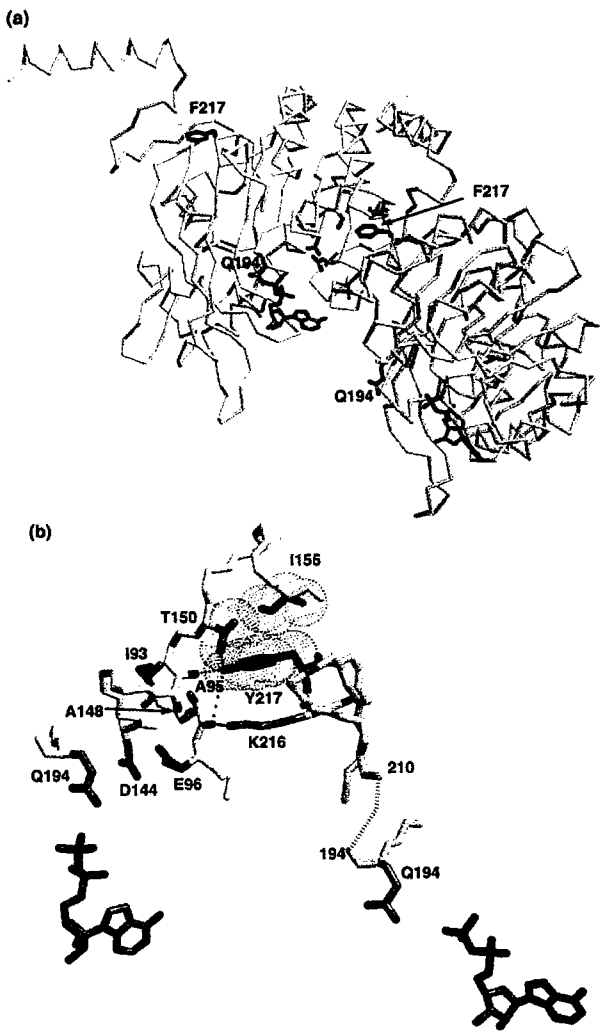


Figure 4.5 - Structure of the RecA protein and specific interactions at the subunit interface. (**A**) An α-carbon trace of dimeric RecA taken from the crystal structure of the helical protein filament (Story et al., 1992) with the main chain of subunit 1 in yellow and subunit 2 in white. Gln194, Phe217 and ADP are shown in both subunits. In subunit 2 side chain carbons of E96, D144, T150 and I155 are dark gray, with side chain oxygens in red. (**B**) Detail of the region of the subunit interface involved in the proposed mechanism for ATP-mediated transfer of allosteric information. Phe217 (here, replaced by Tyr) is within van der Waals distance of Thr150 and I155 in the neighboring subunit. The model proposes that ATP binding in subunit 1 results in conformational changes that are propagated through the L2 region (residues 195-209; disordered in the current RecA structure) and into helix G (residues 212-219), thereby resulting in insertion of the Phe217 side chain further into a pocket in subunit 2 (see text). Residues shown in subunit 1 include 191-194, 210-222 and ADP, and those in subunit 2 include 92-97, 144-155, 191-194 and ADP. Positions in the neighboring subunit within hydrogen bonding distance of the Tyr –OH include the main chain carbonyl oxygens of Ala95 and Ala148, and the –OH of Thr150. Also shown is Lys216 which may stabilize the position of either Phe or Tyr at position 217 through a cation-π interaction (see text). These images were created using the program Midas

immediately downstream of the L2 region, and a pair of Gly residues at positions 211 and 212 that are critical for RecA function (Hortnagel et al., 1999) link L2 with helix G. Therefore, ATP-mediated conformational changes occurring within L2 will propagate through helix G resulting in the insertion of the Phe217 side chain further into a pocket in the neighboring subunit. This insertion may be stabilized by hydrophobic interactions with several residues that lie within this pocket (Ile93, Ala95 and Ala148; Figure 4.5 and 4.6), and likely results in additional changes in nearby cross-subunit interactions that enhance cooperative filament assembly. Upon ATP hydrolysis, Gln194 returns to its position in the inactive form of the enzyme resulting in a relaxation of cross-subunit interactions. The significant increase in cooperative filament assembly afforded by the Tyr substitution likely arises from its ability to form hydrogen bonds with positions in the neighboring subunit (see below).

Modeling a Tyr substitution at position 217 (Figure 4.5B) shows that the Tyr –OH is within hydrogen bonding distance of 3 positions in the neighboring subunit, the main chain carbonyl oxygens of Ala95 and Ala148, and the side chain –OH of Thr150. Also, the RecA structure shows that Lys216 lies immediately underneath Phe217, close enough to provide stabilization of the position of the Phe side chain via a cation-π interaction (Gallivan and Dougherty, 1999). The strength of a cation-π interaction in a Tyr/Lys pair increases if the Tyr –OH serves as a hydrogen bond donor (Mecozzi et al., 1996). Given the proximity of residues in this region (Figure 4.5B and 4.6A), this may also contribute to the increased efficiency of filament formation by the mutant protein.

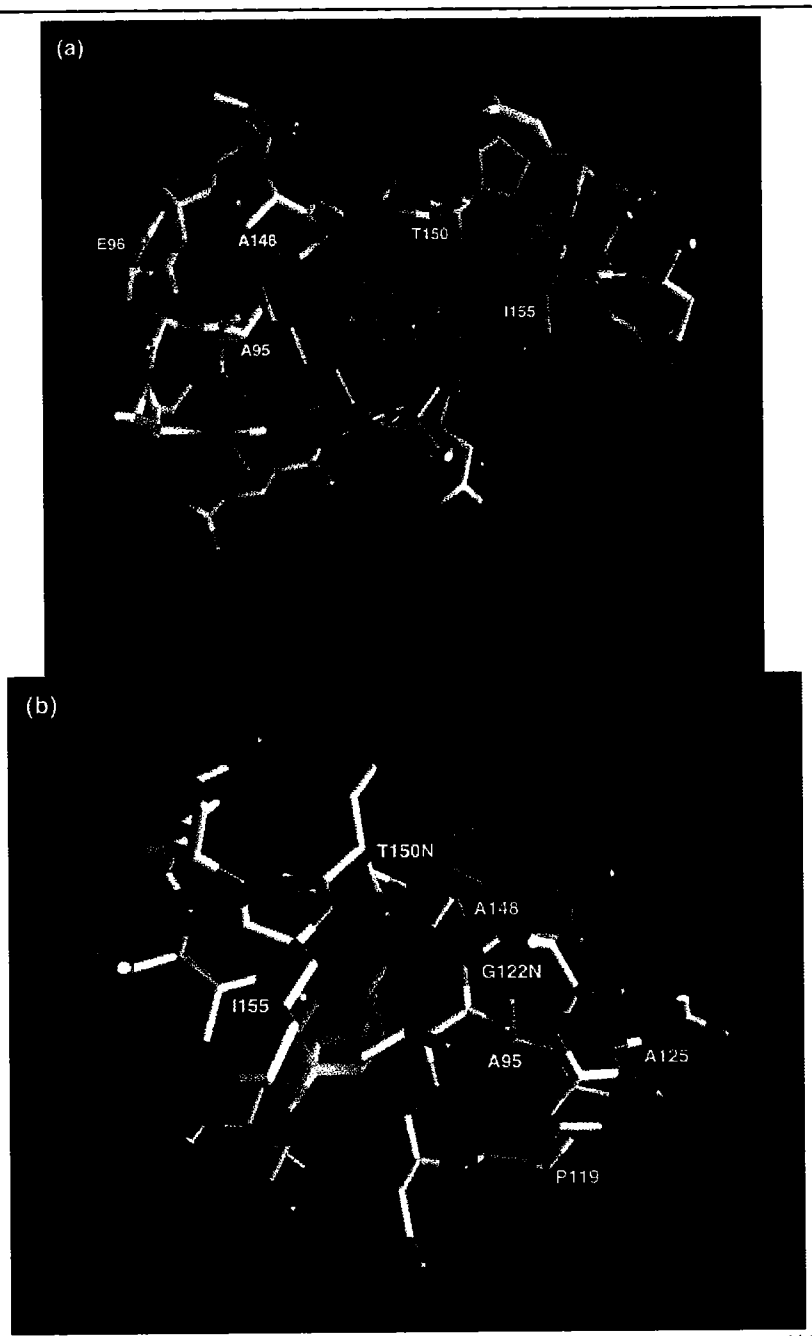


Figure 4.6 - Molecular surface of the neighboring subunit with which residue 217 interacts. (**A**) The surface is colored by atom type (carbon = gray; oxygen = red; nitrogen = blue). In this view, looking from position 217 toward the neighboring subunit, the Tyr substitution at position 217 is seen to lie immediately across from a pocket in the adjacent subunit. (**B**) A top view of the pocket showing positions that may promote stable interactions with a Tyr side chain at position 217 (see text). Additional positions that may participate in hydrogen bond formation with the Tyr -OH are main chain nitrogens of Gly122 (G122N) and Thr150 (T150N). Figures were created using the program GRASP (Nicholls et al.,1993).

The molecular surface shown in Figure 4.6A provides an image of the pocket in the neighboring subunit into which residue 217 may insert. An area in the neighboring subunit immediately in front of position 217 (Figure 4.6A) shows no steric obstruction and could allow insertion of a Phe or Tyr side chain. Again, stabilization of a transient insertion by the wild type Phe side chain may occur by interaction with hydrophobic residues in this pocket. Depending on the degree to which the mutant Tyr side chain inserts into this pocket several other positions appear as candidates for hydrogen bonding interactions, e.g. main chain nitrogens at positions 122 and 150 (G122N and T150N in Figure 4.6B).

The RecA structure also shows that Phe217 lies very close to the ATP binding and catalytic site of the neighboring subunit (Figure 4.5B and 4.6A). Glu96 is proposed to activate a water molecule for an in-line attack of the γ-phosphate of ATP and Asp144 may stabilize binding of the active site Mg^{2+} (Story and Steitz, 1992). The idea that conformational changes in this region of the interface contribute to the cooperativity observed for ATP binding and hydrolysis is supported by our observation that both the affinity for ATP and the rate of ATP hydrolysis is increased by the Phe217Tyr mutation. (Mikawa et al., 1998)

The key roles played by each of the structural elements in this mechanism (***i***) Gln194, (***ii***) Gly211 and Gly212, and (***iii***) Phe217 are supported by previous studies. Gln194 is non-mutable (Kelley and Knight, 1997; Hortnagel et al., 1999) and three mutant proteins, Gln194Asn, Gln194Glu or Gln194Ala are completely inhibited for all ATP-dependent

activities (Kelley and Knight, 1997). Both Gly211 and Gly212 lie immediately next to L2 at the N-terminus of helix G and neither position tolerates any substitution (Hortnagel et al., 1999). Both Gly residues are invariant among eubacterial RecA proteins (Roca and Cox, 1997; Karlin and Brocchieri, 1996) and have been proposed to be involved directly in DNA binding or in mediating ATP-induced conformational changes (Story and Steitz, 1992). Our data supports the idea that the flexibility of the polypeptide backbone at these positions is critical for the propagation of conformational changes transmitted from the ATP binding site to the subunit interface at position 217. Position 217 tolerates only a conservative Tyr substitution while a Phe217Cys change maintains only a low partial activity (approximately 10 – 20% recombination function). All other substitutions, including Trp and other hydrophobic residues result in a *rec*$^-$ phenotype (Skiba and Knight, 1994). These results argue that the specific geometry of the phenyl ring of Phe or Tyr is required at position 217, and supports our idea that ATP-mediated insertion of this side chain into a specifically designed pocket in the neighboring subunit is important to RecA function. Other amino acids in this region of the interface that contact positions in the neighboring subunit (Asn213, Lys216, Tyr218 and Arg222) have a greater tolerance for mutation than does Phe217 (Skiba and Knight, 1994).

Given that the helical pitch of free RecA filaments is ≈ 65 Å (the inactive form) and that of nucleoprotein filaments is ≈ 95 Å (the active form), differences in cross-subunit interactions likely exist between each of these two oligomeric states (Egelman and Stasiak, 1993; Egelman and , 1993). The data in this study show that ATP-mediated cooperative filament assembly is dramatically increased by virtue of a single,

conservative mutation within one region of the RecA subunit interface. The fact that this increase occurs both in the presence and absence of DNA suggests that the position of residue 217 within the protein filament is similar whether RecA polymerizes on its own or on DNA. This idea is supported by a recent study showing that the efficiency of cross-subunit disulfide formation between a Phe217Cys substitution and several Cys substitutions on the surface of the neighboring subunit was similar whether RecA was in the "active" or "inactive" form (Skiba et al., 1999). Additionally, studies of another region of the RecA subunit interface (the N-terminal 28 residues in one subunit and residues 112 – 139 in the neighboring subunit) show that certain mutations destabilize free RecA polymers to a far greater extent than nucleoprotein complexes (Eldin et al., 2000). These results argue that significant differences in cross-subunit interactions between free RecA oligomers *vs.* RecA nucleoprotein complexes occur in this latter area of the interface rather than in the region containing Phe217.

Published alignments comparing the bacterial RecA sequence with the yeast and human Rad51 and DMC1 proteins show that Gln194, Gly211 and Gly212 are conserved (Shinohara et al., 1993; Yoshimura et al., 1993; Story et al., 1993). This suggests that ATP may regulate allosteric events in these 4 eukaryotic proteins using a mechanism similar to that described here for RecA. However, residues in RecA helix G, including Phe217, are not conserved in either of the Rad51 or DMC1 proteins. As with RecA, binding of *S. cerevisiae* Rad51 to ssDNA is dependent on ATP (Namsaraev and Berg, 1998). Unexpectedly, however, the human Rad51 protein binds ssDNA cooperatively and with high affinity in the absence of ATP (De Zutter and Knight, 1999). Therefore,

despite the fact that these residues play important roles in the allosteric mechanism of RecA, ATP-mediated allosteric events and key residues involved in propagating information across the protein filament may be quite different for human Rad51.

Functional and structural studies of helicase enzymes suggest similarities with the RecA protein regarding the use of ATP as an allosteric effector (Namsaraev and Berg, 1998; Soultanas and Wigley, 2000). For example, Gln254 in the *B. stearothermophilus* PcrA helicase aligns with Gln194 in RecA (Subramanya et al., 1996), and the PcrA structure shows that Gln254 is likely to be the switch that communicates ATP binding and hydrolytic events to a DNA binding site immediately downstream (residues 254-264) (Subramanya et al., 1996). Likewise, Sawaya *et al.* (Sawaya et al., 1999) propose that His465 is the γ-phosphate sensor in the NTP binding site of the bacteriophage T7 gene 4 protein and may serve to propagate conformational changes to the adjacent DNA binding motif H4. In fact, in all other DnaB helicase family members residue 465 is Gln (Sawaya et al., 1999). The L2 region in RecA, which is immediately adjacent to Gln194, has been proposed to be the protein's primary DNA binding site (Hortnagel et al., 1999; Voloshin et al., 1996; Wang et al., 1998). Therefore, communication between the ATP and primary DNA binding sites may share mechanistic similarities with helicases. However, other evidence suggests that disordered region L1 (residues 156 – 164) makes up the primary DNA binding site in RecA (Wang and Adzuma, 1996; Cazaux et al., 1998). We note that the effect of ATP on the polymerization of the Phe217Tyr mutant is independent of DNA and, therefore, our proposed mechanism can accommodate either of the disordered regions, L2 or L1, as being the primary DNA binding site. Additionally,

the ATP-induced increase in the DNA binding affinity of RecA results more from an increase in cooperative protein-protein interactions between RecA monomers rather than an increase in the protein's inherent DNA affinity (De Zutter and Knight, 1999). This result is consistent with the model presented here rather than a model in which ATP binding has a direct effect on the intrinsic affinity for DNA. Recent crystallographic studies of the phage T7 g4p helicase shows that a fully active form of the enzyme crystallizes as a closed hexameric ring (Singleton et al., 2000). Therefore, the subunit interface in hexamer helicase structures is very different from RecA and it is unlikely that ATP regulates subunit interactions in helicases in a way related to that in RecA. While the helicase DnaB family may be derived from a *recA* gene duplication (Leipe et al., 2000), RecA appears to have evolved to accommodate the fact that its functional form is a helical protein filament whose assembly and disassembly on DNA substrates is mediated by ATP-induced allosteric events. Therefore, a mechanistic relationship between RecA and helicases remains to be clarified.

Regulated cooperative interaction between subunits in multi-protein complexes is a fundamental mechanism by which protein function is controlled in all biological systems. Point mutations within subunit interfaces that give rise to increases in cooperative behavior have been identified in various proteins. One of the most remarkable, of course, is the β6Glu to Val change in HbS (Eaton and Hofrichter, 1990). Other examples include an Arg152Lys substitution that creates a "hypercooperativity" mutant in *E. coli* phosphofructokinase (Auzat et al., 1995), and similarly, a Thr72Val mutation in *S. inaequivalvis* hemoglobin that results in an increase in cooperative oxygen binding (Royer et al., 1996). Our studies of the Phe217Tyr mutant reveal a striking increase in

ATP-mediated cooperative assembly of a RecA protein filament. Together with previous mutational analyses our data identifies Phe217 as a critical component within the subunit interface that regulates the transmission of allosteric information throughout the protein filament. Interestingly, studies of the RecA-like human Rad51 protein suggest that the allosteric mechanism mediated by ATP binding and hydrolysis is significantly different than that described here for RecA (De Zutter and Knight, 1999). Therefore, despite the structural and catalytic similarities between these two proteins, RecA may serve in only a limited way as a paradigm for understanding the mechanistic properties of its human counterpart. Further studies will be required to complete the molecular description of the allosteric mechanism of RecA, i.e. which residues in the neighboring subunit "sense" the insertion of Phe217, as well as to clearly understand important mechanistic differences between RecA and related eukaryotic strand exchange enzymes.

Materials and methods

Plasmids, proteins and DNA substrates. Wild type and Phe217Tyr *recA* genes are carried on plasmids in which *recA* expression is regulated by p_{tac} (Skiba and Knight, 1994). Purification of both proteins was performed as previously described (Konola et al., 1995). Concentrations of proteins in all assays refer to RecA monomers. 5′-biotinylated phosphoramidite was from Glen research and the biotinylated oligonucleotide used in DNA binding assays was made using an ABI 392 RNA/DNA synthesizer (De Zutter and Knight, 1999). The substrate for electron microscopy (single-stranded circular ϕX174 DNA) was from New England Biolabs. Phage M13 RV-1 single-stranded circular DNA was prepared as described (Zagursky and Berman, 1984).

ATPase assay. DNA dependent ATPase activity was measured as described (Konola et al., 1995). PEI chromatography plates were analyzed using a Molecular Imager FX and QuantityOne software (Bio-Rad). Data are derived from initial rates of ATP hydrolysis determined using various ATP concentrations (1 – 500 μM) and fit to the Hill equation, $v = \frac{V_{max} S^{n(app)}}{K' + S^{n(app)}}$, using KaleidaGraph 3.08 ™ (Synergy Software, Reading, PA.).

Electron microscopy. Samples were prepared for electron microscopy by incubating wild type or mutant RecA protein at 4.0 μM in the absence of DNA, or 2.0 μM in the presence of 0.5 μM phage ϕX174 single-stranded circular DNA. All reactions containing DNA included *E. coli* SSB (0.03 μM) and were pre-incubated at 37 °C for 5 min. Reaction buffer included 25 mM triethanolamine-HCl (pH 7.5), 50 mM KCl and 5 mM $MgCl_2$, as well as 1 mM ATPγS where appropriate. Upon addition of RecA reactions were incubated for 15 min at 37 °C. Reactions were spread onto thin carbon films on holey carbon grids (400 mesh) and stained with 1% uranyl acetate. Samples were visualized by transmission electron microscopy using either a Philips CM10 or a Philips EM400 microscope. *IAsys DNA binding*. Cuvettes containing immobilized ssDNA were prepared using a 5′-biotinylated 86mer oligonucleotide as described (De Zutter and Knight, 1999). Reactions were initiated with addition of protein, and performed at 24 °C in PBS-Tween-Mg buffer (10 mM Na_2HPO_4/NaH_2PO_4, pH 7.4, 138 mM NaCl, 27 mM KCl, 0.05% Tween20 and 5 mM $MgCl_2$) in the absence or presence of 2 mM ATPγS. Protein was preincubated briefly with ATPγS when appropriate (≈ 1 min) prior to addition to the cuvette. Binding was measured for 30 minutes. We performed a number of binding experiments over various times and showed that 25 – 30 min was required to calculate a true equilibrium binding constant for RecA. Following binding, the cuvette

was rapidly washed 3 times with binding buffer and dissociation of the protein from ssDNA was measured for 5 minutes. The immobilized DNA surface was regenerated by addition of 2 M $MgCl_2$ for 2 minutes to strip protein, then washed and re-equilibrated in PBS-Tween-Mg buffer containing NTP where indicated.

Free protein concentration (*S*) was calculated by subtracting the amount of protein-DNA complex from total protein. The amount of complex was determined using a conversion of 600 arc seconds = 1 ng protein/mm^2, with a useable surface area in the biotinylated cuvette of 4 mm^2.Binding is measured in "arc seconds", which corresponds to the accumulation of mass within the optical window at the binding surface, and "extent" refers to the calculated maximum binding at equilibrium for any given protein concentration. Binding data were analyzed using the Fastfit software supplied with the instrument.

PREFACE TO CHAPTER V

In this chapter we report for the first time that Xrcc3 forms distinct foci in human cells and that nuclear Xrcc3 begins to localize at sites of DNA damage very quickly following exposure of cells to radiation damage. Another significant contribution to the field is that Rad51 does not appear to be required for the DNA damage-induced localization of Xrcc3 to DNA breaks. These findings are consistent with a model in which Xrcc3 associates directly with DNA breaks independent of Rad51, and subsequently facilitates formation of the Rad51 nucleoprotein filament.

My specific contributions were development of the cell-based experimental system, RNAi methods, experimental design, interpretation of data and writing of the manuscript. Brian Bennett contributed to this work through image collection on the confocal microscope.

The work presented in this chapter was accepted for publication in the **Journal of Cellular Biochemistry**, Volume 93, (August 2004).

CHAPTER V

XRCC3 IS RECRUITED TO DNA DOUBLE STRAND BREAKS EARLY AND INDEPENDENT OF RAD51

Abstract

Rad51-mediated homologous recombination (HR) is essential for maintenance of genome integrity. The Xrcc3 protein functions in HR DNA repair, and studies suggest it has multiple roles at different stages in this pathway. Defects in vertebrate *XRCC3* result in elevated levels of spontaneous and DNA damage-induced chromosomal abnormalities, as well as increased sensitivity to DNA damaging agents. Formation of DNA damaged-induced nuclear Rad51 foci requires Xrcc3 and the other Rad51 paralog proteins (Rad51B, Rad51C, Rad51D, Xrcc2), thus supporting a model in which an early function of Xrcc3 involves promoting assembly of active Rad51 repair complexes. However, it is not known whether Xrcc3 or other Rad51 paralog proteins accumulate at DNA breaks, and if they do whether their stable association with breaks requires Rad51. Here we report for the first time that Xrcc3 forms distinct foci in human cells and that nuclear Xrcc3 begins to localize at sites of DNA damage within 10 minutes after radiation treatment. RNAi-mediated knock down of Rad51 has no effect on the DNA damage-induced localization of Xrcc3 to DNA breaks. Our data are consistent with a model in which Xrcc3 associates directly with DNA breaks independent of Rad51, and subsequently facilitates formation of the Rad51 nucleoprotein filament.

Introduction

HR is an important pathway in mammalian cells for the repair of DNA double-strand breaks (DSBs) that result from exposure to exogenous DNA damaging agents as well as during normal metabolic processes such as DNA replication and meiotic chromosomal alignment (Pierce et al., 1999; Thompson and Schild, 2001). HR is essential for the maintenance of genome integrity, as defects in this pathway have been shown to result in chromosomal abnormalities that correlate with a number of cancers (Thompson and Schild, 2002). In this pathway, the ends of a DSB are processed by endonucleases to produce a ssDNA tail onto which the Rad51 recombinase is loaded to form a nucleoprotein filament. Rad51 provides the central activity of HR by catalyzing strand exchange between the damaged DNA and an undamaged homologous chromosome, most frequently a sister chromatid, resulting in the formation of cross-over structures referred to as Holliday junctions (Sung et al., 2003; West, 2003). Genetic evidence demonstrates that successful initiation and completion of HR depends on the function of a group of structurally related proteins referred to as Rad51 paralogs: Rad51B, Rad51C, Rad51D, Xrcc2 and Xrcc3 (Tebbs et al., 1995; Liu et al., 1998; Morrison and Takeda, 2000; Takata et al., 2001; Thompson and Schild, 2001; Yoshihara et al., 2004). For example, knock-out of each of the paralog genes in chicken DT40 cells resulted in increased sensitivity to DNA damaging agents and elevated levels of chromosomal abnormalities (Takata et al., 2001). Specific protein-protein interactions between Rad51 paralog proteins have been demonstrated (Schild et al., 2000) and several complexes have been identified (Kurumizaka et al., 2001; Kurumizaka et al., 2002; Masson et al., 2001a; Masson et al., 2001b; Sigurdsson et al., 2001; Wiese et al., 2002).

Recent studies of Xrcc3 suggest that it has a remarkably diverse set of functions and acts both early and late in the HR pathway. Xrcc3 has been shown to play an active role in DNA damage-induced replication fork slowing, a function that occurs early in the HR pathway (Henry-Mowatt et al., 2003). Defects in fork slowing in both hamster and chicken *XRCC3*$^{-/-}$ cells were corrected by either introduction of a human *XRCC3* cDNA or by inclusion of purified human Rad51C-Xrcc3 complex in a permeabilized cell replication assay (Henry-Mowatt et al., 2003). Several lines of work also suggest that Xrcc3 functions during the late stages of HR. For example, defective processing of recombination intermediates is observed in both hamster and *Arabidopsis XRCC3*$^{-/-}$ cells (Bleuyard and White, 2004; Brenneman et al., 2002), and recent studies suggest that human Xrcc3 plays a direct role in Holliday junction resolution (Liu et al., 2004).

Another early function for Xrcc3 likely involves recruitment of Rad51 to the sites of DSBs. Many proteins directly involved in the catalysis of HR appear in distinct nuclear structures termed foci (Haaf et al., 1995; Liu and Maizels, 2000; Essers et al., 2002; Tan et al., 1999) and their accumulation at sites of DNA damage suggests that these are active centers of DNA repair (Raderschall et al., 1999; Tashiro et al., 2000; Aten et al., 2004). To date, only Rad51 has been studied regarding the requirement of other factors for its appearance within DNA damaged-induced foci. For example, in hamster, chicken and human cell lines, formation of damage-induced nuclear Rad51 foci requires Xrcc3 (Bishop et al., 1998; Takata et al., 2001; Yoshihara et al., 2004). Studies using a chicken cell line show that formation of Rad51 foci also requires the other Rad51 paralog proteins

(Takata et al., 2001). Despite their requirement at this early step in the HR pathway, it has not been determined whether any of the five Rad51 paralog proteins accumulate at the site of a DNA break. In the present study, using a combination of immunostaining, transient expression of fluorescent fusion proteins and RNA interference, we show that Xrcc3 forms discrete nuclear foci that localize to DSBs, and that this occurs independent of Rad51.

Results

Immunostaining of HEK293 cells shows the presence of Rad51 in both the cytoplasm and nucleus (Figure 5.1, A-C), consistent with previous results (Yoshikawa et al., 2000).

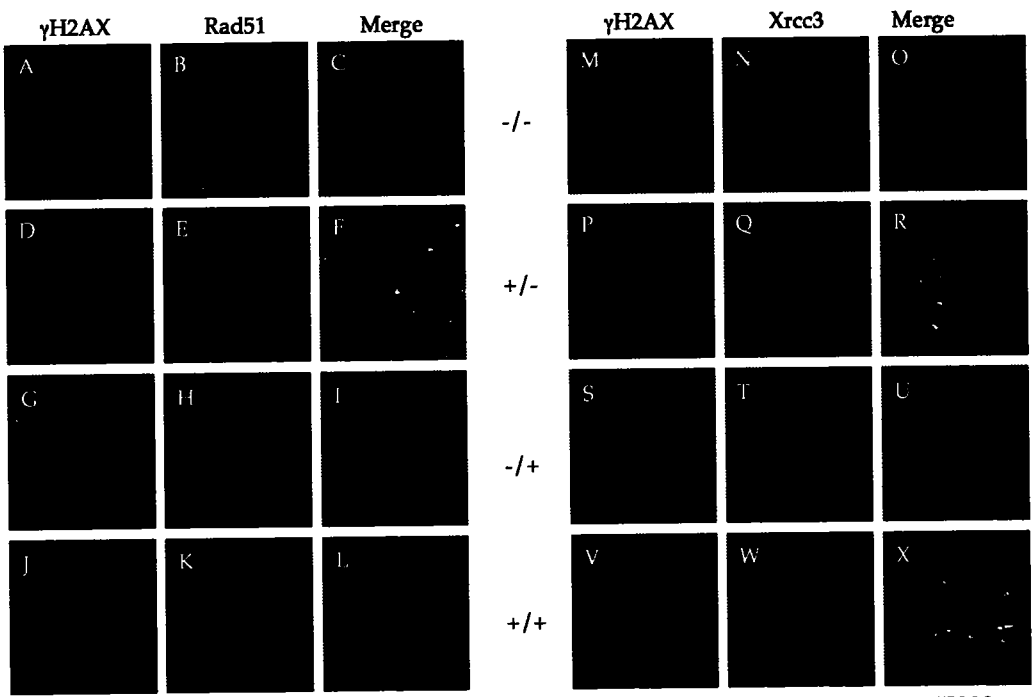


Figure 5.1 - Localization of Xrcc3 to DNA double strand breaks does not require Rad51. HEK293 cells were immunostained for γH2AX (red) and either Rad51 (green) or Xrcc3 (green). Nuclei are stained with DAPI (blue). Where indicated, cells were exposed to 10 Gy ionizing radiation (IR +), and were fixed 60 minutes after exposure. Cells treated with Rad51-specific siRNA (Rad51 siRNA +) were transfected 16 hours prior to ionizing radiation exposure. Cells in each panel are typical of >90% of the total observed in a minimum of three independent experiments.

Exposure to ionizing radiation (10 Gy) results in an increase in both the number and size of nuclear Rad51 foci (Figure 5.1, compare panels B and E). At the one hour time point shown in Figure 5.1 some of the nuclear Rad51 has begun to co-localize with γH2AX (Figure 5.1, D-F), a phosphorylated histone variant (H2AX) that serves as a marker for sites of DSBs (Rogakou et al., 1998). Our data in Figure 5.1 also reveal for the first time the presence of Xrcc3 foci. We find that discrete, small Xrcc3 foci are present in both the cytoplasm and nucleus in the absence of DNA damage (Figure 5.1, M-O). Similar to Rad51, following exposure to ionizing radiation nuclear Xrcc3 foci are larger, greater in number and begin to localize to DNA break sites within one hour (Figure 5.1, P-R). Therefore, it appears that exposure to ionizing radiation results in the redistribution of nuclear Xrcc3 to sites of DNA damage, and that Rad51 and Xrcc3 accumulate at the sites of DNA breaks.

Previous studies have shown that Xrcc3 is required for formation of Rad51 nuclear foci upon DNA damage (Bishop et al., 1998; Takata et al., 2001; Yoshihara et al., 2004). Our results above provide the first evidence that this function of Xrcc3 is likely to occur directly at the site of the DNA break. This, together with the fact that Xrcc3 interacts directly with Rad51 (Schild et al., 2000), raises the question of whether stable association of Xrcc3 with DNA break sites requires the presence of Rad51. Therefore, we asked whether the DNA damage-induced localization of Xrcc3 to the sites of DSBs is dependent on Rad51. HEK293 cells transfected with a Rad51-specific siRNA showed a significant reduction in the amount of Rad51 prior to treatment of cells with ionizing radiation (Figure 5.1, G-I) and eliminated greater than 90% of the damage-induced

nuclear Rad51 foci (Figure 5.1, J-L). However, treatment of cells with Rad51 siRNA had no visible effect on the Xrcc3 staining pattern either before or after DNA damage. Xrcc3 still formed small pre-damage foci in both the cytoplasm and nucleus (Figure 5.1, S-U). Following treatment with ionizing radiation, nuclear Xrcc3 foci increased in both number and size, and showed a partial localization to DSBs similar to that seen in the presence of Rad51 (Figure 5.1, V-X). As expected, treatment of cells with Rad51-specific siRNA prohibited resolution of DSBs and resulted in cell death (data not shown).

The specificity of the Rad51 siRNA was confirmed using a *RAD51-GFP* transgene carrying silent mutations (*RAD51SM-GFP*) rendering it immune to the action of the siRNA. Western blot analysis shows that co-transfection of the siRNA and Rad51SM-GFP depletes the cells of ≥ 90% of the endogenous Rad51 while expression of Rad51SM-GFP is maintained (Figure 5.2A). The absence of Rad51 foci in siRNA treated HEK293 cells was rescued by co-transfection with *RAD51SM-GFP* which forms DNA damage-induced nuclear foci similar to those seen with the endogenous protein (Figure 5.2B and Figure 5.1, J-L). We confirmed the functional relevance of the Rad51SM-GFP protein in the early stages of HR by recapitulating previous results using the Xrcc3-deficient irs1SF hamster cell line (Bishop et al., 1998). Expression of Rad51SM-GFP in irs1SF cells resulted in formation of no damaged-induced Rad51 foci (Figure 5.2C). However, co-expression with Hs*XRCC3* cDNA resulted in recovery of Rad51 focus formation following exposure to ionizing radiation (Figure 5.2C). The fact that Xrcc3 localizes to DSBs independent of Rad51 prompted us to look into the timing of DNA damage-induced Xrcc3 and Rad51 focus formation.

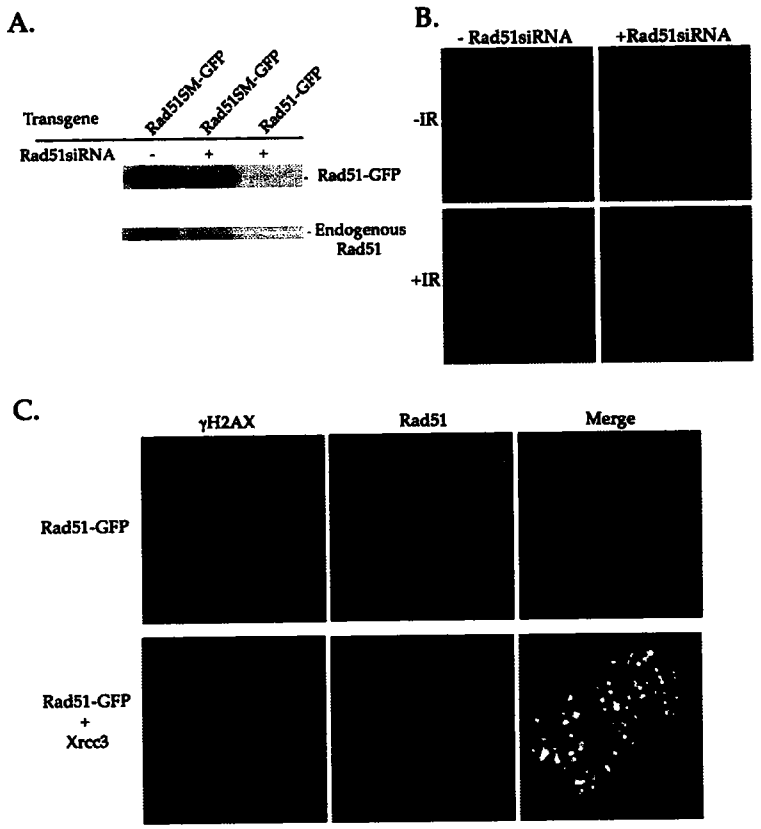


Figure 5.2 - RNAi-mediated knock-down of Rad51 and rescue using a Rad51-GFP fusion protein. (**A**) Western blot showing expression of both endogeneous Rad51 and the Rad51SM-GFP protein (lane 1), specific RNAi-mediated knock-down of endogeneous Rad51 but not the fusion protein carrying silent mutations in the targeted region of the Rad51 sequence, Rad51SM-GFP (lane 2) and RNAi knock-down of both endogenous Rad51 and a Rad51-GFP fusion expressed from a wild type *RAD51-GFP* gene (lane 3). (**B**) HEK293 cells transfected with a plasmid carrying the *RAD51SM-GFP* transgene were co-transfected with a Rad51-specific siRNA duplex and treated with 10 Gy ionizing radiation (IR) as indicated. Cells exposed to radiation were incubated for 60 min before fixation. (**C**) *XRCC3*$^{-/-}$ chinese hamster ovary cells (irs1SF) were transfected with a plasmid carrying the *RAD51SM-GFP* transgene or co-transfected with this plasmid and another carrying the wild type *HsXRCC3* gene. Cells were exposed to 10 Gy ionizing radiation and grown for 60 min before fixation.

If Xrcc3 is required for damage-induced Rad51 focus formation, but not the converse, then Xrcc3 may be localized to the site of a DSB prior to Rad51 in order to facilitate recruitment of Rad51. To observe the timing of Rad51 and Xrcc3 focus formation, HEK293 cells were fixed at 10, 30 and 60 minutes following exposure to 10 Gy ionizing radiation, and immunostained for endogenous Rad51 and Xrcc3. We find that both Xrcc3 and Rad51 nuclear foci begin to appear within 10 minutes after treatment with

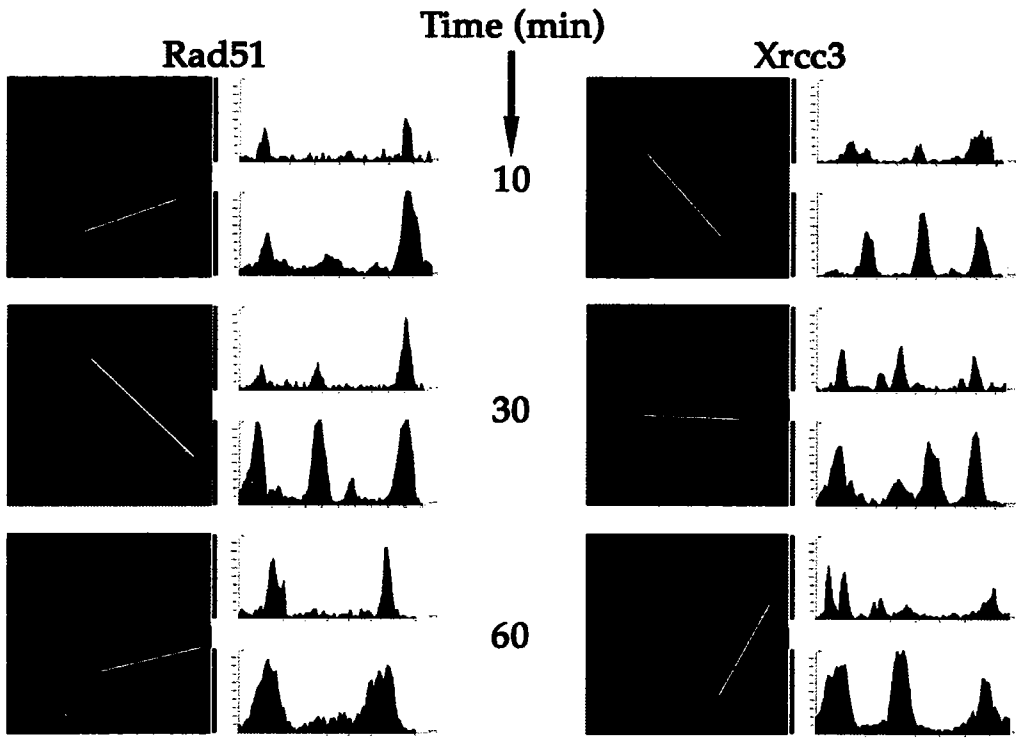


Figure. 5.3 Rad51 and Xrcc3 localize to DNA double strand breaks within 10 min following exposure to ionizing radiation. HEK293 cells were fixed 10, 30 and 60 min following exposure to 10 Gy ionizing radiation. Cells were immunostained for γH2AX (red) and Rad51 (green) in the left three panels, and for γH2AX (red) and Xrcc3 (green) in the right three panels. Profiles at the right of each image indicate the fluorescence intensity of the green and red channels (measured independently) along the yellow line in the corresponding image.

ionizing radiation, and these foci show a partial co-localization with DSBs as indicated by γH2AX foci (Figure 5.3). The incidence of co-localization for several γH2AX foci (red) and either Rad51 or Xrcc3 foci (green) is displayed in the profiles to the right of

each image in Figure 5.3. The fluorescence intensity (y-axis) is plotted against the position of the focus along the yellow line in the image (x-axis). The only other report of Rad51 focus formation at early times after damage (< 60 min) noted that approximately 1% of human fibroblast cells (line Hs68) showed DNA damage-induced nuclear Rad51 foci 10 min after exposure to 9 Gy γ-irradiation (Haaf et al., 1995). However, we find that over 80% of HEK293 cells show an increase in nuclear Rad51 foci 10 min after exposure to 10 Gy γ-irradiation. The importance of our results lies in the fact that we observe a partial co-localization of these foci specifically to the site of DNA breaks and that both Rad51 and Xrcc3 begin to associate with breaks as early as 10 min post DNA damage. Under the conditions used we cannot determine whether both Rad51 and Xrcc3 are associated together at any particular γH2AX focus, but this method is currently under development.

Discussion

The data presented here provide new insights into a developing model regarding the dynamics of recombinational repair proteins (Essers et al., 2002; Yu et al., 2003; Aten et al., 2004) and the function of Rad51 paralogs. We provide the first demonstration of DNA damage-inducible redistribution of Xrcc3 within the cell and formation of Xrcc3 nuclear foci that localize to the sites of DSBs. Additionally, we show that both Xrcc3 and Rad51 appear at the sites of breaks within 10 minutes following exposure to ionizing radiation. Importantly, we demonstrate that formation of DNA break-associated nuclear Xrcc3 foci occurs independent of Rad51. Within the context of other studies regarding the function of Rad51 paralog proteins and the dynamics of recombinational repair

proteins following DNA damage, our data supports the following model (Figure 5.4) for the action of Xrcc3 early in the HR pathway.

The fact that formation of DNA damage-induced Rad51 nuclear foci requires the presence of Xrcc3 (Bishop et al., 1998; Takata et al., 2001; Yoshihara et al., 2004), and that we now show Xrcc3 beginning to localize with DNA breaks within 10 minutes following exposure to DNA damage, strongly suggests that Xrcc3 acts specifically at the site of a DNA break to assist in the formation of Rad51 foci, most likely by promoting assembly of the Rad51 nucleoprotein filament. Yu *et al.* (2003) recently reported that approximately 20% of nuclear Rad51 is sequestered in an immobile complex by virtue of its association with BRCA2, and that it is this pool of Rad51 that is selectively mobilized following replication arrest. However, this mobilization is preceded by a 60-75 minute delay. We find that DNA break-associated Rad51 foci form within the first 10 minutes following DNA damage, suggesting that the Rad51 in these early foci is derived from a pool other than that associated with BRCA2, perhaps either the fraction that is immobile due to Rad51 self-association or the approximate 60% of Rad51 that constitutes the mobile fraction (Yu et al., 2003). Because Xrcc3 forms nuclear foci at the sites of breaks independent of Rad51 we propose that specific protein-protein interactions between Xrcc3 and Rad51 at the DNA break site are directly involved in formation of a Rad51 nucleoprotein filament. This function of Xrcc3 would not necessarily require that it arrives earlier than Rad51 at a DNA break site. We find that both proteins are associated with DNA breaks within 10 minutes after ionizing radiation treatment, but earlier measurements will be needed to provide more detail about the kinetics of the association

of repair proteins with DNA breaks. Whether the BRCA2-associated Rad51 is delivered directly to the site of damage, or upon damage BRCA2 releases bound Rad51 into the mobile pool, specific association of Rad51 with Xrcc3 would again promote assembly of Rad51 into nucleoprotein filaments. Although we currently have no information on the cellular localization of Rad51C either before or after DNA damage, we have included Rad51C in the model (Figure 5.4) because Xrcc3 forms a specific heterodimeric complex with this protein (Masson et al., 2001b; Wiese et al., 2002). The Rad51C/Xrcc3 dimer

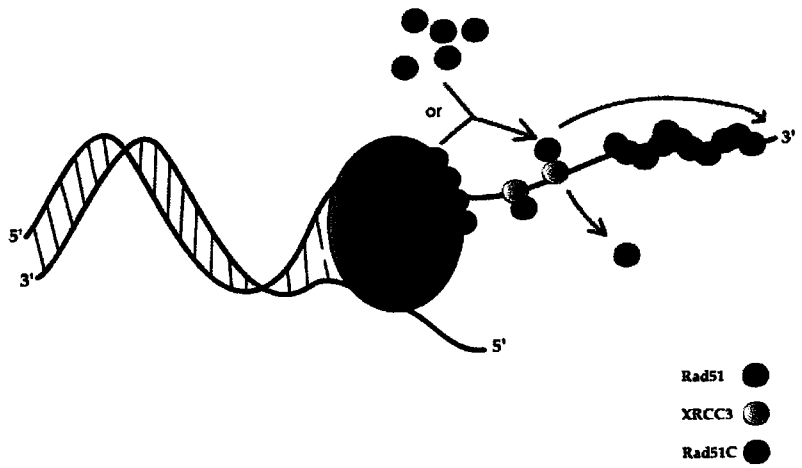


Figure. 5.4 Model for an early function of Xrcc3 in the homologous recombination pathway. Given that our data shows Xrcc3 focus formation at the site of a DNA break 10 minutes after exposure to ionizing radiation, it is likely that at least one function of Xrcc3 occurs directly at the site of the break. The Rad51C/Xrcc3 heterodimer binds single-strand DNA {Masson et al., 2001} at the break and through direct interactions between Xrcc3 and Rad51, mediates the formation of the Rad51 nucleoprotein filament. Rad51 that forms foci within 10 minutes after DNA damage is likely derived from a mobile pool of Rad51 {Yu et al., 2003} whereas BRCA2-bound Rad51 {Yu et al., 2003} may contribute to formation of Rad51 foci at later times.

associates with single-stranded but not double-stranded DNA (Masson et al., 2001a), and therefore may be able to rapidly associate with the single-stranded regions that appear early at a break. Recent data shows that the stability of the Rad51C/Xrcc3 dimer is

regulated by ATP binding and hydrolysis by Xrcc3 (Yamada et al., 2004). Given that Rad51 and each of the five Rad51 paralog proteins has an ATP binding site, regulation of the variety of protein-protein interactions required for the establishment of active repair complexes early in the HR pathway may be mediated by specific ATP binding and turnover events. In fact, recent studies by Shim *et al.* (2004) suggest that Xrcc2 acts as an NTP exchange factor by stimulating ATP processing by Rad51 in a Rad51D-dependent manner.

We consistently find a larger number of Xrcc3 foci relative to Rad51 foci in the nucleus as well as the cytoplasm both before and after exposure to DNA damage. Although we currently do not understand the relationship between these differences in number and localization, further studies are designed to address this issue. While much remains to be discovered about the dynamics and function of recombinational repair proteins, work in this study provides important new information about the DNA damage-induced redistribution and site of action of the Xrcc3 protein early in the homologous recombinational DNA repair pathway.

Materials and Methods

Cell Lines and Transfections. HEK293 cells were obtained from ATCC and were maintained in DMEM supplemented with 10% fetal bovine serum (FBS) and 1% Pen/Strep. In preparation for transfection cells were maintained in DMEM plus 10% FBS. Chinese hamster ovarian (CHO) irs1SF cells (*XRCC3*$^{-/-}$) were maintained in DMEM supplemented with 10% FBS, 1% Pen/Strep and 1% non-essential amino acids.

The *RAD51-GFP* plasmid was made by inserting the *HsRAD51* gene into the SalI-AgeI sites in the multicloning site of pEGFP-N1 (Clontech). The *RAD51SM-GFP* (SM = silent mutations) was made by introducing several silent base changes in the siRNA targeted region of the wild type *RAD51* sequence. Transfection of both a Rad51-specific siRNA duplex (Qiagen) and plasmids was performed using a lipid transfection method (Lipofectamine 2000, Invitrogen). A control siRNA against lamin A/C and a 3´-fluorescein labeled control siRNA with no matches in the human genome (Qiagen, cat# 1022079) showed no effect on Rad51 or Xrcc3 focus formation, or protein levels as determined by Western blots, when transfected into HEK293 cells (data not shown). When used together the siRNA and plasmid were co-transfected.

Antibodies. Primary antibodies used for immunofluorescence staining were mouse anti-phospho-histone H2AX biotin conjugate (clone JBW301, Upstate Biotechnology), mouse anti-Rad51 (clone 3C10, Upstate Biotechnology), mouse anti-Xrcc3 (10F1/6, Novus Biologicals, Inc.) and all were diluted 1:500. Alexa 488 and Alexa 555 (Molecular Probes), and Immunopure Streptavidin Rhodamine Conjugate (Pierce) secondary antibodies were diluted 1:1000. All dilutions were in PBS containing 1% BSA. DNA was counterstained with Vectashield Fluorescent Mounting Media containing DAPI (4´, 6´-diamidino-2-phenylindole; Vector Laboratories).

Immunostaining and Confocal Microscopy. Cells were grown on coverslips in a 6 well dish. For fixation, media was aspirated off and cells were washed once with PBS and immersed in 100% methanol at -20 °C for 5 minutes. Cells were blocked in PBS

containing 4% BSA overnight at 4 °C. After blocking, cells were washed five times for five minutes each with PBS. Incubation with both primary and secondary antibodies was performed in 6 well dishes for 1 hr at 37 °C in a humid environment using a slide warmer (Fisher). Cells were washed five times for five minutes each in PBS after incubation with both primary and secondary antibodies. Coverslips were mounted using Vectashield with DAPI and sealed with polyurethane (nail polish) then stored in the dark at 4 °C. Visualization of immunostains was performed by confocal microscopy using a Leica TCS SP2 AOBS instrument and image processing was performed using the accompanying Leica Confocal Software TCS SP2.

Damage-Induced DNA Double Strand Breaks. Cells were exposed to 10 Gy ionizing radiation (^{137}Cs) using a Gammacell 40 (MDS Nordion Ottawa, ON Canada). After exposure cells were allowed to recover at 37 °C (5% CO_2) for the indicated times. Cells were then methanol fixed and prepared for immunostaining.

Western Blotting. HEK293 cells were transfected with the appropriate transgene and/or siRNA as indicated (Figure 5.2A). Cells were harvested 20 hrs. post transfection washed with PBS and lysed with RIPA buffer (25 mM Tris pH 7.4, 0.5% triton X-100, 0.5% sodium deoxycholate, 0.05% sodium dodecyl sulfate, 0.05 mM EDTA pH 7.0, 75 mM NaCl) and total protein was determined with BCA Protein Assay Kit (Pierce). Acrylamide mini-gels (10%) were run with 80 μg of total protein in each lane and transferred to PVDF membranes overnight at 200 mV in transfer buffer (192 mM glycine, 25mM Tris, 20% methanol). Membranes were incubated in blocking buffer (10

mM Tris-HCL pH 8.0, 300 mM NaCl, 0.025% Tween 20) containing 15% instant nonfat dry milk for 45 min. Rad51 primary antibodies (Oncogene #PC130) were added (1:3,000) in blocking buffer containing 2% instant nonfat dry milk for 1 hr. and membranes were washed five times for 5 min. each in blocking buffer. Peroxidase conjugated anti-rabbit secondary antibodies (Pierce #31462) were added (1:12,000) for 1 hr and membranes washed as above. Membranes were incubated with LumiGLO chemiluminescent substrate (KPL #54-61-01) for 1 min., exposed to X-ray film and developed (Kodak 2000A XOMAT processor).

PREFACE FOR CHAPTER VI

In this chapter I provide data that suggests ATP binding and hydrolysis is required for the function of Rad51 in repairing ionizing radiation induced DNA damage. This is part of an ongoing investigation into the requirement of ATP by human Rad51.

I designed a system utilizing RNAi to efficiently knock-down Rad51 allowing expression of mutant proteins e.g. K133A, K133R, in either the presence or absence of the wild-type endogenous protein. Cells transiently expressing these mutants were evaluated for their ability to repair DNA damage using a comet assay that directly quantifies DNA damage. Yeast two-hybrid and co-immunoprecipitation experiments were performed by Matt Loftus.

CHAPTER VI

ATP BINDING AND HYDROLYSIS IS ESSENTIAL FOR THE ABILITY OF HUMAN RAD51 TO REPAIR IONIZING RADIATION INDUCED DNA DAMAGE

Introduction

The *E. coli* RecA protein forms a nucleoprotein filament in an ATP dependant manner. This RecA/ATP/ssDNA complex is the key active catalytic component in the HR pathway responsible for the efficient repair of DSBs (Roca and Cox, 1990; Kowalczykowski et al., 1994). The human homolog, Rad51, is highly conserved in a 207 amino acid core domain which contains the Walker A and Walker B motifs (Yoshimura et al., 1993; Shinohara et al., 1993). Both RecA and Rad51 proteins share a number of similarities including *in vitro* activities such as ATP binding, DNA-dependent ATP hydrolysis, ssDNA and dsDNA binding, strand annealing and strand exchange (Benson et al., 1994; Baumann et al., 1996; Gupta et al., 1997; De Zutter and Knight, 1999). A combination of electron microscopy and more recently Rad51 X-ray crystallography have revealed many structural similarities between the filaments of RecA and Rad51 from human, yeast and archae (1993; Egelman and Stasiak, 1986; Ogawa et al., 1993; Pellegrini et al., 2002; Shin et al., 2003; Conway et al., 2004).

Despite the high degree of structural and functional similarity, there are fundamental differences in the way that these two homologs catalyze the DNA strand exchange

reaction leading to DSB repair. For example, the DNA dependant ATPase capability of RecA is approximately 30-fold higher than that of Rad51 (Gupta et al., 1997). RecA can independently catalyze *in vitro* strand exchange while Rad51 requires additional cofactors including RPA and/or Rad52 and in some instances Rad54 (Kowalczykowski et al., 1994; Baumann et al., 1996; Baumann and West, 1997; Benson et al., 1998). Additionally, ATP and ATPγS induce a high affinity binding state of RecA for ssDNA while for Rad51, NTP has surprisingly little effect on the equilibrium binding affinity for ssDNA (Silver and Fersht, 1982; Silver and Fersht, 1983; Menetski and Kowalczykowski, 1985; De Zutter and Knight, 1999). While ATP is a required cofactor for HsRad51-mediated strand exchange, its mechanistic role remains undefined.

For RecA, the A site of the NTP binding consensus sequence (GXXXXGKT/S) has been the target of several studies involving a conservative mutation, K→R, that allows binding of ATP but is defective for ATP hydrolysis (Rehrauer and Kowalczykowski, 1993; Bedale and Cox, 1996; MacFarland et al., 1997). Currently in the literature there are two conflicting sets of data acquired through different methods as to whether or not ATP hydrolysis is an essential function of human Rad51. Morrison *et al.* created *RAD51*$^{-/-}$ chicken DT40 cells in which high-level expression of the human Rad51 K133R mutant allowed the cells to remain viable (Morrison et al., 1999). They were unable to make cell lines expressing the human K133A mutant, suggesting that this is due to a dominant negative effect as reported for the same mutation in yeast (Chanet et al., 1996). Upon evaluation of cells expressing the human Rad51 K133R mutant they concluded that these cells carry out normal levels of recombinational repair following treatment with γ-

radiation, showed fewer numbers of DNA damage-induced nuclear Rad51 foci and a reduced level of homologous recombination-dependent gene targeting (Morrison et al., 1999). Another approach to address the role of ATP in Rad51 catalyzed repair of DSBs by Stark *et al.* (2002) was to evaluate the same mutant human proteins (K133A and K133R) in mouse embryonic stem (ES) cell lines. They created a mouse ES cell line expressing the human Rad51 K133R protein at levels comparable to the endogenous mouse Rad51 whose expression was retained in a dominant negative approach (Stark et al., 2002). As in the studies using chicken DT40 cells (Morrison et al., 1999) they were unable to create mouse ES clones expressing the human Rad51 K133A suggesting that its expression is lethal (Stark et al., 2002). They reported that expression of K133R results in multiple types of DNA repair defects including homology directed repair of a chromosomal DSB, as well as repair of damage induced by either mitomycin C or ionizing radiation. In contrast to the findings of Morrison *et al.* (1999) they concluded that ATP hydrolysis by Rad51 plays a key role in HR and DNA repair.

Using the approach of studying human proteins in human cell lines we are in the process of evaluating the functions of the Rad51 K133A and K133R mutants. Recent studies have shown that ATP binding and turnover regulate certain protein-protein interactions relevant to Rad51-mediated recombination (see Figure 6.1). For example, and as mentioned earlier in Chapter V, Yamada *et al.* (2004) have shown that ATP binding and hydrolysis by Xrcc3 regulates the stability of the Xrcc3/Rad51C heterodimer, and Shim *et al.* (2004) have shown that Xrcc2 serves as an NTP exchange factor by stimulating ATP processing by Rad51 in a Rad51D-dependent manner. Therefore, in addition to

measurements of DNA repair, we also asked whether mutations in the Walker A site of Rad51 had an effect on two well characterized protein-protein interactions, Rad51-Xrcc3 and Rad51-Brca2. Below, I describe our initial results using a combination of yeast two-hybrid, co-immunoprecipitation and an *ex vivo* system to evaluate protein-protein interactions and the DNA repair capability of these mutants relative to wild type Rad51.

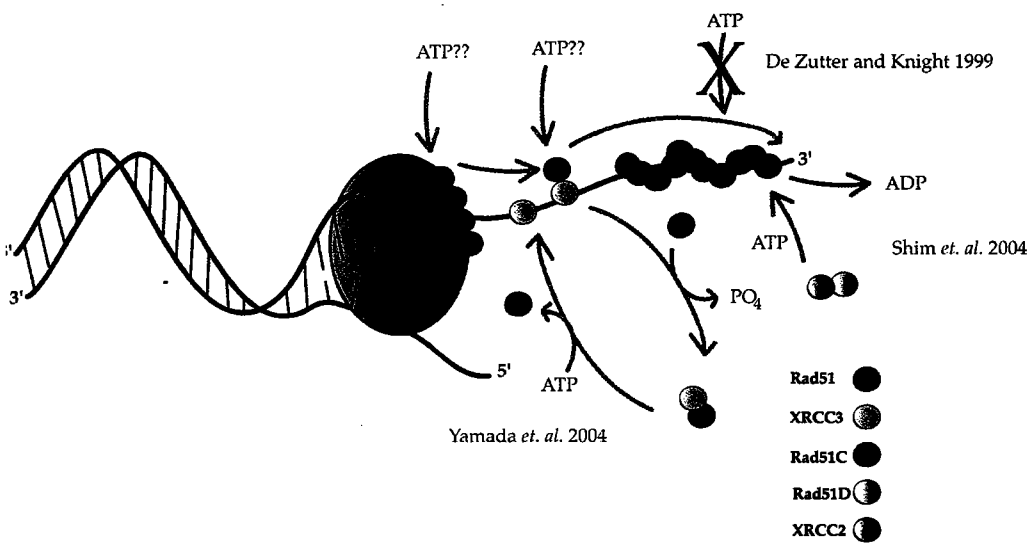


Figure 6.1 - Model for ATP regulation of events at a DSB. Yamada *et al.* have shown that ATP binding to Xrcc3 regulates its interaction with Rad51C and Shim *et al.* have suggested that XRCC2 may act as an ATP exchange factor for Rad51.

Results

To analyze the ability of the Rad51 K133A and K133R proteins to repair radiation-induced DNA damage I utilized a comet assay (single cell gel electrophoresis). Figure 6.2 shows typical HEK293 cells prior to and following damage as indicated. HEK293 cells were transiently transfected with expression vectors carrying either control or mutant transgenes alone or co-transfected with siRNA specific for the endogenous Rad51 mRNA. Following incubation to allow for protein expression, cells were exposed to ionizing radiation and analyzed at 30 min and 10 h for repair of radiation-induced DSBs (see MATERIALS AND METHODS). Expression of transgenes in the absence of endogenous protein is accomplished by putting silent mutations in the coding region that is targeted by the siRNA rendering the transgene message immune to degradation while the endogenous mRNA is still efficiently degraded. As previously reported by Essers *et al.* we found that when GFP is fused to the amino-terminus of Rad51 the transgene is functional but if GFP is fused to the carboxyl-terminus of Rad51 there is a significant

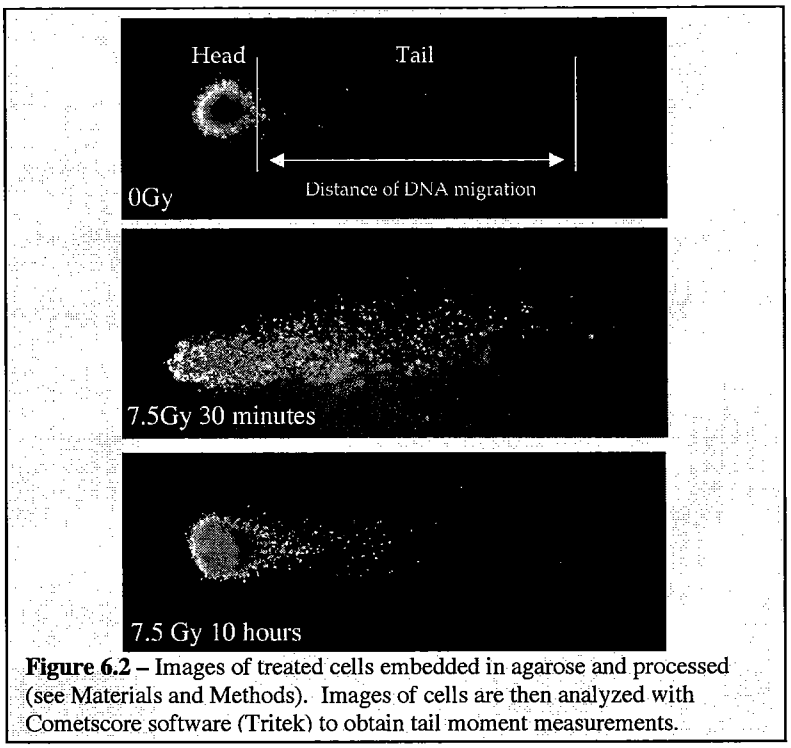


Figure 6.2 – Images of treated cells embedded in agarose and processed (see Materials and Methods). Images of cells are then analyzed with Cometscore software (Tritek) to obtain tail moment measurements.

deficiency in the ability of the cells to undergo repair (Essers et al., 2002). We also observed that in the presence of the endogenous wild-type Rad51 (no Rad51 siRNA transfected) both mutations display a dominant negative phenotype. As shown in Figure 6.3, cells expressing the K133A or K133R mutants present a dominant negative phenotype and show a lack of ability to repair DNA damage similar to results obtained from control experiments where endogenous Rad51 was silenced. The expression of K133R in the absence of endogenous (Rad51K133R + Rad51siRNA) also showed a defect in repair as expected. Surprisingly when we expressed the K133A mutation in the absence of endogenous Rad51 (Rad51K133A + Rad51siRNA) a significant level of repair was observed.

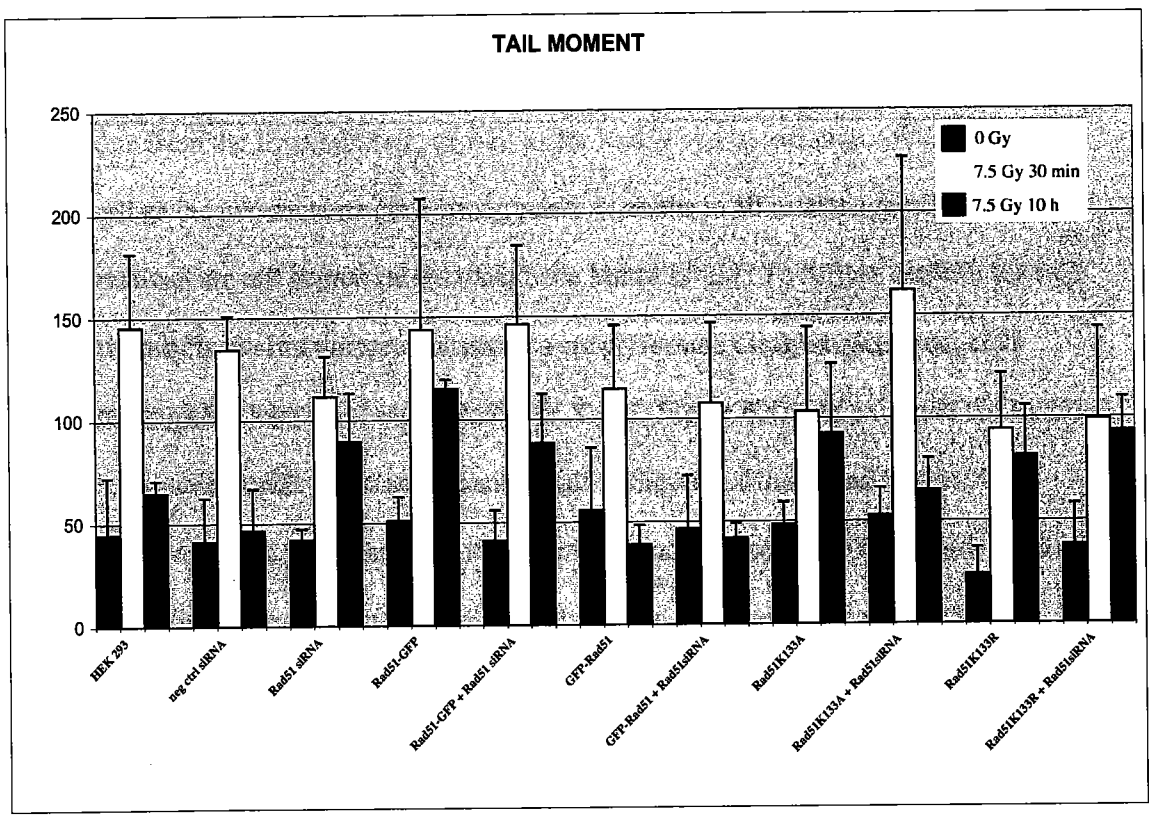


Figure 6.3 - Comet Assay data comparing the ability of HEK293 cells expressing indicated GFP fusions +/- Rad51siRNA to repair γ-radiation induced DNA damage as measured by tail moment. Data points are the mean of three independent experiments analyzing a minimum of 50 cells in each experiment. Error bars were calculated using the three experimental means for each condition.

To test whether the known interactions of Rad51 with Xrcc3 and Brca2 are affected by either the arginine or alanine substitutions at position 133, we used both yeast two-hybrid and co-immunoprecipitation analyses. In a yeast two-hybrid assay full length Rad51 protein was tested for its interaction with the full length Xrcc3 protein or the BRC3

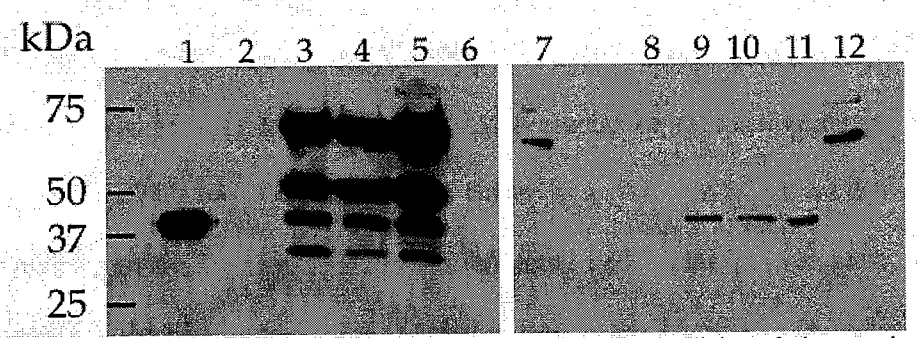


Figure 6.4 - Co-immunoprecipitation assay GFP antibodies were used to pull down fusion proteins along with associated proteins and blotted with Rad51 antibodies (lanes 1-6) or Xrcc3 antibodies (lanes 7-12). Lane 1 purified Rad51 marker. Extracts from cells expressing GFP-fusions as follows; lane 2 GFP, lane 3 Rad51-GFP, lane 4 Rad51K133A-GFP, lane 5 Rad51K133R-GFP, lane 6 Xrcc3-GFP, lane 7 XRCC3-GFP, lane 8 GFP, lane 9 Rad51-GFP, lane 10 Rad51K133A-GFP, lane 11 Rad51K133R-GFP, lane 12 Xrcc3-GFP.

peptide from the Brca2 protein, as well as for Rad51 self-association. Wild type Rad51 as well as the two mutants gave strong positive results in all cases suggesting that the interactions are not compromised (data from Matt Loftus). To further confirm the two-hybrid results, co-immunoprecipitations were performed using extracts from cells expressing GFP fusions of either Rad51 or Xrcc3 (Figure 6.4). As expected the Rad51-GFP was able to pull down endogenous Rad51 (Figure 6.4 lane 3) as well as Xrcc3 (Figure 6.4 lane 9). In lanes 3 – 5 the top-most band represents the full length Rad51-GFP protein whereas bands immediately above and below endogenous Rad51 are fragments of Rad51-GFP that we frequently observe in pull down experiments. Xrcc3-GFP was able to pull down endogenous Rad51 although at minimally detectable levels (Figure 6.4 lane 6). More importantly, Rad51 fusions carrying each of the mutations

(K133A and K133R) showed an interaction with endogenous Rad51 as well as Xrcc3 (lanes 4, 5 and lanes 10, 11, respectively).

Discussion

ATP has now been shown to play a critical role in the regulation of protein-protein interactions essential for the successful repair of DSBs by homologous recombinational repair (Shim et al., 2004; Yamada et al., 2004). The data presented here provide support for the hypothesis that ATP hydrolysis by Rad51 is crucial for its function in repairing radiation-induced damage. For the first time we report a system in which we can study mutant human protein function in the context of human cells. This allowed us to specifically analyze the Rad51 K133R mutant, as well as the Rad51 K133A mutant for which previous attempts were unsuccessful (Morrison et al., 1999; Stark et al., 2002).

We have verified that a fusion of GFP to the terminus-terminus of Rad51 is unable to compensate for the knock-down of endogenous Rad51 yet an amino-terminal fusion is functional when compared to the ability of normal HEK293 cells to repair radiation induced damage (Figure 6.3). In agreement with the findings reported expressing human Rad51 K133R in mouse ES cells, we show that both alanine and arginine substitutions at position 133 result in a dominant negative phenotype and are not able to repair damage induced DSBs (Stark et al., 2002). Surprisingly when we looked at the ability of the mutant proteins to function on their own, in the absence of endogenous (+Rad51siRNA), the Rad51K133A substitution showed significant ability to repair IR induced breaks analyzed by comet assay. This is the first time anyone has been able to observe the functionality of this human mutant protein in the context of human cells or any other cell

line, attempts in mouse and chicken cells were previously unsuccessfull. The result that when K133A is in combination with the wildtype endogenous Rad51 acts as a dominant negative yet when is expressed alone in the absence of endogenous in functional is interesting and currently more experiments are underway to clarify this.

Unlike RecA, the affinity of human Rad51 for DNA is not affected by the presence of ATP. Since ATP has been shown to regulate the interaction between Xrcc3 and Rad51C we tested to see if known interactions between Rad51 and other proteins in the HR pathway were disrupted by these ATP site mutations. We evaluated Rad51's interaction with Xrcc3 and Brca2 through the combination of a yeast two-hybrid assay and co-immunoprecipitation. Interestingly, for both mutant proteins, K133A and K133R, two-hybrid results revealed a strong interaction with wild type Rad51, Xrcc3, and the BRC3 peptide from Brca2 (communication from Matt Loftus). These results were corroborated using co-immunoprecipitation assays in which an Xrcc3-GFP fusion was shown to pull down both mutant Rad51 proteins and GFP fusions to both mutants were able to pull down Xrcc3 (Figure 6.4). Together, these data strongly suggest that interaction of Rad51 with Xrcc3 and Brca2 is not compromised by inhibition of Rad51 ATP hydrolysis or binding.

If ATP does not play a role in DNA binding, Xrcc3 interaction or Brca2 interaction then why is it essential for Rad51-mediated HR? Current studies are underway in our lab to investigate a potential role in the regulation of other essential protein-protein interactions. Also, we are developing an assay to assess the possibility that ATP is required by the

active Rad51 nucleoprotein filament to bind a homologous dsDNA template. Regardless of specific mechanistic role for ATP, we conclude that ATP hydrolysis by Rad51 is indeed essential for the repair of radiation induced breaks by HR in human cells.

Materials and Methods

Cells HEK293 cells were obtained from ATCC and were maintained in DMEM supplemented with 10% fetal bovine serum (FBS) and 1% Pen/Strep. In preparation for transfection cells were maintained in DMEM plus 10%FBS.

Vectors and siRNA The Rad51-GFP and GFP-Rad51 plasmids were constructed by inserting the human *RAD51* gene into the SalI-AgeI sites in the multicloning site of pEGFP-N1 or pEGFP-C1 vectors respectively (Clontech). The GFP-Rad51SM (SM = silent mutations) was made by introducing several silent base changes in the siRNA targeted region of the wild type *RAD51* sequence making the message immune to the effect of ad51 siRNA. The K133A and K133R mutations were constructed from the parental GFP-Rad51SM vectors with Quickchange mutagenesis kit (Stratagene). Xrcc3-GFP was constructed by inserting the HsXrcc3 gene into the SaI-AgeI sites in the multicloning site of pEGFP-N1 vector (Clontech). SiRNA for Rad51 was purchased from Qiagen. When transfected into HEK293 cells a control 3´-fluorescein labeled control siRNA with no matches in human genome (Qiagen, cat# 1022079) had no effect on protein levels as determined by Western blots (data not shown). When used together the siRNA and plasmid were co-transfected. Transfections of DNA and/or siRNA (4μg DNA or 10 nM siRNA per well of a 6-well plate) were performed using a lipid transfection method (Lipofectamine 2000, Invitrogen).

Comet assay Cells were seeded in a 6-well plate at $0.8x10^6$ 24 hours prior to transfection. The indicated expression vectors and/or siRNA were transfected. Following a 24 hour incubation to allow for uptake and expression or knock-down cells were exposed to 7.5 Gy of ionizing radiation (^{137}Cs) using a Gammacell 40 (MDS Nordion Ottawa, ON Canada). 30 minutes or 10 hours post irradiation cells were collected and mixed with 0.5% lo-melt argarose. ~10,000 cells in a volume of 50μL were spotted on a glass slide previously coated with 1% normal-melt argarose and a coverslip was placed immediately over the cells. Once the agarose solidified the coverslip was removed and an additional 50μL of 0.5% low-melt agarose without cells was layered on top and the coverslip replaced to allow for the agarose to harden. The coverslips are then removed and the slides placed in fresh Lysing solution (2.5M NaCl, 100mM EDTA, 10mM Trizma base, 1% Triton X-100, 10% DMSO) and kept at 4 C overnight. Following lysis slides were rinsed 3X for 5 minutes each washed (0.4M Tris pH7.5). Slides were then placed in electrophoresis buffer (300mM NaOH, 1mM EDTA) in horizontal gel boxes and incubated for 20 minutes prior to running them at 25 volts for 15 minutes. The slides were then removed from electrophoresis buffer and washed 3X for 5 minutes each in neutralization buffer (0.4M Tris pH7.5). Slides were then stained with 2μg/mL ethidium bromide in water and images were obtained with a fluorescent microscope (Axioskop2 plus, Zeiss). Images were analyzed with Cometscore software (Tritek software). Tail moment is defined as %DNA in Tail * Tail Length.

Co-immunoprecipition Cells were transfected with appropriate vector in a 6-well plate in triplicate. 24 hours post transfection cells were collected and washed with PBS. Pelleted

cells were resuspended in 150μL lysis buffer (10 mM Hepes, pH 7.4, 150 mM KCl, 10mM MgCl2, and 50 μg/mL digitonin) with protease inhibitors and incubated on ice for 10 minutes. Following centrifugation at max speed in a microcentrifuge supernatant was transferred to a new eppendorf tube and assayed for total protein content using BCA assay (Pierce). Pre-clearing was accomplished by mixing ~200μg total protein with 25μl protein G magnetic beads (NEB S1425S) and incubated at 4°C with gentle rocking. The tubes were then placed in a magnetic rack for 1 minute and the supernatant was transferred to a clean tube. 12.5 μl (5μg) of anti-GFP mouse monoclonal IgG antibody was added to the pre-cleared supernatant and gently rocked for 1 hour at 4°C. Beads were washed 3X with lysis buffer. Beads were then resuspended in 30μl of Laemmli loading buffer incubated at 100°C and placed in the magnetic rack to separate beads out. The entire sample was then loaded on SDS-PAGE gel. Western blots were then performed as described in Chapter V using primary antibodies for either Rad51 (1:3,000 Oncogene PC130) or Xrcc3 (1:5,000 Novus NB100-165) and goat anti-rabbit HRP conjugate (1:12,000 Pierce 31462).

CHAPTER VII

FUTURE DIRECTIONS

The structural and mechanistic studies I performed on the bacterial RecA protein described in Chapters II-IV, provide novel information regarding two classes of residues that have specific functional and/or structural roles at the subunit interface in the RecA filament. Initially I we identified residues involved in maintaining the structural stability of the filament, e.g. Lys6, Arg28 and Asp139. We then identified Phe217 as a key residue in the transmission of allosteric information from one subunit to the next upon ATP binding. This finding is not only significant to the RecA field but to others interested in the mechanistic details of NTP mediated allosteric events. For studies of the human Rad51 protein I realized that it would be difficult to take a similar structure/function approach because a method to accurately analyze mutant protein function in the context of a living human cell had yet to be developed. As described in Chapters V and VI, I established a method that now permits this type of analysis. We are now able to evaluate the function of any given mutant DNA repair protein in the presence or absence of the wild-type endogenous protein in human cells, even in the case of essential genes for which knockout cell lines cannot be made. Prior to this development, researchers in the field were forced to express human proteins in other mammalian cell lines such as chicken, hamster or mouse, clearly this provided valuable information, but recent work shows that human cells may respond quite differently to defects in HR than

do other mammalian lines. Therefore, there was an obvious need to develop a cell biological system using human cells.

In brief this system utilizes RNAi to knock-down a specific target gene while the transgene carries silent base changes rendering it immune to the action of the siRNA. Cells can then be assayed for their ability to repair induced DNA damage. Another benefit is the ability to visualize and monitor specific proteins within the cell. This can be accomplished in live cells in real-time through fusions to fluorescent proteins such as GFP or in fixed cells that are processed and stained with various antibodies. Other researchers in our lab are now building on my basic set-up to knock-down specific HR proteins, analyze the overall DNA repair capability of the cell, and assess the localization of other HR proteins. With these tools now in hand, the potential exists to explore the timing and order-of-addition as HR proteins assemble at the sites of DSBs. For example, one could knock-down a specific protein whose presence or interaction with other proteins is implicated in the progression of HR and simultaneously track the effect on localization of multiple other proteins.

A combination of this cellular system, traditional biochemical assays and genetic analyses will allows us to analyze many components of the human HR pathway, and will provide a better understanding of the mechanistic details, as well as the links between HR and other cellular pathways involved in DNA damage signaling, DNA replication and cell cycle progression.

REFERENCES

Albala, J., Thelen, M., Prange, C., Fan, W., Christensen, M., Thompson, L. and Lennon, G. (1997) Identification of a Novel Human Rad51 Homolog, Rad51b. *Genomics* **46**, 476-479

Aten, J., Stap, J., Krawczyk, P., Van Oven, C. H., Hoebe, R., Essers, J. and Kanaar, R. (2004) Dynamics of DNA Double-Strand Breaks Revealed By Clustering of Damaged Chromosome Domains. *Science* **303**, 92-95

Auzat, I., Le Bras, G. and Garel, J. (1995) Hypercooperativity Induced By Interface Mutations in the Phosphofructokinase From Escherichia Coli. *J Mol Biol* **246**, 248-253

Baumann, P., Benson, F. and West, S. (1996) Human Rad51 Protein Promotes ATP-Dependent Homologous Pairing and Strand Transfer Reactions in Vitro. *Cell* **87**, 757-766

Baumann, P. and West, S. (1997) The Human Rad51 Protein: Polarity of Strand Transfer and Stimulation By Hrp-a. *EMBO J* **16**, 5198-5206

Bedale, W. and Cox, M. (1996) Evidence for the Coupling of ATP Hydrolysis to the Final (Extension) Phase of RecA Protein-Mediated DNA Strand Exchange. *J Biol Chem* **271**, 5725-5732

Benson, F., Baumann, P. and West, S. (1998) Synergistic Actions of Rad51 and Rad52 in Recombination and DNA Repair. *Nature* **391**, 401-404

Benson, F., Stasiak, A. and West, S. (1994) Purification and Characterization of the Human Rad51 Protein, an Analogue of E. Coli RecA. *EMBO J* **13**, 5764-5771

Bezzubova, O., Shinohara, A., Mueller, R., Ogawa, H. and Buerstedde, J. (1993) A Chicken Rad51 Homologue is Expressed At High Levels in Lymphoid and Reproductive Organs. *Nucleic Acids Res* **21**, 1577-1580

Bianco, P., Tracy, R. and Kowalczykowski, S. (1998) DNA Strand Exchange Proteins: a Biochemical and Physical Comparison. *Front Biosci* **3**, D570-603

Bishop, D., Ear, U., Bhattacharyya, A., Calderone, C., Beckett, M., Weichselbaum, R. and Shinohara, A. (1998) Xrcc3 is Required for Assembly of Rad51 Complexes in Vivo. *J Biol Chem* **273**, 21482-21488

Bleuyard, J. and White, C. (2004) The Arabidopsis Homologue of Xrcc3 Plays an Essential Role in Meiosis. *EMBO J* **23**, 439-449

Brenneman, M., Wagener, B., Miller, C., Allen, C. and Nickoloff, J. (2002) Xrcc3 Controls the Fidelity of Homologous Recombination: Roles for Xrcc3 in Late Stages of Recombination. *Mol Cell* **10**, 387-395

Brenner, S., Zlotnick, A. and Griffith, J. (1988) RecA Protein Self-Assembly. Multiple Discrete Aggregation States. *J Mol Biol* **204**, 959-972

Cartwright, R., Tambini, C., Simpson, P. and Thacker, J. (1998) The Xrcc2 DNA Repair Gene From Human and Mouse Encodes a Novel Member of the RecA/Rad51

Family. *Nucleic Acids Res* **26**, 3084-3089
Cazaux, C., Blanchet, J., Dupuis, D., Villani, G., Defais, M. and Johnson, N. (1998) Investigation of the Secondary DNA-Binding Site of the Bacterial Recombinase RecA. *J Biol Chem* **273**, 28799-28804
Chanet, R., Heude, M., Adjiri, A., Maloisel, L. and Fabre, F. (1996) Semidominant Mutations in the Yeast Rad51 Protein and Their Relationships With the Srs2 Helicase. *Mol Cell Biol* **16**, 4782-4789
Clark, A. and Margulies, A. (1965) Isolation and Characterization of Recombination-Deficient Mutants of *Escherichia Coli* K12. *Proc Natl Acad Sci U S A* **53**, 451-459
Conway, A., Lynch, T., Zhang, Y., Fortin, G., Fung, C., Symington, L. and Rice, P. (2004) Crystal Structure of a Rad51 Filament. *Nat Struct Mol Biol* **11**, 791-796
Cui, X., Brenneman, M., Meyne, J., Oshimura, M., Goodwin, E. and Chen, D. (1999) The Xrcc2 and Xrcc3 Repair Genes Are Required for Chromosome Stability in Mammalian Cells. *Mutat Res* **434**, 75-88
De Zutter, J. K. and Knight, K. (1999) The Hrad51 and RecA Proteins Show Significant Differences in Cooperative Binding to Single-Stranded DNA. *J Mol Biol* **293**, 769-780
Di Capua, E., Engel, A., Stasiak, A. and Koller, T. (1982) Characterization of Complexes Between RecA Protein and Duplex DNA By Electron Microscopy. *J Mol Biol* **157**, 87-103
Dosanjh, M., Collins, D., Fan, W., Lennon, G., Albala, J., Shen, Z. and Schild, D. (1998) Isolation and Characterization of Rad51c, a New Human Member of the Rad51 Family of Related Genes. *Nucleic Acids Res* **26**, 1179-1184
Eaton, W. and Hofrichter, J. (1990) Sickle Cell Hemoglobin Polymerization. *Adv Protein Chem* **40**, 63-279
Egelman, E. (1998) Bacterial Helicases. *J Struct Biol* **124**, 123-128
Egelman, E. (1993) What Do X-Ray Crystallographic and Electron Microscopic Structural Studies of the RecA Protein Tell Us About Recombination. *Curr Opin Struct Biol* **3**, 189-197
Egelman, E. and Stasiak, A. (1986) Structure of Helical RecA-DNA Complexes. Complexes Formed in the Presence of ATP-Gamma-S Or ATP. *J Mol Biol* **191**, 677-697
Egelman, E. and Stasiak, A. (1988) Structure of Helical RecA-DNA Complexes. Ii. Local Conformational Changes Visualized in Bundles of RecA-ATP Gamma S Filaments. *J Mol Biol* **200**, 329-349
Egelman, E. and Stasiak, A. (1993) Electron Microscopy of RecA-DNA Complexes: Two Different States, Their Functional Significance and Relation to the Solved Crystal Structure. *Micron* **24**, 309-324
Eggleston, A. and West, S. (1996) Exchanging Partners: Recombination in E. Coli. *Trends Genet* **12**, 20-26
Eldin, S., Forget, A., Lindenmuth, D., Logan, K. and Knight, K. (2000) Mutations in the N-Terminal Region of RecA That Disrupt the Stability of Free Protein Oligomers But Not RecA-DNA Complexes. *J Mol Biol* **299**, 91-101

Essers, J., Houtsmuller, A., Van Veelen, L., Paulusma, C., Nigg, A., Pastink, A., Vermeulen, W., Hoeijmakers, J. and Kanaar, R. (2002) Nuclear Dynamics of Rad52 Group Homologous Recombination Proteins in Response to DNA Damage. *EMBO J* **21**, 2030-2037

Forget, A., Bennett, B. and Knight, K. (2004) Xrcc3 is Recruited to DNA Double Strand Breaks Early and Independent of Rad51. *J Cell Biochem* (in press)

Gallivan, J. and Dougherty, D. (1999) Cation-Pi Interactions in Structural Biology. *Proc Natl Acad Sci U S A* **96**, 9459-9464

Game, J. and Mortimer, R. (1974) A Genetic Study of X-Ray Sensitive Mutants in Yeast. *Mutat Res* **24**, 281-292

Griffith, J. and Formosa, T. (1985) The Uvsx Protein of Bacteriophage T4 Arranges Single-Stranded and Double-Stranded DNA Into Similar Helical Nucleoprotein Filaments. *J Biol Chem* **260**, 4484-4491

Gupta, R., Bazemore, L., Golub, E. and Radding, C. (1997) Activities of Human Recombination Protein Rad51. *Proc Natl Acad Sci U S A* **94**, 463-468

Haaf, T., Golub, E., Reddy, G., Radding, C. and Ward, D. (1995) Nuclear Foci of Mammalian Rad51 Recombination Protein in Somatic Cells After DNA Damage and Its Localization in Synaptonemal Complexes. *Proc Natl Acad Sci U S A* **92**, 2298-2302

Hazes, B. and Dijkstra, B. (1988) Model Building of Disulfide Bonds in Proteins With Known Three-Dimensional Structure. *Protein Eng* **2**, 119-125

Henry-Mowatt, J., Jackson, D., Masson, J., Johnson, P., Clements, P., Benson, F., Thompson, L., Takeda, S., West, S. and Caldecott, K. (2003) Xrcc3 and Rad51 Modulate Replication Fork Progression on Damaged Vertebrate Chromosomes. *Mol Cell* **11**, 1109-1117

Heuser, J. and Griffith, J. (1989) Visualization of RecA Protein and Its Complexes With DNA By Quick-Freeze/Deep-Etch Electron Microscopy. *J Mol Biol* **210**, 473-484

Hortnagel, K., Voloshin, O., Kinal, H., Ma, N., Schaffer-Judge, C. and Camerini-Otero, R. D. (1999) Saturation Mutagenesis of the E. Coli RecA Loop L2 Homologous DNA Pairing Region Reveals Residues Essential for Recombination and Recombinational Repair. *J Mol Biol* **286**, 1097-1106

Karlin, S. and Brocchieri, L. (1996) Evolutionary Conservation of RecA Genes in Relation to Protein Structure and Function. *J Bacteriol* **178**, 1881-1894

Kelley De Zutter, J., Forget, A., Logan, K. and Knight, K. (2001) Phe217 Regulates the Transfer of Allosteric Information Across the Subunit Interface of the RecA Protein Filament. *Structure (Camb)* **9**, 47-55

Kelley, J. and Knight, K. (1997) Allosteric Regulation of RecA Protein Function is Mediated By Gln194. *J Biol Chem* **272**, 25778-25782

Kiselev, V., Glukhov, A., Tarasova, I. and Shchepetov, M. (1988) [accumulation of N-Terminal Fragment of RecA Protein in the Htpr- Mutant Impairs the Sos-Function of Escherichia Coli Cells]. *Mol Biol (Mosk)* **22**, 1198-1203

Kiselev, V., Tarasova, I., Malinin, A., Kiselev, O. and Glukhov, A. (1988) [properties of Thermostable Htpr-Mutant of Escherichia Coli]. *Mol Gen Mikrobiol Virusol* **9**, 21-26

Kobayashi, N., Knight, K. and Mcentee, K. (1987) Evidence for Nucleotide-Mediated Changes in the Domain Structure of the RecA Protein of Escherichia Coli. *Biochemistry* **26**, 6801-6810

Konola, J., Nastri, H., Logan, K. and Knight, K. (1995) Mutations At Pro67 in the RecA Protein P-Loop Motif Differentially Modify Coprotease Function and Separate Coprotease From Recombination Activities. *J Biol Chem* **270**, 8411-8419

Kowalczykowski, S. (1991) Biochemistry of Genetic Recombination: Energetics and Mechanism of DNA Strand Exchange. *Annu Rev Biophys Biophys Chem* **20**, 539-575

Kowalczykowski, S., Dixon, D., Eggleston, A., Lauder, S. and Rehrauer, W. (1994) Biochemistry of Homologous Recombination in Escherichia Coli. *Microbiol Rev* **58**, 401-465

Kowalczykowski, S., Lonberg, N., Newport, J. and Von Hippel, P. H. (1981) Interactions of Bacteriophage T4-Coded Gene 32 Protein With Nucleic Acids. I. Characterization of the Binding Interactions. *J Mol Biol* **145**, 75-104

Kurumizaka, H., Ikawa, S., Nakada, M., Eda, K., Kagawa, W., Takata, M., Takeda, S., Yokoyama, S. and Shibata, T. (2001) Homologous-Pairing Activity of the Human DNA-Repair Proteins Xrcc3.Rad51c. *Proc Natl Acad Sci U S A* **98**, 5538-5543

Kurumizaka, H., Ikawa, S., Nakada, M., Enomoto, R., Kagawa, W., Kinebuchi, T., Yamazoe, M., Yokoyama, S. and Shibata, T. (2002) Homologous Pairing and Ring and Filament Structure Formation Activities of the Human Xrcc2*Rad51d Complex. *J Biol Chem* **277**, 14315-14320

Leipe, D., Aravind, L., Grishin, N. and Koonin, E. (2000) The Bacterial Replicative Helicase DNAB Evolved From a RecA Duplication. *Genome Res* **10**, 5-16

Levinson, A., Silver, D. and Seed, B. (1984) Minimal Size Plasmids Containing an M13 Origin for Production of Single-Strand Transducing Particles. *J Mol Appl Genet* **2**, 507-517

Liu, N., Lamerdin, J., Tebbs, R., Schild, D., Tucker, J., Shen, M., Brookman, K., Siciliano, M., Walter, C., Fan, W., Narayana, L., Zhou, Z., Adamson, A., Sorensen, K., Chen, D., Jones, N. and Thompson, L. (1998) Xrcc2 and Xrcc3, New Human Rad51-Family Members, Promote Chromosome Stability and Protect Against DNA Cross-Links and Other Damages. *Mol Cell* **1**, 783-793

Liu, Y. and Maizels, N. (2000) Coordinated Response of Mammalian Rad51 and Rad52 to DNA Damage. *EMBO Rep* **1**, 85-90

Liu, Y., Masson, J., Shah, R., O'regan, P. and West, S. (2004) Rad51c is Required for Holliday Junction Processing in Mammalian Cells. *Science* **303**, 243-246

Lloyd, J., Forget, A. and Knight, K. (2002) Correlation of Biochemical Properties With the Oligomeric State of Human Rad52 Protein. *J Biol Chem* **277**, 46172-46178

Logan, K., Forget, A., Verderese, J. and Knight, K. (2001) ATP-Mediated Changes in Cross-Subunit Interactions in the RecA Protein. *Biochemistry* **40**, 11382-11389

Logan, K. and Knight, K. (1993) Mutagenesis of the P-Loop Motif in the ATP Binding Site of the RecA Protein From Escherichia Coli. *J Mol Biol* **232**, 1048-1059

Logan, K., Skiba, M., Eldin, S. and Knight, K. (1997) Mutant RecA Proteins Which Form Hexamer-Sized Oligomers. *J Mol Biol* **266**, 306-316

Macfarland, K., Shan, Q., Inman, R. and Cox, M. (1997) RecA as a Motor Protein. Testing Models for the Role of ATP Hydrolysis in DNA Strand Exchange. *J Biol Chem* **272**, 17675-17685

Maeshima, K., Morimatsu, K., Shinohara, A. and Horii, T. (1995) Rad51 Homologues in Xenopus Laevis: Two Distinct Genes Are Highly Expressed in Ovary and Testis. *Gene* **160**, 195-200

Masson, J., Stasiak, A., Stasiak, A., Benson, F. and West, S. (2001) Complex Formation By the Human Rad51c and Xrcc3 Recombination Repair Proteins. *Proc Natl Acad Sci U S A* **98**, 8440-8446

Masson, J., Tarsounas, M., Stasiak, A., Stasiak, A., Shah, R., Mcilwraith, M., Benson, F. and West, S. (2001) Identification and Purification of Two Distinct Complexes Containing the Five Rad51 Paralogs. *Genes Dev* **15**, 3296-3307

Masui, R., Mikawa, T. and Kuramitsu, S. (1997) Local Folding of the N-Terminal Domain of Escherichia Coli RecA Controls Protein-Protein Interaction. *J Biol Chem* **272**, 27707-27715

Mcghee, J. and Von Hippel, P. H. (1974) Theoretical Aspects of DNA-Protein Interactions: Co-Operative and Non-Co-Operative Binding of Large Ligands to a One-Dimensional Homogeneous Lattice. *J Mol Biol* **86**, 469-489

Mecozzi, S., West, A. J. and Dougherty, D. (1996) Cation-Pi Interactions in Aromatics of Biological and Medicinal Interest: Electrostatic Potential Surfaces as a Useful Qualitative Guide. *Proc Natl Acad Sci U S A* **93**, 10566-10571

Menetski, J. and Kowalczykowski, S. (1985) Interaction of RecA Protein With Single-Stranded DNA. Quantitative Aspects of Binding Affinity Modulation By Nucleotide Cofactors. *J Mol Biol* **181**, 281-295

Mikawa, T., Masui, R. and Kuramitsu, S. (1998) RecA Protein Has Extremely High Cooperativity for Substrate in Its ATPase Activity. *J Biochem (Tokyo)* **123**, 450-457

Mikawa, T., Masui, R., Ogawa, T., Ogawa, H. and Kuramitsu, S. (1995) N-Terminal 33 Amino Acid Residues of Escherichia Coli RecA Protein Contribute to Its Self-Assembly. *J Mol Biol* **250**, 471-483

Morimatsu, K. and Horii, T. (1995) Analysis of the DNA Binding Site of Escherichia Coli RecA Protein. *Adv Biophys* **31**, 23-48

Morita, T., Yoshimura, Y., Yamamoto, A., Murata, K., Mori, M., Yamamoto, H. and Matsushiro, A. (1993) A Mouse Homolog of the Escherichia Coli RecA and Saccharomyces Cerevisiae Rad51 Genes. *Proc Natl Acad Sci U S A* **90**, 6577-6580

Morrical, S. and Cox, M. (1985) Light Scattering Studies of the RecA Protein of Escherichia Coli: Relationship Between Free RecA Filaments and the RecA X ssDNA Complex. *Biochemistry* **24**, 760-767

Morrison, C., Shinohara, A., Sonoda, E., Yamaguchi-Iwai, Y., Takata, M., Weichselbaum, R. and Takeda, S. (1999) The Essential Functions of Human Rad51 Are Independent of ATP Hydrolysis. *Mol Cell Biol* **19**, 6891-6897

Morrison, C. and Takeda, S. (2000) Genetic Analysis of Homologous DNA Recombination in Vertebrate Somatic Cells. *Int J Biochem Cell Biol* **32**, 817-831

Namsaraev, E. and Berg, P. (1998) Binding of Rad51p to DNA. Interaction of Rad51p With Single- and Double-Stranded DNA. *J Biol Chem* **273**, 6177-6182

Nastri, H. and Knight, K. (1994) Identification of Residues in the L1 Region of the RecA Protein Which Are Important to Recombination Or Coprotease Activities. *J Biol Chem* **269**, 26311-26322

Nayak, S. and Bryant, F. (1999) Differential Rates of Ntp Hydrolysis By the Mutant [s69g]RecA Protein. Evidence for a Coupling of Ntp Turnover to DNA Strand Exchange. *J Biol Chem* **274**, 25979-25982

Nguyen, T., Muench, K. and Bryant, F. (1993) Inactivation of the RecA Protein By Mutation of Histidine 97 Or Lysine 248 At the Subunit Interface. *J Biol Chem* **268**, 3107-3113

Nicholls, A., Bharadwaj, R. and Honig, B. (1993) Grasp: a Graphical Representation and Analysis of Surface Properties. *Biophys. J.* **64**, A166

Ogawa, T., Yu, X., Shinohara, A. and Egelman, E. (1993) Similarity of the Yeast Rad51 Filament to the Bacterial RecA Filament. *Science* **259**, 1896-1899

Pellegrini, L., Yu, D., Lo, T., Anand, S., Lee, M., Blundell, T. and Venkitaraman, A. (2002) Insights Into DNA Recombination From the Structure of a Rad51-Brca2 Complex. *Nature* **420**, 287-293

Pierce, A., Johnson, R., Thompson, L. and Jasin, M. (1999) Xrcc3 Promotes Homology-Directed Repair of DNA Damage in Mammalian Cells. *Genes Dev* **13**, 2633-2638

Pittman, D., Weinberg, L. and Schimenti, J. (1998) Identification, Characterization, and Genetic Mapping of Rad51d, a New Mouse and Human Rad51/RecA-Related Gene. *Genomics* **49**, 103-111

Radding, C. (1989) Helical RecA Nucleoprotein Filaments Mediate Homologous Pairing and Strand Exchange. *Biochim Biophys Acta* **1008**, 131-145

Raderschall, E., Golub, E. and Haaf, T. (1999) Nuclear Foci of Mammalian Recombination Proteins Are Located At Single-Stranded DNA Regions Formed After DNA Damage. *Proc Natl Acad Sci U S A* **96**, 1921-1926

Ranatunga, W., Jackson, D., Lloyd, J., Forget, A., Knight, K. and Borgstahl, G. (2001) Human Rad52 Exhibits Two Modes of Self-Association. *J Biol Chem* **276**, 15876-15880

Register, J. r. and Griffith, J. (1985) The Direction of RecA Protein Assembly Onto Single Strand DNA is the Same as the Direction of Strand Assimilation During Strand Exchange. *J Biol Chem* **260**, 12308-12312

Rehrauer, W. and Kowalczykowski, S. (1993) Alteration of the Nucleoside Triphosphate (Ntp) Catalytic Domain Within Escherichia Coli RecA Protein Attenuates Ntp Hydrolysis But Not Joint Molecule Formation. *J Biol Chem* **268**, 1292-1297

Rice, M., Smith, S., Bullrich, F., Havre, P. and Kmiec, E. (1997) Isolation of Human and Mouse Genes Based on Homology to Rec2, a Recombinational Repair Gene From the Fungus Ustilago Maydis. *Proc Natl Acad Sci U S A* **94**, 7417-7422

Roca, A. and Cox, M. (1990) The RecA Protein: Structure and Function. *Crit Rev Biochem Mol Biol* **25**, 415-456

Roca, A. and Cox, M. (1997) RecA Protein: Structure, Function, and Role in Recombinational DNA Repair. *Prog Nucleic Acid Res Mol Biol* **56**, 129-223

Rogakou, E., Pilch, D., Orr, A., Ivanova, V. and Bonner, W. (1998) DNA Double-Stranded Breaks Induce Histone H2ax Phosphorylation on Serine 139. *J Biol Chem* **273**, 5858-5868

Roman, L. and Kowalczykowski, S. (1986) Relationship of the Physical and Enzymatic Properties of Escherichia Coli RecA Protein to Its Strand Exchange Activity. *Biochemistry* **25**, 7375-7385

Royer, W. J., Pardanani, A., Gibson, Q., Peterson, E. and Friedman, J. (1996) Ordered Water Molecules as Key Allosteric Mediators in a Cooperative Dimeric Hemoglobin. *Proc Natl Acad Sci U S A* **93**, 14526-14531

Ruigrok, R. and Dicapua, E. (1991) On the Polymerization State of RecA in the Absence of DNA. *Biochimie* **73**, 191-198

Sawaya, M., Guo, S., Tabor, S., Richardson, C. and Ellenberger, T. (1999) Crystal Structure of the Helicase Domain From the Replicative Helicase-Primase of Bacteriophage T7. *Cell* **99**, 167-177

Schild, D., Lio, Y., Collins, D., Tsomondo, T. and Chen, D. (2000) Evidence for Simultaneous Protein Interactions Between Human Rad51 Paralogs. *J Biol Chem* **275**, 16443-16449

Segel, I. (1975) Enzyme Kinetics, T. Hoffman, Ed. 346-385

Shim, K., Schmutte, C., Tombline, G., Heinen, C. and Fishel, R. (2004) Hxrcc2 Enhances ADP/ATP Processing and Strand Exchange By Hrad51. *J Biol Chem* **279**, 30385-30394

Shin, D., Pellegrini, L., Daniels, D., Yelent, B., Craig, L., Bates, D., Yu, D., Shivji, M., Hitomi, C., Arvai, A., Volkmann, N., Tsuruta, H., Blundell, T., Venkitaraman, A. and Tainer, J. (2003) Full-Length Archaeal Rad51 Structure and Mutants: Mechanisms for Rad51 Assembly and Control By Brca2. *EMBO J* **22**, 4566-4576

Shinohara, A., Ogawa, H., Matsuda, Y., Ushio, N., Ikeo, K. and Ogawa, T. (1993) Cloning of Human, Mouse and Fission Yeast Recombination Genes Homologous to Rad51 and RecA. *Nat Genet* **4**, 239-243

Sigurdsson, S., Van Komen, S., Bussen, W., Schild, D., Albala, J. and Sung, P. (2001) Mediator Function of the Human Rad51b-Rad51c Complex in Rad51/Rpa-Catalyzed DNA Strand Exchange. *Genes Dev* **15**, 3308-3318

Silver, M. and Fersht, A. (1982) Direct Observation of Complexes Formed Between RecA Protein and a Fluorescent Single-Stranded Deoxyribonucleic Acid Derivative. *Biochemistry* **21**, 6066-6072

Silver, M. and Fersht, A. (1983) Investigation of Binding Between RecA Protein and Single-Stranded Polynucleotides With the Aid of a Fluorescent Deoxyribonucleic Acid Derivative. *Biochemistry* **22**, 2860-2866

Singleton, M., Sawaya, M., Ellenberger, T. and Wigley, D. (2000) Crystal Structure of T7 Gene 4 Ring Helicase Indicates a Mechanism for Sequential Hydrolysis of Nucleotides. *Cell* **101**, 589-600

Skiba, M. and Knight, K. (1994) Functionally Important Residues At a Subunit Interface Site in the RecA Protein From Escherichia Coli. *J Biol Chem* **269**, 3823-3828

Skiba, M., Logan, K. and Knight, K. (1999) Intersubunit Proximity of Residues in the RecA Protein as Shown By Engineered Disulfide Cross-Links. *Biochemistry* **38**,

11933-11941

Sonoda, E., Sasaki, M., Buerstedde, J., Bezzubova, O., Shinohara, A., Ogawa, H., Takata, M., Yamaguchi-Iwai, Y. and Takeda, S. (1998) Rad51-Deficient Vertebrate Cells Accumulate Chromosomal Breaks Prior to Cell Death. *EMBO J* **17**, 598-608

Soultanas, P. and Wigley, D. (2000) DNA Helicases: 'Inching Forward'. *Curr Opin Struct Biol* **10**, 124-128

Sowdhamini, R., Srinivasan, N., Shoichet, B., Santi, D., Ramakrishnan, C. and Balaram, P. (1989) Stereochemical Modeling of Disulfide Bridges. Criteria for Introduction Into Proteins By Site-Directed Mutagenesis. *Protein Eng* **3**, 95-103

Stark, J., Hu, P., Pierce, A., Moynahan, M., Ellis, N. and Jasin, M. (2002) ATP Hydrolysis By Mammalian Rad51 Has a Key Role During Homology-Directed DNA Repair. *J Biol Chem* **277**, 20185-20194

Story, R., Bishop, D., Kleckner, N. and Steitz, T. (1993) Structural Relationship of Bacterial RecA Proteins to Recombination Proteins From Bacteriophage T4 and Yeast. *Science* **259**, 1892-1896

Story, R. and Steitz, T. (1992) Structure of the RecA Protein-ADP Complex. *Nature* **355**, 374-376

Story, R., Weber, I. and Steitz, T. (1992) The Structure of the E. Coli RecA Protein Monomer and Polymer. *Nature* **355**, 318-325

Subramanya, H., Bird, L., Brannigan, J. and Wigley, D. (1996) Crystal Structure of a Dexx Box DNA Helicase. *Nature* **384**, 379-383

Sung, P., Krejci, L., Van Komen, S. and Sehorn, M. (2003) Rad51 Recombinase and Recombination Mediators. *J Biol Chem* **278**, 42729-42732

Takata, M., Sasaki, M., Tachiiri, S., Fukushima, T., Sonoda, E., Schild, D., Thompson, L. and Takeda, S. (2001) Chromosome Instability and Defective Recombinational Repair in Knockout Mutants of the Five Rad51 Paralogs. *Mol Cell Biol* **21**, 2858-2866

Tan, T., Essers, J., Citterio, E., Swagemakers, S., De Wit, J., Benson, F., Hoeijmakers, J. and Kanaar, R. (1999) Mouse Rad54 Affects DNA Conformation and DNA-Damage-Induced Rad51 Foci Formation. *Curr Biol* **9**, 325-328

Tashiro, S., Walter, J., Shinohara, A., Kamada, N. and Cremer, T. (2000) Rad51 Accumulation At Sites of DNA Damage and in Postreplicative Chromatin. *J Cell Biol* **150**, 283-291

Tebbs, R., Zhao, Y., Tucker, J., Scheerer, J., Siciliano, M., Hwang, M., Liu, N., Legerski, R. and Thompson, L. (1995) Correction of Chromosomal Instability and Sensitivity to Diverse Mutagens By a Cloned cDNA of the Xrcc3 DNA Repair Gene. *Proc Natl Acad Sci U S A* **92**, 6354-6358

Thompson, L. and Schild, D. (2001) Homologous Recombinational Repair of DNA Ensures Mammalian Chromosome Stability. *Mutat Res* **477**, 131-153

Thompson, L. and Schild, D. (2002) Recombinational DNA Repair and Human Disease. *Mutat Res* **509**, 49-78

Tsuzuki, T., Fujii, Y., Sakumi, K., Tominaga, Y., Nakao, K., Sekiguchi, M., Matsushiro, A., Yoshimura, Y. and Moritat (1996) Targeted Disruption of the Rad51 Gene Leads to Lethality in Embryonic Mice. *Proc Natl Acad Sci U S A* **93**, 6236-6240

Voloshin, O., Wang, L. and Camerini-Otero, R. D. (1996) Homologous DNA Pairing Promoted By a 20-Amino Acid Peptide Derived From RecA. *Science* **272**, 868-872

Wang, L., Voloshin, O., Stasiak, A. and Camerini-Otero, R. D. (1998) Homologous DNA Pairing Domain Peptides of RecA Protein: Intrinsic Propensity to Form Beta-Structures and Filaments. *J Mol Biol* **277**, 1-11

Wang, Y. and Adzuma, K. (1996) Differential Proximity Probing of Two DNA Binding Sites in the Escherichia Coli RecA Protein Using Photo-Cross-Linking Methods. *Biochemistry* **35**, 3563-3571

Weinstock, G., Mcentee, K. and Lehman, I. (1981) Hydrolysis of Nucleoside Triphosphates Catalyzed By the RecA Protein of Escherichia Coli. Characterization of ATP Hydrolysis. *J Biol Chem* **256**, 8829-8834

Weisemann, J. and Weinstock, G. (1988) Mutations At the Cysteine Codons of the RecA Gene of Escherichia Coli. *DNA* **7**, 389-398

West, S. (1992) Enzymes and Molecular Mechanisms of Genetic Recombination. *Annu Rev Biochem* **61**, 603-640

West, S. (2003) Molecular Views of Recombination Proteins and Their Control. *Nat Rev Mol Cell Biol* **4**, 435-445

Wiese, C., Collins, D., Albala, J., Thompson, L., Kronenberg, A. and Schild, D. (2002) Interactions Involving the Rad51 Paralogs Rad51c and Xrcc3 in Human Cells. *Nucleic Acids Res* **30**, 1001-1008

Wilson, D. and Benight, A. (1990) Kinetic Analysis of the Pre-Equilibrium Steps in the Self-Assembly of RecA Protein From Escherichia Coli. *J Biol Chem* **265**, 7351-7359

Yamada, N., Hinz, J., Kopf, V., Segalle, K. and Thompson, L. (2004) Xrcc3 ATPase Activity is Required for Normal Xrcc3-Rad51c Complex Dynamics and Homologous Recombination. *J Biol Chem* **279**, 23250-23254

Yarranton, G. and Sedgwick, S. (1982) Cloned Truncated RecA Genes in E. Coli Ii. Effects of Truncated Gene Products on in Vivo RecA+ Protein Activity. *Mol Gen Genet* **185**, 99-104

Yoshihara, T., Ishida, M., Kinomura, A., Katsura, M., Tsuruga, T., Tashiro, S., Asahara, T. and Miyagawa, K. (2004) Xrcc3 Deficiency Results in a Defect in Recombination and Increased Endoreduplication in Human Cells. *EMBO J* **23**, 670-680

Yoshikawa, K., Ogawa, T., Baer, R., Hemmi, H., Honda, K., Yamauchi, A., Inamoto, T., Ko, K., Yazumi, S., Motoda, H., Kodama, H., Noguchi, S., Gazdar, A., Yamaoka, Y. and Takahashi, R. (2000) Abnormal Expression of Brca1 and Brca1-Interactive DNA-Repair Proteins in Breast Carcinomas. *Int J Cancer* **88**, 28-36

Yoshimura, Y., Morita, T., Yamamoto, A. and Matsushiro, A. (1993) Cloning and Sequence of the Human RecA-Like Gene cDNA. *Nucleic Acids Res* **21**, 1665

Yu, D., Sonoda, E., Takeda, S., Huang, C., Pellegrini, L., Blundell, T. and Venkitaraman, A. (2003) Dynamic Control of Rad51 Recombinase By Self-Association and Interaction With Brca2. *Mol Cell* **12**, 1029-1041

Yu, X. and Egelman, E. (1992) Structural Data Suggest That the Active and Inactive

Forms of the RecA Filament Are Not Simply Interconvertible. *J Mol Biol* **227**, 334-346

Yu, X., Shibata, T. and Egelman, E. (1998) Identification of a Defined Epitope on the Surface of the Active RecA-DNA Filament Using a Monoclonal Antibody and Three-Dimensional Reconstruction. *J Mol Biol* **283**, 985-992

Zagursky, R. and Berman, M. (1984) Cloning Vectors That Yield High Levels of Single-Stranded DNA for Rapid DNA Sequencing. *Gene* **27**, 183-191

Zaitsev, E. and Kowalczykowski, S. (1998) Essential Monomer-Monomer Contacts Define the Minimal Length for the N-Terminus of RecA Protein. *Mol Microbiol* **29**, 1317-1318

Zaitsev, E. and Kowalczykowski, S. (1999) Enhanced Monomer-Monomer Interactions Can Suppress the Recombination Deficiency of the RecA142 Allele. *Mol Microbiol* **34**, 1-9

Zlotnick, A., Mitchell, R., Steed, R. and Brenner, S. (1993) Analysis of Two Distinct Single-Stranded DNA Binding Sites on the RecA Nucleoprotein Filament. *J Biol Chem* **268**, 22525-22530